TÉCNICO LISBOA

Seismic Behaviour and Design of Frame Buildings with Discontinued Columns

José Pedro Cristo Ferreira Marques Alexandre

Dissertation to obtain the Master of Science Degree in

Civil Engineering

Supervisors: Professor Jorge Miguel Silveira Filipe Mascarenhas Proença
Professor José Manuel Matos Noronha da Camara

Examination Committee

Chairperson: Professor José Joaquim Costa Branco de Oliveira Pedro
Supervisor: Professor Jorge Miguel Silveira Filipe Mascarenhas Proença
Members of the Committee: Professor João José Rio Tinto de Azevedo

November 2015

Abstract

Structural irregularities in which a vertical element is interrupted and indirectly supported on beams are associated with a poor seismic behaviour and are often avoided by designers. The main objectives of this dissertation are the assessment of the consequences of this irregularity and the identification of the structural layouts in which it proves to be more detrimental to the seismic behaviour of reinforced concrete frame structures.

In the first part a parametric study based on the linear elastic properties of the materials was carried out. In that study, the values of the internal forces in the structures, corresponding to the gravity loads and the seismic loads, were compared with the objective of determining the load combination which led to the most unfavourable condition.

In the following part, both static and dynamic non-linear time-history analyses were performed, comparing the most detrimental layout identified in the parametric study with the corresponding regular model. This study was carried out to evaluate the influence of the irregularity on both the non-linear behaviour and on the dynamic effects.

The possibility of taking into account this irregularity at the design stage through a reduction of the behaviour factor was also considered.

It was concluded that a careful design and detailing may be the key to assure that structures with this irregularity have a suitable behaviour under seismic actions. Failing to properly approach this kind of irregularity, may lead to severe structural damage and eventually to collapse, as seen in past occurrences.

Key-words

Discontinued columns; Structural irregularities; RC structures; Seismic behaviour; Non-linear analysis

Resumo

Irregularidades estruturais em que um elemento vertical é interrompido e apoiado indiretamente em vigas estão associadas a um inadequado comportamento sísmico, sendo frequentemente preteridas pelos projetistas. Os principais objetivos desta dissertação foram a identificação das configurações que se mostram ser mais prejudiciais para o comportamento sísmico de estruturas porticadas de betão e a avaliação das suas implicações em termos de desempenho sísmico.

Numa primeira fase foi realizado um estudo paramétrico com base em modelos de comportamento linear. Nesse estudo e tendo como objetivo a determinação da combinação de ações prevista pelos Eurocódigos que levaria à condição de dimensionamento mais desfavorável, foram comparados os esforços internos correspondentes à combinação fundamental e à combinação sísmica.

A segunda fase do estudo compreendeu a realização de análises estáticas não-lineares e análises dinâmicas não-lineares no domínio do tempo, comparando o desempenho da solução estrutural considerada mais negativa no estudo paramétrico com o do modelo regular correspondente. Esta fase do estudo foi realizada para avaliar a influência da irregularidade, tanto no comportamento não-linear como nos efeitos dinâmicos.

Foi concluído que um dimensionamento e pormenorização adequados são a chave para garantir que estruturas com esta irregularidade têm um comportamento sísmico adequado. Não abordar convenientemente este tipo de irregularidade pode levar a danos severos a nível estrutural e até mesmo colapso, como observado em casos anteriores.

Palavras-chave

Pilares interrompidos; Irregularidades estruturais; Estruturas de BA; Comportamento sísmico, Análise não linear

Acknowledgements

My first acknowledgement is directed to my supervisors to whom I would like to express my utmost gratitude for giving me the opportunity to develop this dissertation. Both Professors, Jorge Proença and José Camara, guided and supported me throughout the different steps of this work. In particular to Professor Jorge Proença, who closely supervised and reviewed this work and with whom I discussed most of the results achieved. His constant guidance and concern was crucial and words cannot possibly describe the value of his support.

I am also thankful to all the professors of Instituto Superior Técnico who, along the last five years, showed availability and dedication to assist whenever was necessary. Their contribution could not go unmentioned.

To all my friends and colleagues, that were there through the development of this dissertation. Their friendship is greatly valued as is their support, either direct or indirect.

For the great dedication in all aspects of her life, for the kind words and love shown, a special thanks to Inês. She has been the key stone in this defining part of my life.

Finally, to all my family who defined the person I am and accompanied me through the years. To Francisca for sharing my concerns and cheering me up day and night, to my father with whom I share a contagious passion for civil engineering and to my mother for nurturing me along the way.

Contents

List of Figures

List of Tables

List of Symbols

Latin upper case letters:

A_c	Area of the cross-section
$A_{s,a}$	Adopted cross-sectional area of longitudinal steel reinforcement
$A_{s,d}$	Design cross-sectional area of longitudinal steel reinforcement
$A_{s,min}$	Minimum cross-sectional area of longitudinal steel reinforcement to the Eurocodes
$A_{s,PE}$	Adopted cross-sectional area of pre-stress reinforcement
A_{sw}	Adopted cross-sectional area of transversal steel reinforcement
$A_{sw,d}$	Design cross-sectional area of transversal steel reinforcement
A_{sx}	Adopted cross-sectional area of longitudinal steel reinforcement in the direction x
E_0	Initial modulus of elasticity in the steel model proposed by Menegotto and Pinto [28]
E_c	Initial modulus of elasticity of the concrete
$E_{C,28}$	Tangent modulus of elasticity of normal weight concrete at 28 days
E_S	Design value of modulus of elasticity of reinforcing steel
E_{sec}	Secant modulus of elasticity at peak stress off the concrete
E_P	Design value of modulus of elasticity of prestressing steel
E_T	Variable of the steel model proposed by Menegotto and Pinto [28]
E_X	Value of an internal force for a load combination where X is a specific load combination
F_b	Base shear
F_B^{lin}	Base shear obtained from a linear elastic analysis
F_B^{Nlin}	Base shear obtained from a non-linear inelastic analysis
$F_{B,ED}$	Design value of the base shear
$F_{B,RD}$	Resisting value of the base shear
F_y	Yielding force
L	Span Length
L_V	Ratio moment/shear at the end section
M_{ED}	Design value of the bending moment
M_{RD}	Resisting value of the bending moment
M_X	Bending moment for a specific load combination (X)
N_{ED}	Design value of the axial force
P	Pre-stress pushing force
P_∞	Pre-stress pushing force at infinite time
R	Variable of the steel model proposed by Menegotto and Pinto [28]
R_0	Experimentally determined parameter of the steel model proposed by Menegotto and Pinto [28]
S	Soil factor

S_e Spectral acceleration of the elastic response spectrum defined in EN1998-1 [15]

T Fundamental period

T_{LSNC} Return period associated with the limit state of near collapse

T_{LSSD} Return period associated with the limit state of significant damage

U_X $=\left(\sqrt{\nu^2+\mu_x^2+\mu_y^2}\right)_X$ where X is a specific load combination

V_{CD} Shear force according with the rules of capacity design

V_{ED} Design value of the shear force

V_X Shear force for a specific load combination (X)

$V_{zcot\theta}$ Shear force at a distance $zcot\theta$ of the support

Latin lower case letters:

a_1 Experimentally determined parameter of the steel model proposed by Menegotto and Pinto [28]

a_2 Experimentally determined parameter of the steel model proposed by Menegotto and Pinto [28]

a_3 Experimentally determined parameter of the steel model proposed by Filippou *et al.* [19]

a_4 Experimentally determined parameter of the steel model proposed by Filippou *et al.* [19]

a_M Proportionality constant between damping matrix and mass matrix

a_K Proportionality constant between damping matrix and stiffness matrix

a_{gR} Reference peak ground acceleration

a_g Design ground acceleration

a_{vg} Design ground acceleration in the vertical direction

b Width of the cross-section. Strain hardening parameter in the steel model proposed by Menegotto and Pinto [28]

b_c Cross-sectional dimension of the column

b_0 Width of confined core in a column (to centreline of hoops)

b_w Width of the compressive zone of the cross-section

d Displacement

d_{1st} Displacement at the level of the 1st floor

d_{2nd} Displacement at the level of the 2nd floor

d_{el} Elastic displacement

d_t Target displacement

d_y Yielding displacement

e Slab thickness

f Frequency of vibration

f_c Compressive concrete stress

f'_{c0} Unconfined concrete compressive strength

f'_{cc} Confined concrete compressive strength

f_{cd} Design value of the concrete compressive strength

f_{ck} Characteristic compressive cylinder strength of concrete at 28 days

f_{cm} Mean compressive strength

f_t' Concrete tensile strength

f_{ctm} Mean value of axial tensile strength of concrete

f_{pk} Characteristic tensile strength of prestressing steel

$f_{p0.1k}$ Characteristic 0,1 % proof-stress of prestressing steel

f_{yd} Design yield strength of reinforcement

f_{yk} Characteristic yield strength of reinforcement

f_{yw} Stirrups yielding strength

g Acceleration of gravity

h Height of the cross-section

h_0 Depth of confined core in a column (to centreline of hoops)

h_c Cross-sectional depth of column in the direction of interest

k Exponent dependent of the seismic action used to define equation (4.18)

m Mass

n Number of floors above the ground

q Behaviour factor

q_{EC8} Behaviour factor defined according to the EN1998-1 [15]

q_F Behaviour factor obtained from the analyses computed

r Parameter of the concrete model proposed by Mander *et al.* [26]

s Spacing

s_h Stirrups spacing

t Time

Greek upper case letters:

$\Delta\sigma_I$ Variable of the steel model proposed by Filippou *et al.* [19]

Greek lower case letters:

α Confinement effectiveness factor

α_b Adimentional parameter for comparing the internal forces on the beams

$\alpha_{b,M}$ Particular case of α_b for bending moments

$\alpha_{b,V}$ Particular case of α_b for shear force

α_c Adimentional parameter for comparing the internal forces on the columns

β Seismic coefficient

γ_C Specific weight of concrete

γ_{cl} Variable associated with the importance of the seismic elements (primary or secondary)

γ_G Partial factor for permanent actions

γ_I Importance factor

γ_P Partial factor for actions associated with prestressing

γ_Q	Partial factor for variable actions
γ_C	Specific weight of steel
ε^*	Normalised strain in the steel model proposed by Menegotto and Pinto [28]
ε	Strain in the steel model proposed by Menegotto and Pinto [28]
ε_0	Variable of the steel model proposed by Menegotto and Pinto [28]
ε_c	Compressive concrete strain
ε_{c0}	Strain corresponding to f'_{c0}
ε_{cc}	Strain corresponding to f'_{cc}
ε_{cu}	Ultimate strain of confined concrete
ε_{max}	Variable of the steel model proposed by Filippou *et al.* [19]
ε_r	Variable of the steel model proposed by Menegotto and Pinto [28]
ε_r^n	Variable of the steel model proposed by Menegotto and Pinto [28]
ε_{sp}	Ultimate strain of unconfined concrete
$\varepsilon_{sy,d}$	Design value of the steel strain at yield
ε_t	Strain corresponding to f'_t
ε_y	Yielding strain
ε_y^n	Yielding strain in the steel model proposed by Menegotto and Pinto [28]
θ_{um}	Ultimate chord rotation capacity
ν	Normalized axial force
μ	Normalized bending moment
μ_ϕ	Curvature ductility factor
ξ	Viscous damping ratio (in percent)
ξ_p^n	Plastic excursion at semicycle *n* in the steel models proposed by Menegotto and Pinto [28]
ρ_{sx}	Ratio of transverse steel parallel to the direction x of the loading
σ^*	Normalised stress in the steel model proposed by Menegotto and Pinto [28]
σ	Stress in the steel model proposed by Menegotto and Pinto [28]
σ_0	Variable of the steel model proposed by Menegotto and Pinto [28]
σ_r	Variable of the steel model proposed by Menegotto and Pinto [28]
σ_y	Yielding stress
ψ_2	Factor defining representative values of variable actions for quasi-permanent values
ψ_E	Combination coefficient to be used when determining the effects of the design seismic action
ω	Mechanical ratio of steel reinforcement. Mechanical ratio of steel reinforcement of the tension zones. Circular frequency in equations (4.14).
ω'	Mechanical ratio of steel reinforcement of the compression zones
ω_{wd}	Mechanical volumetric ratio of confining reinforcement

List of Acronyms

DL – Dead Loads

FEM – Finite Element Method

FLC – Fundamental Load Combination

LL – Live Loads

LSNC – Limit State of Near Collapse

LSSD – Limit State of Significant Damage

ODL – Other Dead Loads

PS – Pre-Stress

QPLC – Quasi-Permanent Load Combination

RC – Reinforced Concrete

RSA – Response Spectrum Analysis

RV – Relative Value

SA – Seismic Action

SL – Seismic Loads

SLS – Serviceability Limit State

SLC – Seismic Load Combination

TB – Transfer Beam

ULS – Ultimate Limit State

Chapter 1

Introduction

Since ancient times men have sought for more imposing and memorable structures, and builders had to search for new and ingenious solutions to solve the tasks at hand. In modern days, architects seek that acknowledgement and it falls to the structural engineer the task of making the vision of the architect possible. One of these cases is the ever-growing increase in span in order to create larger volumes that allow for a better interpretation and experience of the space. Clear examples of the use of longer spans are the entrance hall of hotels, movie theatres, auditoriums, parking lots, etc. In some of these cases the larger span is mostly necessary in the lower levels, therefore, the usage of the same span typology in upper floors would be a waste of space with a large economic impact. One of the ways to conciliate these two requirements consists in the adoption of a transfer structure.

There are different types of transfer structures, some more global and others more local. One solution consists in the so-called transfer floors (which may be of four types: girder, truss, plate and box, being the first two the most common), whereas for more local situations, a single beam may suffice. It is important to notice that a transfer girder may be seen as an intermediate solution.

Given the fact that transfer floors are more common in high rise-buildings, in which the wind loading gains relevance to the seismic loading, in the present work only transfer beams are considered. Therefore, only one frame of the buildings under study is deemed to be irregular.

Other case in which discontinued columns may also be considered is in retrofitting and strengthening of structures. In this case, also with the purpose of increasing the span, an existing column is removed and the existing beams reinforced. These situations need additional care regarding the limitations of the existing building that affect the height of the transfer beam, the position of the pre-stress cable, among others. Another situation in which the study of discontinued columns applies, although in a different scope, is the study of progressive collapse resulting from the unpredicted failure of a column.

The two latter cases mentioned before are not considered in this work. It is basically assumed for the development work that the irregularity is defined in the architectural project from the very beginning.

1.1. Objectives

The objective of this dissertation resides in the determination if a structure in which a column is discontinued and supported in a beam (discontinued column) constitutes a problem to the desirable seismic behaviour and, if so, what are the situations in which that detrimental effect is more conditioning.
All the results presented were obtained using different numerical modelling programs based on the finite element method (FEM). In this work the aspects regarding the FEM computation are not addressed in detail, once it falls outside the predetermined scope. Nonetheless, the non-linear modelling aspects are sufficiently explained and with the necessary detail to understand the adopted solutions.
A parametric study is carried out to assess the effect of considering a discontinued column, regarding distinct structural layouts as well as the in-plan position of that irregularity. The number of situations taken into account is sufficient to allow for significant conclusions to be taken. The results are compared mostly in terms of internal forces at the floor level of the irregularity and displacements at the different floor levels of the structure.
The non-linear implications of the discontinued column, in the global and local behaviour of the structure, are studied in a tridimensional FEM model. The linear and non-linear response of the model without discontinued columns (regular model) and of the model with a discontinued column (irregular model), are compared in terms of structural displacements, total base shear, axial forces and chord rotations.
The main objective for this dissertation is to identify the most unfavourable layout, to ascertain whether the effect of this irregularity is local or global and identifying the most suitable ways to account for the irregularity at the design stage. This establishes a framework for future studies.

1.2. Organization of the Dissertation

This dissertation is divided into five chapters which include introduction and conclusions. It is duly noted that the used methodologies are defined in each chapter, in accordance with the needs for each of these, rather than being condensed in an independent chapter.
This first chapter presents the main objectives of the work as well as the overall organization and the content of each chapter.
In the second chapter, a review of the state of the art concerning this irregularity is presented in order to understand and interpret current analyses, methodologies, results and conclusions. That chapter also presents the definitions for some of the expressions used throughout the work; the study of situations in which the present irregularity led to structural collapse; and also the provisions contained in the Eurocodes regarding this irregularity, as well as other aspects important in the development of the work.
In the third chapter, a parametric study based on the linear elastic properties of the materials is presented considering a representative number of situations. As a whole, five case studies are considered in which the height, span and presence of shear walls is altered. For each of these cases nine positions for the discontinued column are considered apart from the corresponding regular model (without any irregularity). The situations are compared in terms of internal forces (for different combinations) and of displacements (for the seismic combination).

The fourth chapter presents a comparative study of tridimensional frame structures considering non-linear inelastic behaviour of the materials and geometrical non-linear behaviour. In that chapter only one irregular model and a regular model are considered due to the complexity of these type of analyses. Both structures were studied under static and dynamic time-history loading, leading to the comparison of the global behaviour (displacements, base shear and collapse mechanism) and local behaviour (chord rotation and accumulation of inelasticity).

Finally, in the fifth chapter conclusions are drawn about the results obtained. Synthesising this way, the main aspects of this work, as well as set the basis for future studies.

Chapter 2

Literature Review

Irregularities in which the continuity of the structural system that transfers the horizontal loads to the foundations is interrupted or disturbed are nowadays currently used but lack, in some cases, adequate study. As stated by Fardis [17] regarding these irregularities:

> *"The current State-of-the-Art is not sufficiently advanced to describe with much confidence the behaviour under cyclic loading of regions of discontinuity…"*

This statement is in line with a reduced number of research studies on these issues, of which the irregularity studied in this work is part.

In the present chapter the results obtained in previous research studies are presented, as well as, the applicable prescriptions in the European structural design framework (the Eurocodes). The results considered regard, not only vertically discontinued columns, but also other types of irregularities. The present chapter also addresses cases of previous earthquake occurrences in which the existence of this irregularity led to severe damage and sometimes collapse.

This chapter intends to set the bases for the following studies as well as a form of compiling the results already presented by various authors. By carefully analysing the results is possible to avoid repeating studies similar to the already made extending the knowledge on this subject.

2.1. Definitions

Some definitions for the expressions used along this work are presented in the following.

Discontinued column – also referred to as “floating” column or “cut-off” column is a vertical element that, due to architectural needs, is discontinued at a certain level and rested on a beam with special characteristics (transfer beam) that is supported in several columns. The beam is responsible for transferring the vertical load to the other vertical elements below it.

“Hanging” column – is a vertical element that is discontinued at a certain level and rested on a cantilever. The major difference to a “floating” column is the static resisting mechanism where the column is rested, being, in this case, a cantilever instead of a beam.

Transfer beam – is one among other ways to transfer vertical loads from one or more elements to adjacent vertical elements. This beam should present special geometry and detailing in order to accommodate the high levels of internal forces associated with the load transfer of the rested column.

Regular beam – is used in this work to refer to beams that are not the transfer beam, having therefore no additional care apart from what is commonly taken.

In Figure 2.1 is presented a scheme of the previously defined expressions.

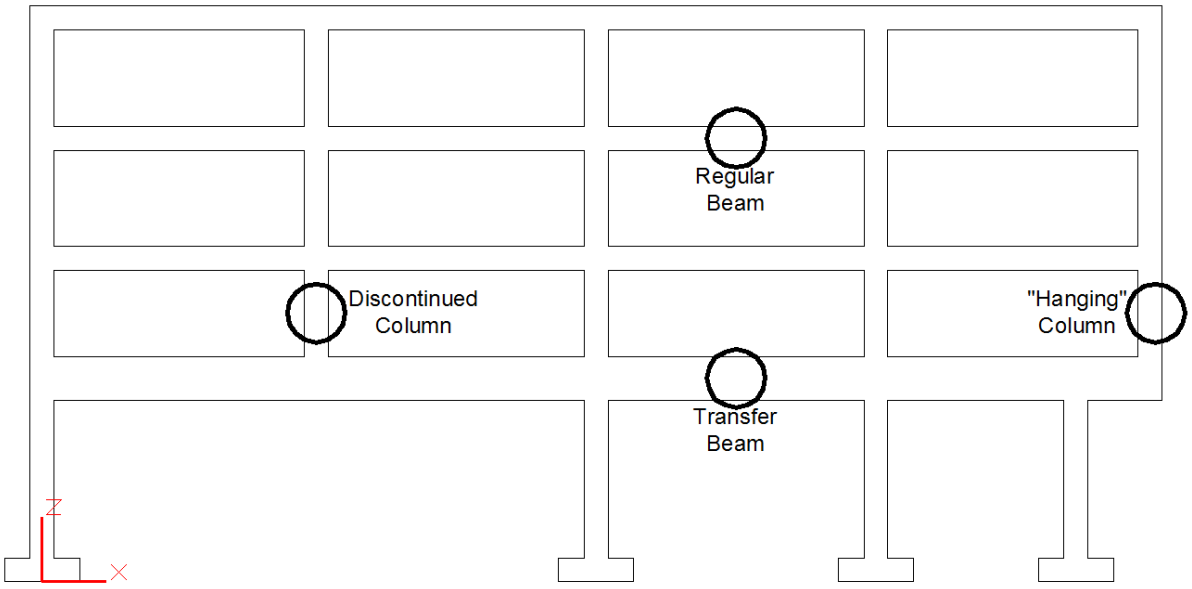

Figure 2.1 – Scheme representing the defined expressions

2.2. Research Review

The most significant results obtained regarding the studies developed by other authors are presented here. Only the most significant will be addressed in detail being the remaining just mentioned.

In the work of Poonam *et al*. [34] various types of structural irregularities are studied and their effect on horizontal displacement, storey drift and storey shear compared. Apart from the regular model, five other situations are considered by altering the regular model. Among the irregularities considered are: the case of the discontinued column; the suppression of the slab of the first two floors (creating a case of soft-storey); a heavier load on the top floor and others.

Based on their results, the irregularity that leads to the higher horizontal displacement and storey drift is the case where the discontinued columns are considered. Although the results are in accordance with what was expected, in the irregular cases the redesign of the elements (beams and columns) was not considered. This led to results that might not be completely consistent with common design practises.

If the irregular structures were to be redesigned, not only to resist to the seismic actions but also for reasons of serviceability under gravity loads, the results would expectedly lead to different conclusions, namely, lower displacements.

In the research of Singla and Rahman [42] the effect of discontinued columns is studied in three different 3D models: the first one is a regular model without any discontinued columns and two irregular models with the discontinued columns in the ground and first floor, respectively. For each of the irregular models three cases are considered which represent different positions (in the plan) for the discontinued columns. The compared parameter are the fundamental time period, the spectral acceleration, the base shear and the storey displacement.

The results obtained can be synthesized as follows: the irregular models have a fundamental period higher than that of the regular model, which indicates that the irregularity leads to a softer structure. This is possible to confirm with the results for all other parameters.

The main conclusion of this work is that “the effect on various parameters reflects the deficiencies, if floating columns are incorporated in a building without considering any measure for safer construction. The failure of storeys having floating columns can have a serious effect on progressive collapse of the building. Hence, floating columns should be avoided as far as possible in seismic regions and if they are unavoidable, then the structure should be strengthened by adopting some remedial features.” This conclusion is aligned with the expectations that simply considering a current building and removing a column without no further alterations on the structure leads to a severe error not only for the seismic actions but also for the gravity actions.

The study conducted by Harugoppa and Muranal [23] compares the effect of discontinued columns in the internal forces of the beams (M and V). It also compares the effect of the consideration of the infill.

The results obtained lead to the conclusion that the consideration of this irregularity has a negative effect on the beams. These results are important but the comparison between the regular and the irregular models might not be entirely correct. The fact that in the irregular models the static system is different (longer spans and the presence of cantilevers) leads directly to higher internal forces. For a proper comparison to be made other parameters should be considered.

Apart from the mentioned, the main conclusions that are possible to draw from the results presented in this study are that the consideration of the studied irregularity leads to an increase in span and therefore the need for sections with different dimensions. The author also alerts that the shear force in the cantilevers is 6 times higher in the irregular model and that this should be taken in consideration in order to avoid shear failure, generally considered to be brittle.

In the article of Mundada and Sawdatkar [30] the bending moments and shear force in columns of three 3D building models are compared. One model is regular while the other two have discontinued columns wherein one of the models struts are considered beneath the discontinued columns. The results are attained by using an equivalent static method.

The results of this study show that the case where the columns are removed leads to a higher probability of failure. Although, by considering the presence of struts beneath the discontinued columns the behaviour of the structure is substantially improved, reducing the probability of failure. The struts balance the moments conferring more stability to the structure.

After the conclusions the authors indicate some possibilities for future studies. Among them, analysing the structures with a pushover analysis in order to determine whether the plastic hinges are forming in the discontinued column and testing this irregularity in a shake table with a real model.

In Sabari and Praveen [37] a comparison of the effect of the geometry of the columns is made. Although only two 2D models of four floors (a regular and an irregular) were considered, for each of them 5 cases of column geometry were considered. The conclusions presented were quite trivial and somehow expected: for a stiffer structure the displacements and storey drift are lower. Apart from this not much was concluded.

Even so, the results presented suggests that by increasing the size of the columns in the level below the irregularity leads to a significant variation in stiffness. Although, keeping increasing the size of columns on upper floors leads to a lower variation in the overall stiffness of the structure. This indicates that the best way to enhance the behaviour of a structure with this irregularity is to alter the size of elements below the irregularity.

In the work of Nanabala *et al.* [32] a very consistent study of the effect of discontinued columns is done. The authors consider 3 different 3D models: the first is a regular 6 floor building with a plan of five spans (5m long) in each direction; the second model is similar to the first although all the peripheral columns are discontinued below the first floor; the third model is based on the second model but the cross-section of the beams and columns are different. The study is made first by an equivalent static method and then the results are compared with the results attained by a linear time-history analysis.

The models are compared based on their displacement due to lateral loads, lateral stiffness and quantity of steel rebars.

The results obtained in this work are in accordance with what was expected. The consideration of the irregularity increases the displacement of the structure but by considering different cross-sections the displacements reduce significantly, being lower than in the regular model as can be seen in Figure 2.2. In both figures Model 1 regards the regular model, Model 2 the irregular with normal cross-sections and Model 3 the irregular with larger cross-sections.

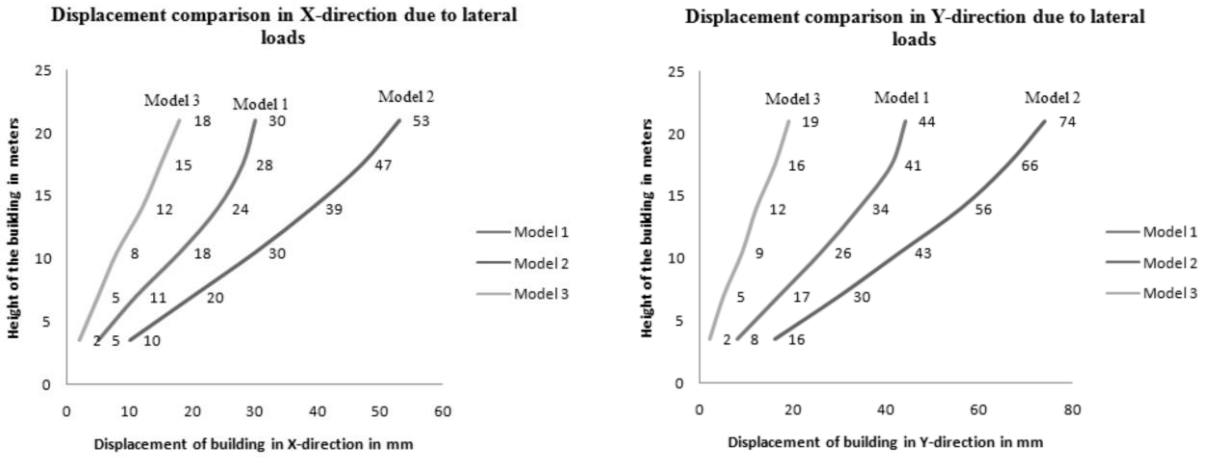

Figure 2.2 – Displacement for three models due to lateral loads for the x direction (left) and y direction (right) [32]

The irregularity considered leads to a structure with serious problems of soft-storey. This does not occur in the regular model. The results indicate also that by considering the mentioned irregularity, there is an increase of approximately 40% in the quantity of both concrete and rebars, which is to be expected.

When the results of the time-history are compared with the ones of the equivalent static method it is possible to conclude that the horizontal displacements of the regular model and of the irregular model with larger cross-sections are approximate, although the irregular model has slightly higher displacements at the top.

Rohilla *et al.* [36] thoroughly studied various possible positions for the irregularity in different types of structures. In the first part of this work four different models are compared, there are two different heights (6 and 8 floors) and for each of them, 2 types of building are considered. For each of these models different positions for the discontinued column are modelled and all of the mentioned cases are studied for two different seismic zones. On the second part the effect of the variation in the size of both columns and beams is studied considering the highest building (with 8 floors), the most unfavourable position of the discontinued column and the seismic zone that leads to the highest displacements.

Some of the main conclusions presented by the authors are the following: “ii) Storey displacement and storey drift increases due to presence of floating column; iii) Storey displacement increases with increase in load on floating column; iv) Storey shear decreases in presence of floating column because of reduction mass of column in structure; v) Increase in size of beams and columns improve the performance of building with floating column by reducing the values of storey displacement and storey drift; vi) Increasing dimensions of beams and columns of only one floor does not decreases storey displacement and storey drift in upper floors so dimensions should be increased in two consecutive floors for better performance of building.”

In the work of Nautiyal *et al.* [33] the effect of “floating” columns under seismic action is studied and a magnification factor (factor that compares the regular and irregular models) is determined. For this work two 2D frame models were considered, one of four floors and other of six floors. For each model various positions for the discontinued column were considered.

The authors used a linear dynamic response spectrum analysis for two different types of soil in order to determine, for each model, the base shear and bending moment on the columns along the height.

The most relevant conclusions are that, regarding base shear, the irregular models, are more favourable than the regular ones, for being more flexible. The bending moments in columns and beams is more variable, with some cases in which the irregular models are more conditioning and others in which the contrary is observed. In the case of the beams this is justified by the increase in span although for the columns the reason is not so implicit. A possible explanation is that the reduction in base shear does not compensate for the removal of one of the columns.
Although not addressed in detail, the methodologies and results presented by other authors were considered in the development of this dissertation, namely, the studies carried out by Bhensdadia and Shah [4], Shah and Patodi [41] and Dubal *et al.* [10] were of importance for the understanding of aspects regarding discontinued columns.

Based on all that was presented the main conclusions that are taken from previous studies are the following:

- The presence of discontinued column reduces the stiffness of a structure if no other alteration is considered;
- The studied irregularity is one of the vertical structural irregularities that leads to more problems if not properly taken in consideration in the design phase;
- When a discontinued column is included in a building, a clear load path must be defined, adopting transfer structures for the effect;
- In order for the building to be stable under both seismic and gravity loads the beams that support columns and columns that are below the irregularity should have larger cross-sections than in regular buildings;
- The consideration of discontinued columns leads to larger amounts of structural materials.

2.2.1. Other Consulted Documents

In addition to the works mentioned above there are other, of a more general nature, which were used in the development of this work. Among them stands out the book "*Sismos e Edifícios*" [24], regarding the general seismic behaviour of structures and the study of vertical irregularities developed by Arlekar *et al.* [3] and Chintanapakdee and Chopra [6]. Also, most of the concrete design related aspects, as predesign criteria, reinforcement detailing among others, were based on the book "*Estruturas de Betão*" [2]

2.3. Structural Response During Previous Earthquakes

The 2001 Bhuj earthquake in India was, among recent recorded events, the one that had more situations of collapse due to the existence of this irregularity. The Mw 7.7 earthquake that struck the region was the most damaging of their last 50 years, in part due to: the type of construction, non-ductile detailing, stiffness discontinuity (or soft-storey), torsion, materials quality and discontinuity on the vertical load path.

In India was common at the time the use (sometimes excessively) of this type of irregularity (not only "floating" columns but also "hanging columns") in order to bypass the floor surface index imposed by the local municipal corporation. This problematic is well addressed and explained by Murty *et al.* [31].

According to Agarwal *et al.* [1], among the causes of collapse during this earthquake, this was the second most notable. He also indicates that during the earthquake a clear load path for the horizontal loading was not available, leading to the development of overturning forces that overstress the columns at the ground floor, which caused significant deformations and buckling in the columns, resulting in total collapse. The main reasons for the collapse were: the strength of the columns at the ground level (which was deficient), the cantilever where the columns were rested on and the inadequate detailing of the ductile connection beam-column.

Figure 2.3 illustrates two situations of collapse due to this irregularity.

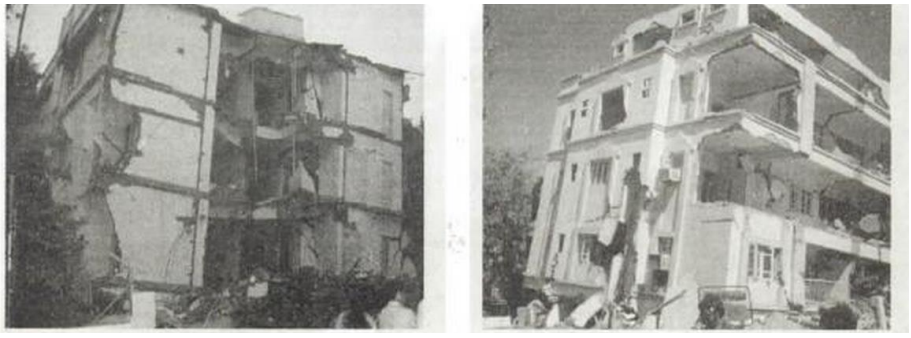

Figure 2.3 – Failure of reinforced concrete buildings with "hanging" columns [1]

Also, according to Murty *et al.* [31] some structures, besides having "hanging" columns, also had open ground storey and random masonry infill which led to irregularities in strength and stiffness. The paper under study also states that even in buildings that did not collapse the discontinued columns led to significant damage.

Other authors ([21] and [22]) also concluded that the presence of this kind of irregularity was one of the major causes for collapse during this earthquake. They also indicated that the structures were mainly designed for gravity loads and there was the possibility that in some cases the seismic actions were not considered in the design in the proper way, leading to widespread damage and promoting global collapses.

According to the EERI [11], in the city of Ahmedabad, at the level of the first floor, the cantilevers in which columns were supported were built with about 1.5m. In most cases, after the earthquake the cantilevers shown diagonal cracking due to shear.

Although of a different nature, the collapse of the Alfred P. Murrah Federal Building in Oklahoma City due to a bombing that destroyed one of the columns that supported the transfer beam is also relevant for the present study. The collapse of this column led to the failure, by shear, of two other and subsequently the collapse of close to 50% of the floor area.

The study carried out by Corley [8] addresses the possibility of applying earthquake resistant detailing to reduce the losses caused by this kind of actions. It is mentioned that adopting special moment frames, which are detailed based on principles similar to the capacity design (shear strength to resist maximum probable moments, confinement at zones where plastic hinges might occur and continuity of the reinforcement), might improve the capacity to dissipate energy in situations of extreme loading such as earthquakes and, in this case, blasts.

It is possible to conclude from this work that the consideration of a discontinued column solution, induces situations where some elements become more important for the resistance of the building, of which transfer beams are an example. These elements have almost no structural redundancy which, in case of failure, may lead to total collapse.

Situations of progressive collapse are not directly addressed in the present dissertation, although some of the conclusions taken may apply to such cases.

2.4. Normative Prescriptions

The present work is based on the normative prescriptions of the Eurocodes. Regarding the combination of actions, it is based on the EN1990 [12] and the load combinations considered are the following:

- Quasi-Permanent Load Combination (QPLC)

$$S_{QPLC} = DL + \psi_2 \cdot LL + PS$$

- Fundamental Load Combination (FLC)

$$S_{FLC} = \gamma_G \cdot DL + \gamma_Q \cdot LL + \gamma_P \cdot PS$$

- Seismic Load Combination (SLC)

$$S_{SLC} = DL + \psi_E \cdot LL + PS \pm SA$$

The gravity loads considered previously are defined according with the EN1991-1-1 [13] and the design and detailing of the steel reinforcement, as well as other aspects related with the behaviour of the concrete, follow the EN1992-1-1 [14].

For the definition of the seismic loads the EN1998-1 [15] was used and complemented with the clarifications presented by Fardis *et al.* [18]. Also, regarding the detailing of the horizontal loading resisting system, the EN1998-1 [15] superseded the EN1992-1-1 [14]. The EN1998-3 [16] was also considered in this dissertation for the definition of the limit state of near collapse.

In paragraph 5.4.1.2.5 the EN1998-1 [15] indicates a set of specific rules for beams supporting discontinued vertical elements, which are:

- There shall be no eccentricity of the column axis with respect to that of the beam;
- The beam shall be supported by at least two direct supports, such as walls or columns.

Apart from this, the only implications of considering such irregularity according to the EN1998-1 [15] are the following:

- The structure is considered irregular in elevation given that the condition 4.2.3.3. (2), that states that all lateral load-resisting systems shall run without interruption from their foundations to the top of the building, is not met. This implies a reduction in 20% on the behaviour factor of the structure.
- According to 4.3.3.5.2 the vertical component of the seismic action, for a_{vg} greater than 0.25g, should be considered, given that the structures include beams supporting columns.

Regarding the time-history representation used for this work, the EN1998-1 [15] refers, in paragraph 3.2.3.1, the following:

- When using a spatial model, the seismic motion shall consider accelerograms acting in the three directions simultaneously, given that the same accelerogram should not be considered for both horizontal directions.
- It is allowed to describe the seismic motion by using artificial accelerograms given that:

- The accelerogram shall be generated in order to match the elastic response spectrum;
- The duration shall be consistent with the magnitude and other features of the seismic event;
- The minimum duration of the stationary part of the accelerograms should be equal to 10s.
- Follow specific rules for the suite of accelerograms.

Chapter 3

Parametric Linear Elastic Analysis

In this chapter a parametric study was developed in order to determine the situations in which the considered irregularity leads to the most unfavourable situation.
The following parameters were considered:

- Height of the building (number of floors);
- Span between vertical elements;
- Presence of shear walls;
- Position of the discontinued columns.

Considering the first three parameters, five case studies were defined. For each case study, a structurally regular model, that has no discontinued columns, was established. This model is briefly compared with the **regular base model** and then used as reference to compare with the irregular ones. The **regular base model** is the regular model for the case used as reference to define the others.
Apart from the regular models, nine other models with one (or two) discontinued columns, at the ground level of each case study, are considered. In these models only the position of the irregularity and direction of the transfer beam (TB) is altered. The redesign of the cross-sections of the irregular frame, deemed to be necessary for endowing the structure with a suitable behaviour, is also considered in this study.
As concluded from the literature review some of the examples of situations considered when studying this type of irregularity are “hanging” columns and not only “floating” columns. As mentioned before, “hanging” columns are discontinued columns in peripheral alignments that are supported by cantilevers rather than a multi-supported beam. In the present work this irregularity is not considered.
In order to allow for simpler models and for better comparison between them, some simplifications and approximations were considered, which are explained throughout the chapter.

3.1. Methodologies

3.1.1. Definition of the Case Studies

i.Floor Plan

The floor plan of the case study building is defined by a grid of 4 by 3 spans in the ***x*** and ***y*** directions respectively (Figure 3.1).

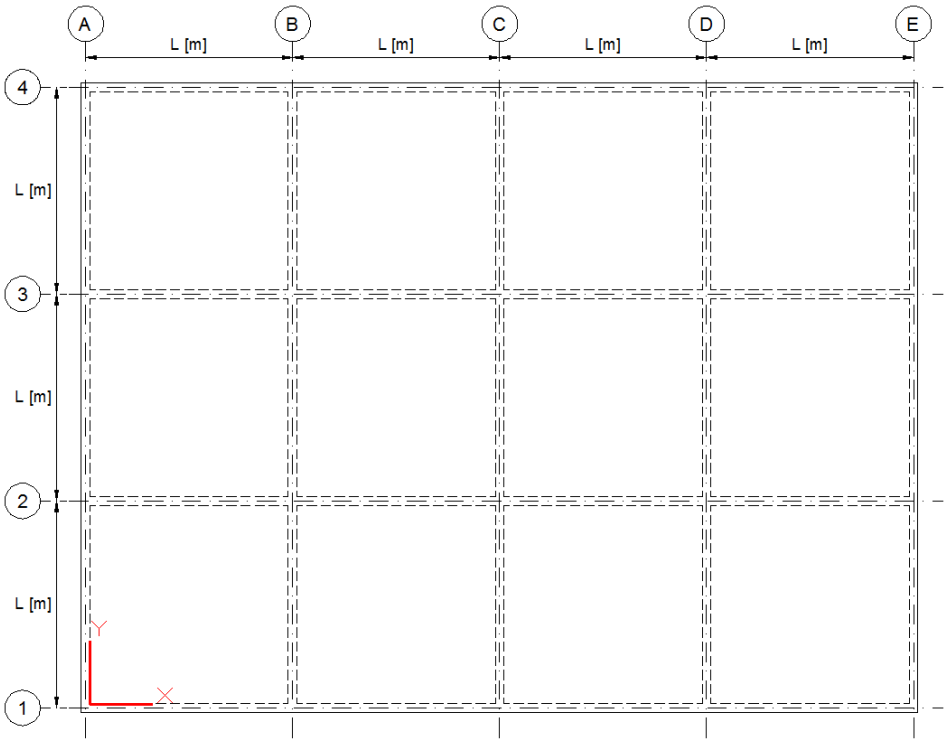

Figure 3.1 – Definition of the structural plan grid and axes

As mentioned before, the considered parameters pertaining to the floor plan layout are the span between columns (L) and the presence (or absence) of shear walls.

Regarding the span, two situations were considered: one with a larger span of 7 meters (plan A) and another with a shorter span of 4 meters (plan C).

The first case corresponds to a more recent type of building, trying to meet the growing demands for larger spans brought by updated architectural constraints and trends. This span length is quite normal in cases where discontinued columns are used.

The second case corresponds to a current building situation, with normal/shorter spans.

The case study with shear walls corresponds to floor plan B, a derivation of floor plan A. The shear walls could eventually be placed at different positions, however the only situation taken into consideration is the one illustrated in Figure 3.2. The reason for this choice is to try keeping the models as simple as possible and to minimize the torsional effects on the building.

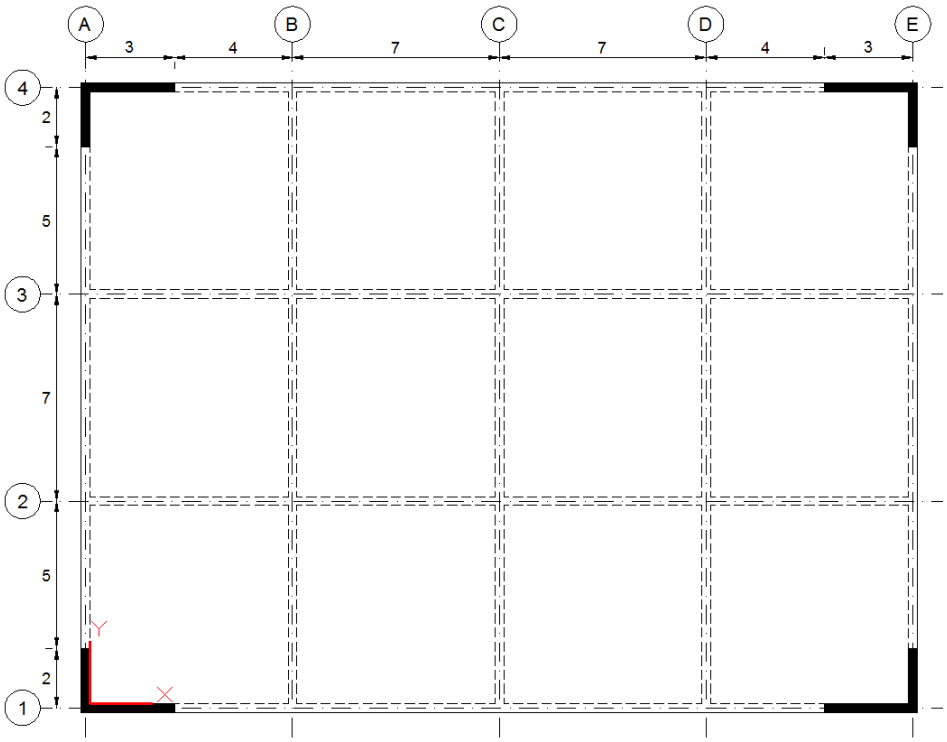

Figure 3.2 – Position and dimensions [m] of the shear walls

ii.Elevation

The elevation of the building is defined by the number ***n*** of floors with a regular height of 3.0m. Again, the option for this height between floors is related to the current architectural constraints. The considered situations are presented in Table 3.1.

Table 3.1 – Elevations considered

Elevation	*n*
I	6 floors
II	2 floors
III	10 floors

By using these values of ***n,*** provision was made to cover the current heights of buildings.

iii.Case Study Models

The **regular base model** corresponds to the combination of floor plan **A** and elevation **I**. This was the starting point for the other models. For example, when studying any other of the plans (**B** or **C**) the elevation was always elevation **I**. On the other hand, when studying one of the elevations, other than **I** (**II** or **III**), the plan was always plan **A**. By using this method, the number of models becomes manageable and the loss of significance in the results and conclusions should be minimized. Table 3.2 presents the definition of all the cases considered in this parametric study.

Table 3.2 – Definition of the adopted cases

Case	Span (L)	Shear Walls	*n* floors
A.I	7 m	No	6
B.I	7 m	Yes	6
C.I	4 m	No	6
A.II	7 m	No	2
A.III	7 m	No	10

iv.Position of Discontinued Columns

For each model the position of the discontinued columns varies and the direction of the transfer beam also varies accordingly. The main constraints (rules) considered in the choice of the discontinued column were:

- There cannot be two consecutive discontinued columns;
- If a peripheral column is eliminated, the transfer beam must be positioned along the same peripheral alignment, avoiding the situation of “hanging” column;
- Situations symmetrical to the ones following were not considered.

Based on these principles, the possible combinations of discontinued columns were those presented in Table 3.3. The situation reference was of the type **A.B** being **A** the direction of the transfer beam and **B** the grid coordinates of the discontinued column according with Figure 3.1**.**

Table 3.3 – Definition of the adopted irregular situation

Situation Reference	Direction of the transfer beam	Alignment of the transfer beam	Discontinued Column
R	Base model with no discontinued columns		
X-b1	X	1	B1
X-c1	X	1	C1
X-bd1	X	1	B1+D1
X-b2	X	2	B2
X-c2	X	2	C2
X-bd2	X	2	B2+D2
Y-a2	Y	A	A2
Y-b2	Y	B	B2
Y-c2	Y	C	C2

The identification of the irregular models combines the identification of the reference model (without discontinued columns) with the position of the discontinued columns (irregular situation). For example, **M_A.II_X-c1** refers to the irregular model with plan A and elevation II where the discontinued column is C1 and the transfer beam oriented in the x direction.

3.1.2. Definition of the Analysis Parameters

The analysis and comparison of the internal forces in the models was performed through the definition of the adimensional parameters $\boldsymbol{\alpha_b}$ and $\boldsymbol{\alpha_c}$, respectively for the beam and column structural elements.
The parameter $\boldsymbol{\alpha_b}$, used to compare both the bending moments and shear forces in the beams, is defined in expression (3.1).

$$\alpha_b = \frac{E_{SLC}}{E_{FLC}} \tag{3.1}$$

Where $\boldsymbol{E_{SLC}}$ is the maximum value per alignment of a given internal force for the seismic load combination and $\boldsymbol{E_{FLC}}$ is the maximum value of a given internal force for the fundamental load combination per alignment. This parameter provides information if, in a given alignment and in terms of maxima, the seismic load combination is more or less relevant than the gravity load combination.
The fact that the columns are subjected to the interaction effects of the axial force and bending moments led to the definition of parameter $\boldsymbol{\alpha_c}$. That parameter is used to compare the level of the internal forces in the columns and is defined in expression (3.2).

$$\alpha_c = \frac{U_{SLC}}{U_{FLC}} = \frac{\left(\sqrt{\nu^2 + \mu_x^2 + \mu_y^2}\right)_{SLC}}{\left(\sqrt{\nu^2 + \mu_x^2 + \mu_y^2}\right)_{FLC}} \tag{3.2}$$

Where $\boldsymbol{\nu}$ is the normalized axial force, $\boldsymbol{\mu_x}$ and $\boldsymbol{\mu_y}$ are the normalized bending moment in the $\boldsymbol{x}$ and $\boldsymbol{y}$ direction, respectively. Also, $\boldsymbol{U_{SLC}}$ refers the maximum value of $\sqrt{\nu^2 + \mu_x^2 + \mu_y^2}$ for a given alignment for the seismic load combination and $\boldsymbol{U_{FLC}}$ the maximum value of $\sqrt{\nu^2 + \mu_x^2 + \mu_y^2}$ for a given alignment for the fundamental load combination. Similarly to the parameter $\boldsymbol{\alpha_b}$, the parameter $\boldsymbol{\alpha_c}$ gives information if, for a certain alignment, the seismic action effects in the columns is more or less relevant than those due to the gravity loads.
For both parameters if the value is larger than one the seismic load combination is more relevant than the gravity load combination.
Apart from the defined parameters that compare the internal forces between the models, the displacements at each floor level were also compared.

3.1.3. Definition of the Structural Elements

The definition of the beams and columns cross-sections as well as the thickness of the floor slabs were performed adopting pre-design criteria that normally ensure a good behaviour both for Ultimate Limit and Serviceability Limit States.
More important than assuring a careful and detailed design of the structure (cross-sections), the focus was on keeping it simple, in order to make it easy to adapt the **regular base model** to conform with the needs of each specific model. It is important to stress that no additional verifications were made in order to confirm the adequacy of the cross-section dimensions, hence no reinforcement was determined nor ductility or security checks were made.

i.Materials

The materials chosen and used throughout the work were a concrete C30/37, a steel reinforcement A500 NR and a pre-stress steel A1860/1670 with the characteristics presented in Table 3.4.

Table 3.4 – Properties of the materials

Concrete C30/37	f_{ck} [MPa]	30.0
	f_{cd} [MPa]	20.0
	f_{ctm} [MPa]	2.9
	$E_{c,28}$ [GPa]	33.0
Ordinary Steel Reinforcement A500 NR	f_{yk} [MPa]	500.0
	f_{yd} [MPa]	435.0
	E_S [GPa]	200.0
Pre-stress Steel Reinforcement A1860/1670	f_{pk} [MPa]	1860.0
	$f_{p0.1k}$ [MPa]	1670.0
	E_P [GPa]	195.0 $\pm$ 5

ii.Beams

For a beam span **L** and a height **h** the adopted pre-design criterion was:

$$L/h = 10\ to\ 12$$

The considered cross-sections are presented in Table 3.5. The element reference is of the type **Vn_AxB** being **A** the height and **B** the width of the cross-section.

Table 3.5 – Geometry of the beams cross-section

Element Reference	Span (L) [m]	Height (h) [m]	Width (b) [m]
V1_0.6x0.3	7.00	0.60	0.30
V2_1.6x0.6	14.00	1.60	0.60
V3_1.4x0.5	14.00	1.40	0.50
V4_1.3x0.5	14.00	1.30	0.50
V5_1.1x0.4	14.00	1.10	0.40
V6_1.8x0.6	14.00	1.80	0.60
V7_1.6x0.5	14.00	1.60	0.50
V8_0.4x0.3	4.00	0.40	0.30
V9_1.0x0.4	8.00	1.00	0.40
V10_0.8x0.4	8.00	0.80	0.40

It should be noted that the pre-stressed beams do not follow the mentioned criteria. The reason for this is related to the high stresses originated by the discharge (reaction) of the discontinued column, for these beams lower values of slenderness (L/h) were considered. A remark should be made to the fact that the dimensions presented were considered exclusively from an academic point of view and, in some cases, might not be practicable.

iii.Columns

The pre-design criterion was based on the normalized axial force ($\boldsymbol{\nu}$) of each column in the fundamental load combination:

$$\nu_{FLC} \approx 0.6$$

This condition normally ensures a ductile behaviour under seismic loads (with values of ν between 0.3 and 0.4).

In order to limit the diversity in columns the following criteria were adopted:

- Preferentially all columns should have a squared cross-section with sides of $[h \times b]$. Although exceptions can be made to verify the secondary criterion.
- The dimension of the beam width should be equal to or lower than the perpendicular side of the column supporting it.

The considered cross-sections are presented in Table 3.6. The element reference is of the type **Pn_A** if $h = b$ or **Pn_AxB** if $h \neq b$ being **A** and **B** the largest and smallest dimension of the cross-section, respectively.

Table 3.6 – Geometry of the columns cross-section

Element Reference	h $[m]$	b $[m]$	A_c $[m^2]$
P1_0.3	0.30	0.30	0.09
P2_0.4	0.40	0.40	0.16
P3_0.5	0.50	0.50	0.25
P4_0.6	0.60	0.60	0.36
P5_0.7	0.70	0.70	0.49
P6_0.8	0.80	0.80	0.64
P7_0.9	0.90	0.90	0.81
P8_1.0	1.00	1.00	1.00
P9_1.1	1.10	1.10	1.21
P10_1.2	1.20	1.20	1.44
P11_0.5x0.6	0.50	0.60	0.30
P12_0.3x0.4	0.30	0.40	0.12
P13_0.3x0.5	0.30	0.50	0.15
P14_0.4x0.5	0.40	0.50	0.20

iv.Slab

The adopted pre-design criteria for a two-way slab with a span ***L*** and a thickness ***e*** was:

$$L/e = 35 \; to \; 40$$

Given the fact that there are only two different spans, the adopted thickness for the slab is presented in Table 3.7. The element reference is of the type **Sn_A** being A the thickness of the slab.

Table 3.7 – Thickness of the slabs

Element Reference	Span (L) [m]	Thickness (e) [m]
S1_0.20	7	0.20
S2_0.15	4	0.15

v.Pre-Stress Tendon

For this parametric analysis, given the large number of considered cases and that the determined values will be compared to each other, the effect of the pre-stress will not be taken in consideration. This simplifying assumption is made with full knowledge that this is an approximation and that some factors may not be taken in consideration.

It is also important to refer that the design of the pre-stress is very variable depending not only on the adopted criteria but also in its layout. By not considering the effect of the pre-stress the effort put in the definition of the models is drastically reduced.

On the subsequent part of this study (non-linear analysis) the effect of the pre-stress is duly considered.

vi.Model Assignments

Given the amount of models considered for this study it is difficult to describe them deeply. Therefore, they are generally described here regarding details that affect each case study and doesn't vary to the irregular models as is the case of the slabs and regular beams.

Table 3.8 presents the slabs and regular beams assigned to each of the case studies and in the Annex A is possible to visualize the differences between the regular and irregular models with detail.

Table 3.8 – Assigned sections for each study case

	M_A.I	M_A.II	M_A.III	M_B.I	M_C.I
Slab	S1_0.20	S1_0.20	S1_0.20	S1_0.20	S2_0.15
Regular beams	V1_0.60	V1_0.60	V1_0.60	V1_0.60	V8_0.40

3.1.4. Definition of the Load Patterns

The definition of the loads was based on the EN1991 [13] and the EN1998-1 [15] for the gravity and seismic loads, respectively.

i.Dead Loads

a) Structural Self-Weight

For the self-weight of the structure (being of structural concrete) the following specific weight was considered:

$$\gamma_c = 25\ kN/m^3$$

b) Other Dead Loads

The adopted value for the uniformly distributed area load that is used to account for the weight of partition walls, floor and ceiling cover is:

$$\text{ODL} = 3\ kN/m^2$$

ii.Live Loads

Based on EN1991 [13] and for a Category A, buildings with habitational usage, the value for the live load in all floors is:

$$\text{LL} = 2\ kN/m^2$$

iii.Seismic Loads

In this chapter the seismic action is taken into consideration by an analysis by response spectrum defined in accord with the EN1998-1 [15].

Considering a building with a importance class II ($\gamma_I = 1.0$), located in Lisbon (zones 1.3 and 2.3, respectively for the distant and close earthquake scenarios) and a soil type B, the design response spectrum, present in Figure 3.3, may be generated for seismic action type 1 and 2 (again, distant and close earthquake scenarios in mainland Portugal). Based on the Portuguese National Annex, a reduction in the soil factor depending in the values of a_g was considered. The behaviour factor (q) considered were of $q = 3.0$ for the regular models and of $q = 2.4$ for the irregular models. In Table 3.9 are presented the values considered for the definition of the response spectrum.

Table 3.9 – Values considered for the definition of the response spectrum

Seismic action	Type 1	Type 2
a_g $[m/s^2]$	1.50	1.70
S_{max} [-]	1.35	1.35
S [-]	1.29	1.27
T_B [s]	0.10	0.10
T_C [s]	0.60	0.25
T_D [s]	2.00	2.00
q [-]	3.0 (2.4)	3.0 (2.4)

According to the paragraph 4.3.3.5.2 of the EN1998-1 [15], a vertical component of the seismic action should be considered for the case where beams support columns which happens in all irregular cases. For the definition of the vertical response spectrum the following is considered, $S = 1.0$, $q = 1.5$, for seismic action type 1 $a_{vg}/a_g = 0.75$; $T_B = 0.05s$; $T_C = 0.25s$; $T_D = 1.0s$ and for seismic action type 2 $a_{vg}/a_g = 0.95$; $T_B = 0.05s$; $T_C = 0.15s$; $T_D = 1.0s$.

Figure 3.3 and Figure 3.4 present the horizontal and vertical design response spectrum for ξ=5%, respectively. Both charts were drawn considering a unitary behaviour factor, whereas in the parametric analysis the design spectra were considered (grossly dividing the elastic spectra by the corresponding behaviour factor).

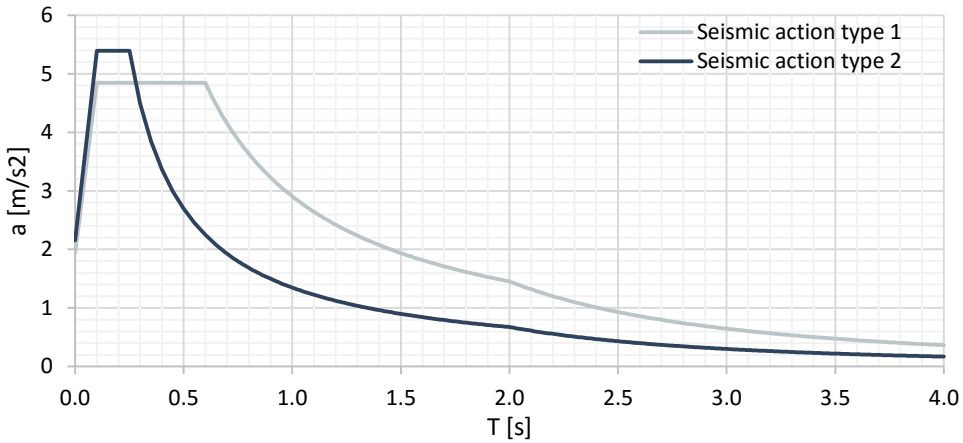

Figure 3.3 – Design response spectrum for the horizontal component of the seismic action for $q = 1.0$

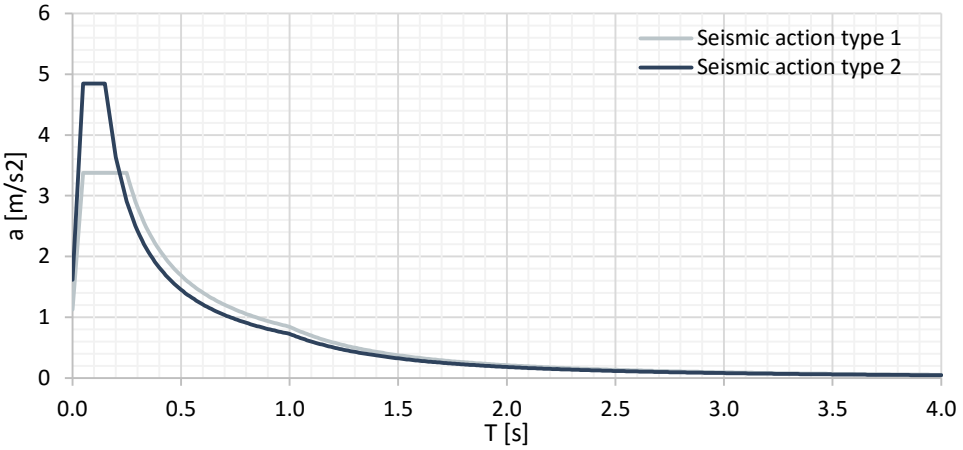

Figure 3.4 – Design response spectrum for the vertical component of the seismic action for $q = 1.0$

3.2. Presentation and Discussion of Results

3.2.1. Initial Analysis

In this section of the subchapter, the models **M_A.I** (**R**, **X-b1** and **X-c1**) are compared in order to determine the most relevant aspects to take into consideration on the study.

As obtained from the analytical models (SAP2000 [38]) the frequency (f) of the most relevant vibration mode for the different structures is indicated in Table 3.10, where the type relates to the predominant movement of the vibration mode (in the x direction, in the y direction or torsional).

Table 3.10 – Frequency of main vibration mode shapes

		1st Mode	2nd Mode	3rd Mode	4th Mode	5th Mode
M_A.I_R	f [Hz]	0.8540	0.8618	0.9471	2.4672	2.4835
	Type	Y	X	T	Y	X
M_A.I_X-b1	f [Hz]	0.8519	0.8771	0.9685	2.4688	2.5243
	Type	Y	X	T	Y	X
M_A.I_ X-c1	f [Hz]	0.8519	0.8769	0.9713	2.4681	2.5243
	Type	Y	X	T	Y	X

It is possible to conclude from the analysis of the values that there are no major variations in the irregular models in terms of frequency of vibration. Although, the following is possible to be concluded: the existence of the irregularity leads to an increase in stiffness in the direction of the transfer beam but also a reduction in the perpendicular direction which, for the case, is negligible. It is also possible to conclude that the torsional stiffness is also higher in the irregular models.

These results indicate that the presence of the irregularity has no highly noticeable effects on the linear elastic dynamic properties of the structures as a whole.

i.<u>Gravity Loads</u>

To allow for a better understanding of the behaviour of the structure, the loads due to the gravity forces (dead and live loads) will be analysed separately from the seismic loads.

Figure 3.5 to Figure 3.7 illustrate the bending moment diagrams in the beams X1 (transfer beam), YB and YC of the building. The values indicated correspond to the quasi-permanent load combination for the beams of the first floor. For the remaining beams there were no variations worth mentioning between the three models regarding the bending moment diagrams, although those diagrams are presented in Annex B.

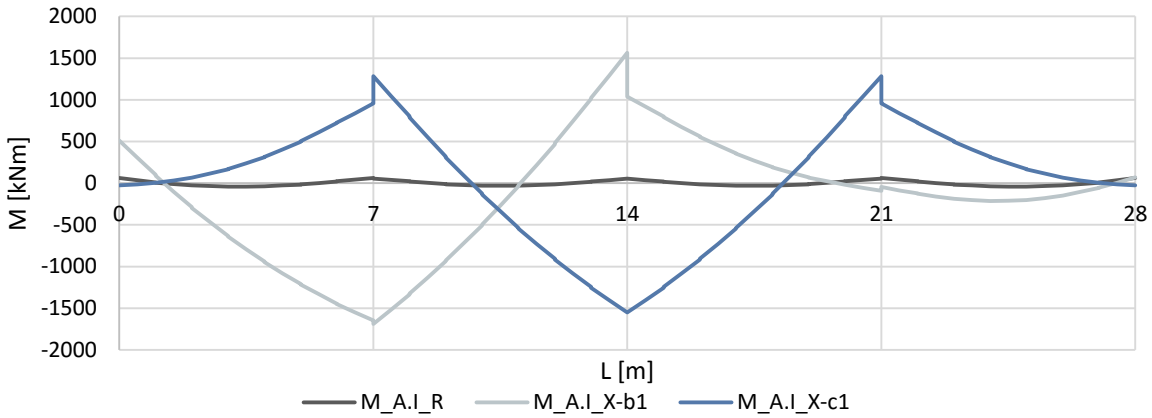

Figure 3.5 – Bending moments for the Quasi-Permanent Load Combination on beam X1

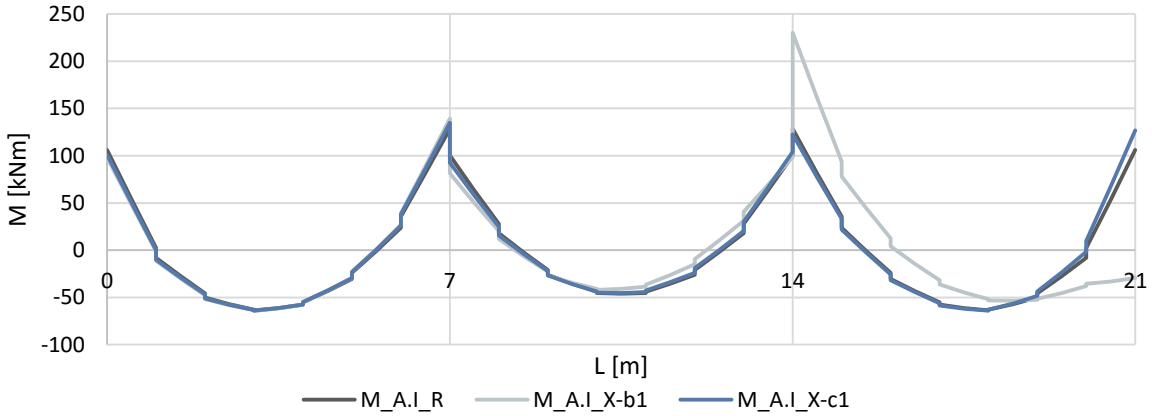

Figure 3.6 – Bending moments for the Quasi-Permanent Load Combination on beam YB

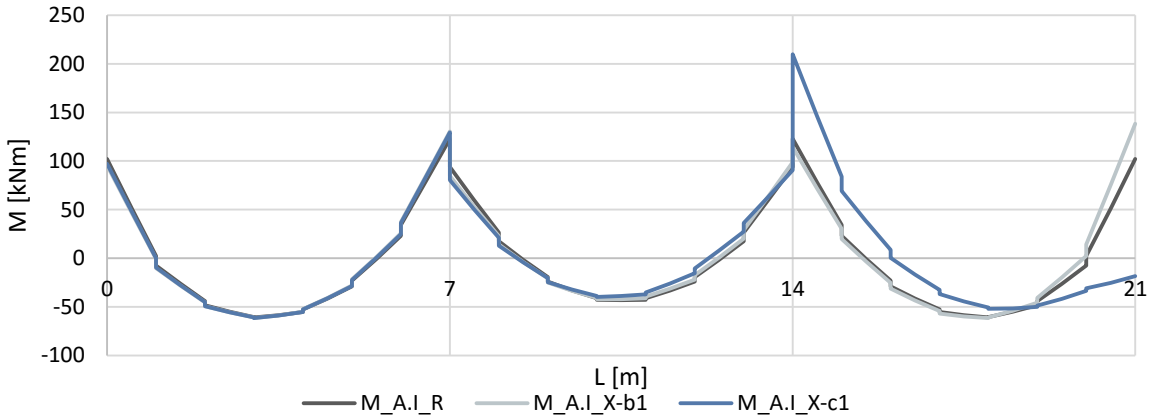

Figure 3.7 – Bending moments for the Quasi-Permanent Load Combination on beam YC

Based on the bending moment diagrams presented, the following conclusions can be drawn:

- The variation of the bending moments on the transfer beam is particularly significant, as could be expected due, not only to the reaction of the discontinued column, but also to the increase in the span. Furthermore, model **M_A.I_X-b1** is more conditioning than **M_A.I_X-c1** because, in the first, the discontinued column is a lateral one and in the second case an interior one.
- Apart from the transfer beam (TB), the **x** oriented beams (parallel to the TB) show a slight variation from the regular to the irregular cases. This is related to the low variation in the static load-resisting system in this direction.
- Concerning the beams oriented in the y direction (perpendicular to the TB), the only change worth mentioning is on the YB and YC beams for the **M_A.I_X-b1** and **M_A.I_X-c1** models, respectively.

  For the those beams, between the grid alignments 1 and 2, a radical change may be observed in the static load-resisting system due to the loss of continuity introduced by the interruption of the column. The fact that the bending moment in the end of the beam is practically nil, leads to a significant increase of the bending moment over the first continuous column when compared to that of the **M_A.I_R** model.

Although only the bending moments for the Quasi-Permanent Load Combination (QPLC) are presented, for the Fundamental Load Combination (FLC) the same conclusions could be taken. The scale factor between the QPLC and the FLC is in average:

$$FLC/QPLC \cong 1.55$$

ii.<u>Seismic Loads</u>

To analyse the effects of the seismic action on the structure, the bending moment diagrams for each direction (horizontal in the *x* and *y* direction and vertical) are presented. For these, the behaviour factor is considered unitary to facilitate the comparison between models. To be noted that, with the exception of the transfer beam, the diagrams are shown only for the seismic action acting in the direction of the beam axis.

The directional combination of the diagrams, affected by the behaviour coefficient, is then performed, based on the SRSS (Square-Root-of-Sum-of-Squares).

Figure 3.8 through Figure 3.10 show the bending moment diagrams for the transfer beam. For the remaining beams the same diagrams are presented in Figure 3.11 to Figure 3.18.

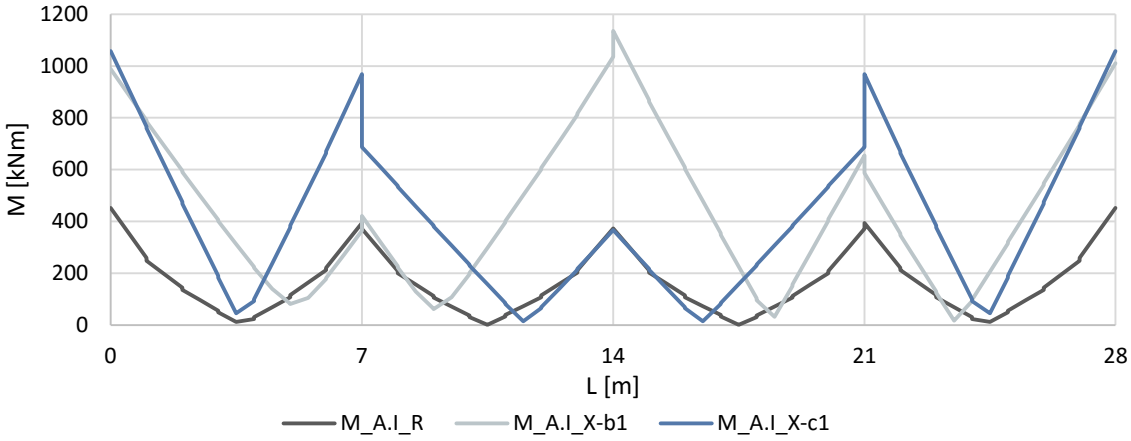

Figure 3.8 – Bending moments for the Seismic Action in the x direction on beam X1

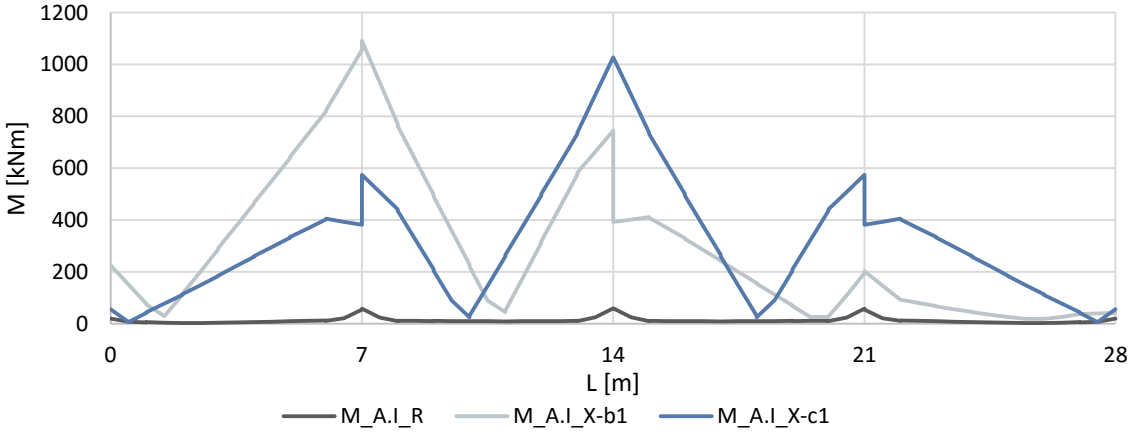

Figure 3.9 – Bending moments for the Seismic Action in the y direction on beam X1

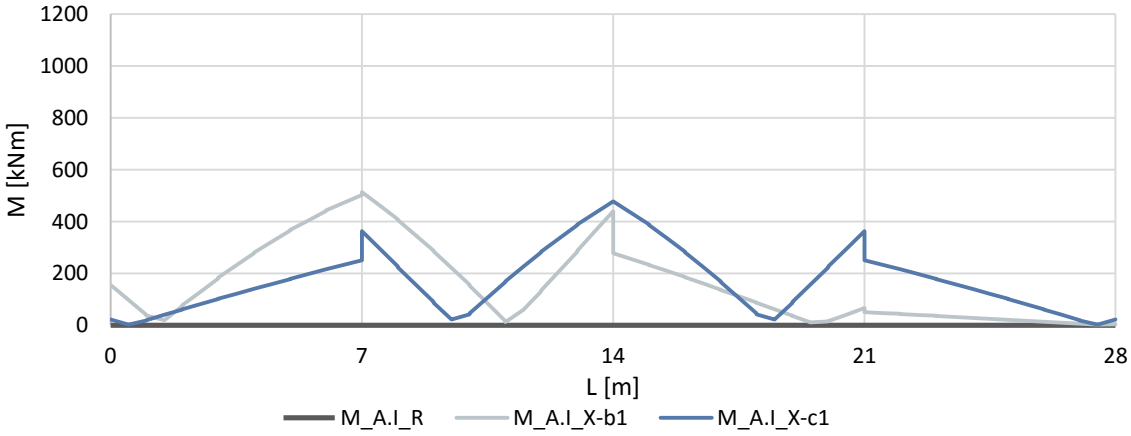

Figure 3.10 – Bending moments for the Seismic Action in the z direction on beam X1

Based on the bending moment diagrams presented, the following conclusions can be drawn:

- The absolute value of the bending moment increases in the x direction. This does not occur beneath the discontinued column but rather in the adjacent column as a consequence of the alteration on the load-resisting system.

- In the irregular models, when compared to regular one, an increase in the relevance of the vertical component of the seismic action was noted. This is to be expected given that there is a significant increase in the oscillating mass and in the span length between continuous columns. Although with lower absolute value than the horizontal components, the contribution of the vertical modes of vibration is relevant and its own specific evaluation is of great importance.
- Finally, despite not being the most common situation, the seismic action component in the direction perpendicular to the beam axis gains relevance, along with the other components. This is not a regular occurrence in structures but in the case of the transfer beam can be explained by the following reasons:
    - In a case where there are no discontinued columns and given a seismic action acting upon a structure, there is a main load transfer mechanism brought by the mobilization of the frame effect. However, there is also a load transfer mechanism based on the tension of some columns and compression of others. In the case of a discontinued column, the tensile and compressive forces lead to bending in the beam which supports the column. This is the reason for the seismic action in the perpendicular direction to the TB to originate bending moments with this level of relevance.
    - Given the reason indicated above, it is reasonable to expect that, the further away the discontinued column is from the centre of the building, the more expressive this effect will be.

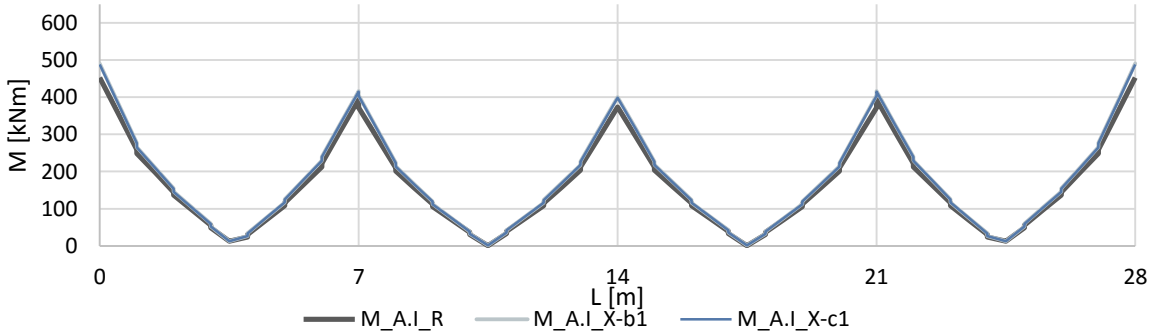

Figure 3.11 – Bending moments for the Seismic Action in the x direction on beam X2

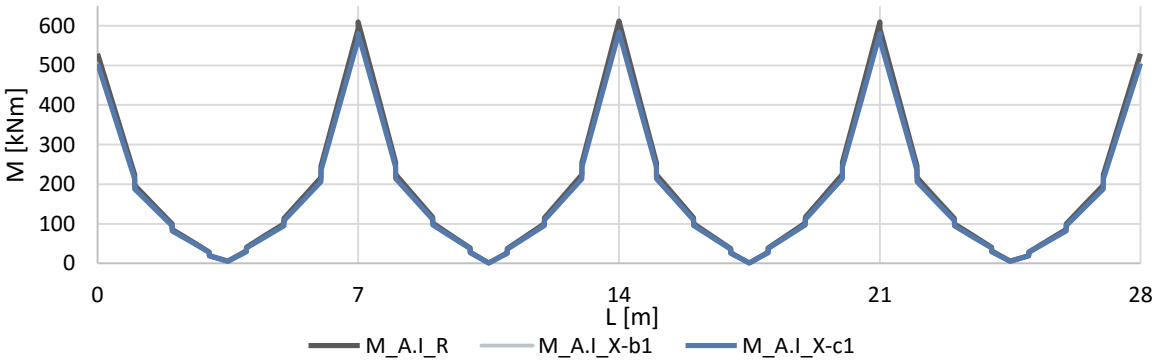

Figure 3.12 – Bending moments for the Seismic Action in the x direction on beam X3

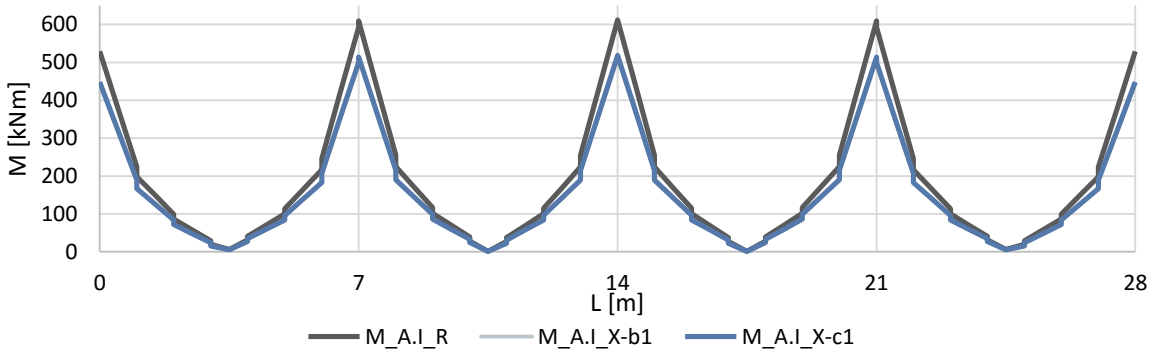

Figure 3.13 – Bending moments for the Seismic Action in the x direction on beam X4

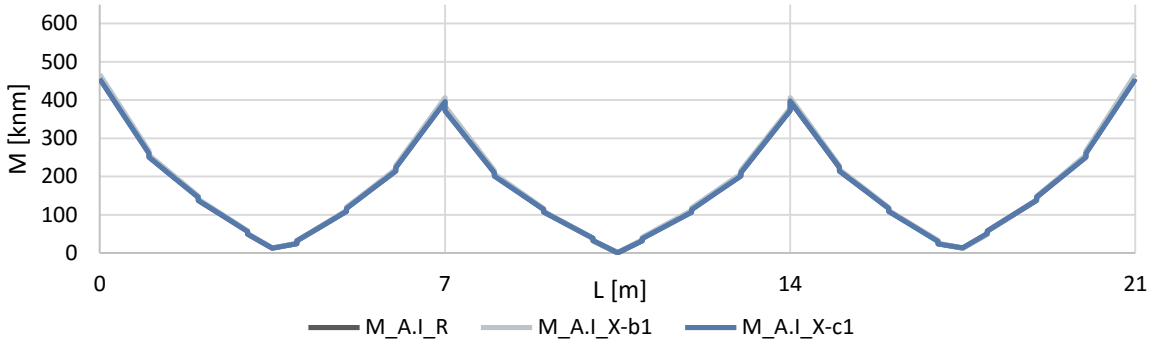

Figure 3.14 – Bending moments for the Seismic Action in the y direction on beam YA

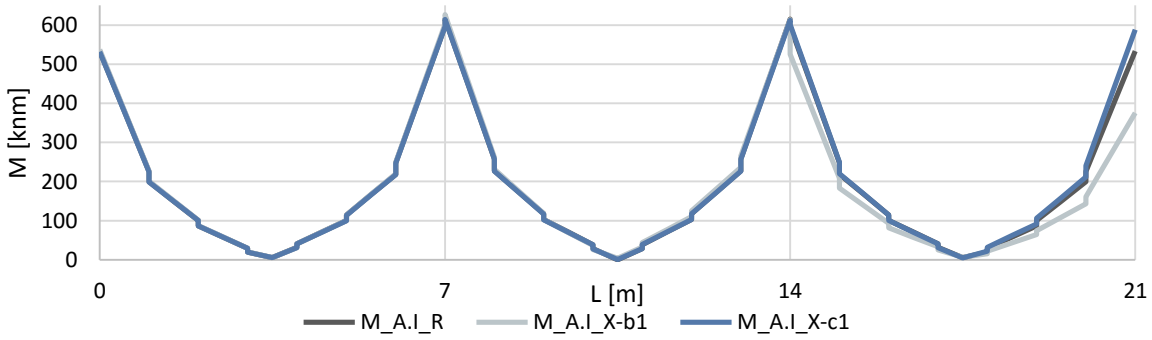

Figure 3.15 – Bending moments for the Seismic Action in the y direction on beam YB

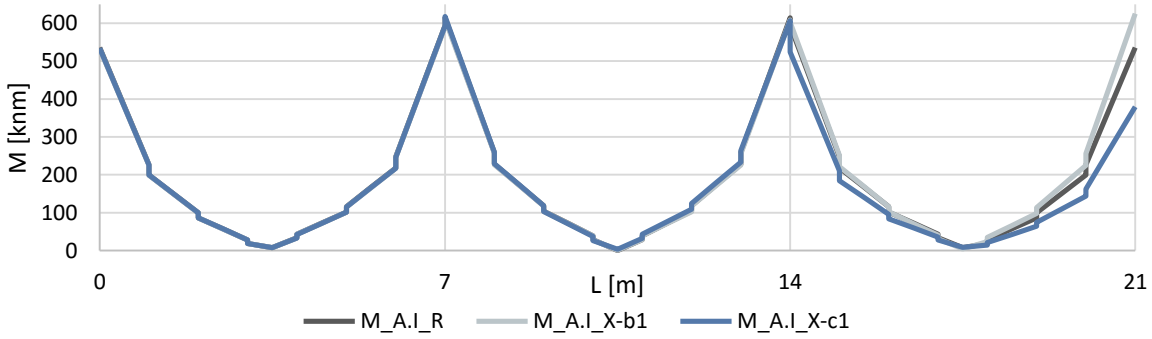

Figure 3.16 – Bending moments for the Seismic Action in the y direction on beam YC

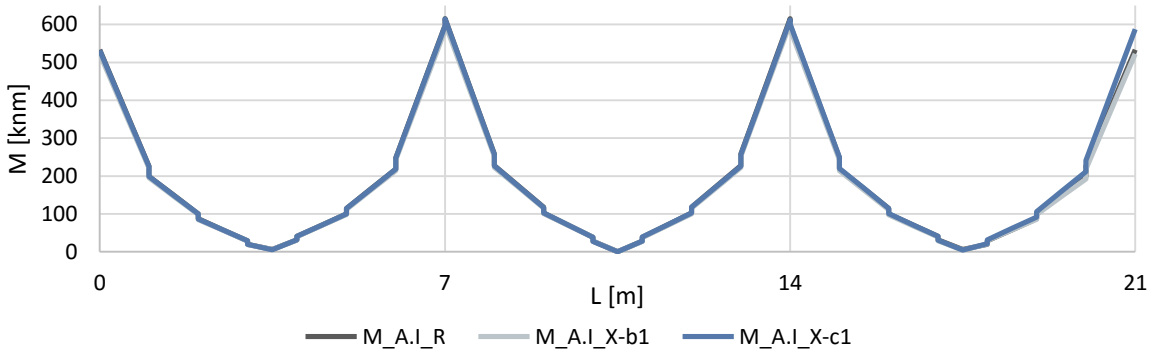

Figure 3.17 – Bending moments for the Seismic Action in the y direction on beam YD

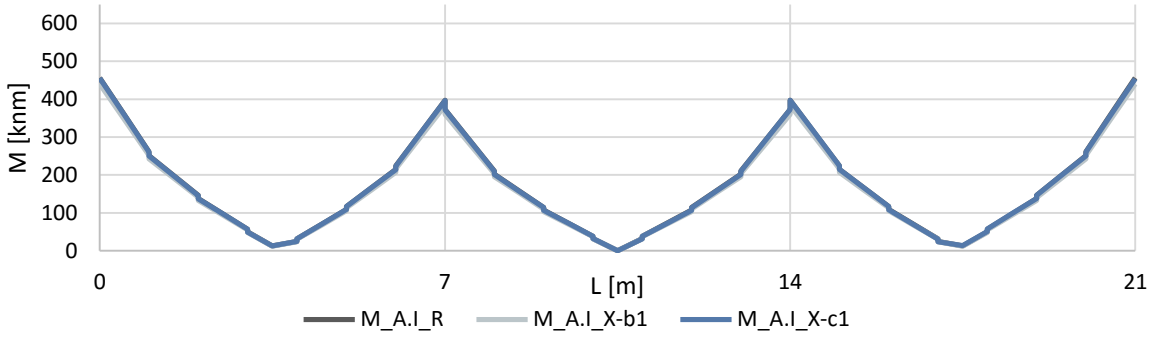

Figure 3.18 – Bending moments for the Seismic Action in the y direction on beam YE

Based on the bending moment diagrams presented the following conclusions can be drawn:

- Analysing the bending moments in the beams oriented in the x direction it is possible to conclude that the regular model present higher values of bending moment in the regular beams than the irregular ones. The reason for this is that the alignment of the transfer beam is stiffer than in the regular model, which means that a larger percentage of the base shear force is resisted by this frame. Given the fact that the base shear force is similar in all models, the regular model will expectedly present higher values of bending moment for the beams parallel to the TB (that are not the TB).
- Regarding the beams oriented in the y direction (perpendicular to the TB) there is a slight difference between the regular and the irregular models. The only major difference that is important to take into consideration is in the beams YB and YC where, for the same reasons presented in the analysis of the gravity loads, a variation in the bending moment next to the discontinued column occurs. In the model **M_A.I_X-b1** there is a reduction in the beam YB because of the absence of the column and an increase in the beam YC because of the increase of the cross-section of the column. The same can be seen for model **M_A.I_X-c1**, but in this case the reduction occurs in beam YC and the increase in beam YB.
- Table 3.11 summarizes the base shear force (F_b) distribution per alignment.

Table 3.11 – Base shear per alignment for the models M_A.I (R, X-b1 and X-c1)

		M_A.I_R	M_A.I_X-b1	M_A.I_X-c1
x direction	$\sum F_b$ [kN]	8392.1	8402.8	8400.7
	X1	16.2%	24.9%	24.2%
	X2	33.8%	26.3%	27.0%
	X3	33.8%	31.3%	31.5%
	X4	16.2%	17.5%	17.3%
y direction	$\sum F_b$ [kN]	8322.1	8534.9	8521.2
	YA	12.8%	13.4%	12.9%
	YB	24.8%	21.2%	26.7%
	YC	24.8%	29.2%	20.7%
	YD	24.8%	23.6%	26.7%
	YE	12.8%	12.6%	12.9%

iii.Comparison

To conclude this initial analysis, Figure 3.19 to Figure 3.21 present the bending moment diagrams for each model with the fundamental load combination and the seismic load combination, only for the transfer beam.

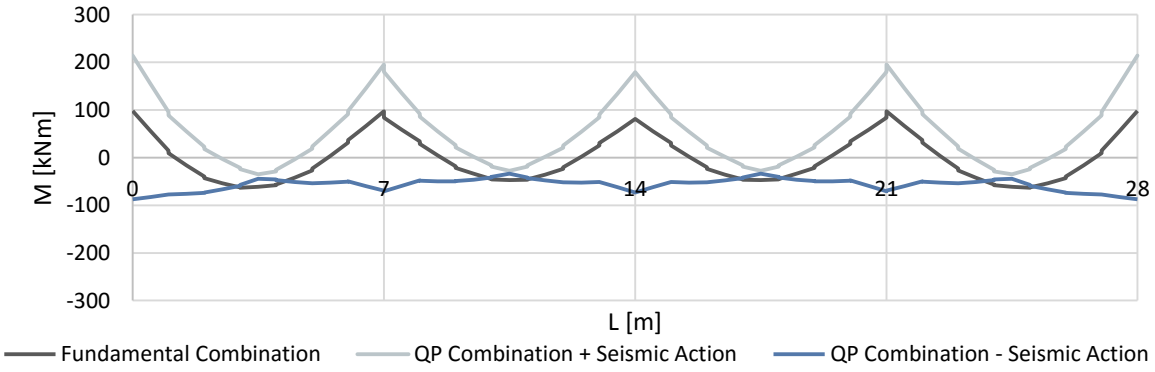

Figure 3.19 – Bending moment diagrams for the FLC and SLC in the beam X1 for the model M_A.I_R

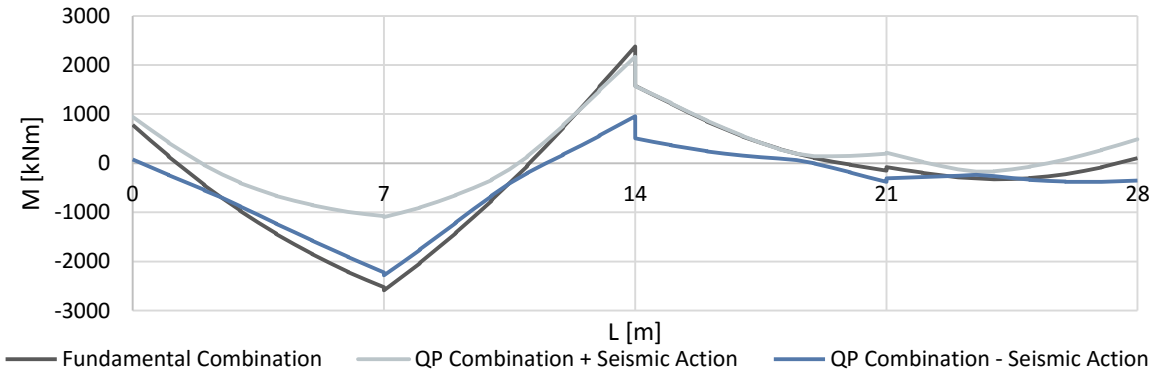

Figure 3.20 – Bending moment diagrams for the FLC and SLC in the beam X1 for the model M_A.I_X-b1

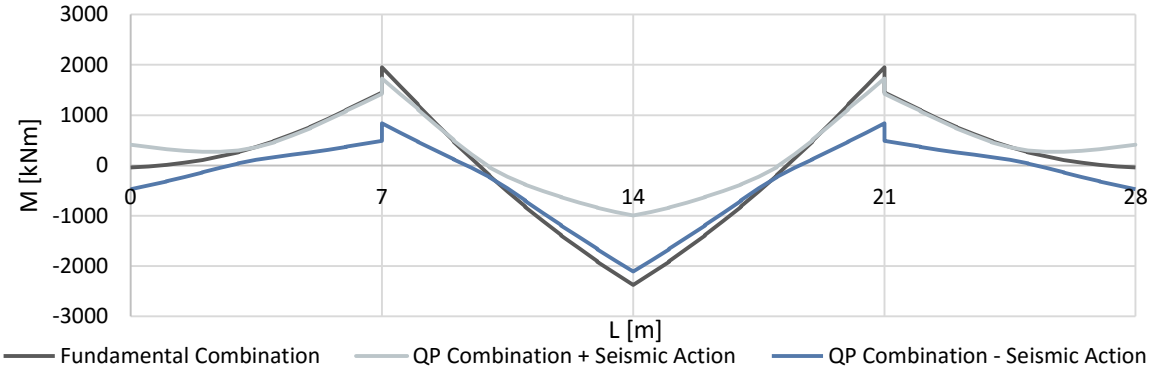

Figure 3.21 – Bending moment diagrams for the FLC and SLC in the beam X1 for the model M_A.I_X-c1

As can be seen in the presented figures and according to expectations, there is a severe increase in the bending moments when comparing the regular with the irregular model. Also from the figures it is possible to conclude that the fundamental load combination is the one that influences the design of the beam. On the other hand, for the regular beams, the most influent loading combination is the seismic load combination.

From this point on, the other models will be analysed and compared based on the previously defined parameters. The analysis performed in this chapter is of relevance as a basis to better understand and explain the results of the analysis of the parameters.

3.2.2. Parametric Analysis

For each model the values obtained for the defined parameters (α_b and α_c) are presented and compared with the conclusions taken from the initial analysis. The main similarities and differences between the cases are appointed always highlighting the one with higher values and providing, when possible, a justification for the results.

The following tables present the results obtained from the parametric analysis, where $\alpha_{b,M}$ regards to the parameter α_b for the bending moments and $\alpha_{b,V}$ regards the same parameter but for the shear force. Also, highlighted with grey are the values of the parameter for the transfer beam and the bold value identifies the maximum value attained for each case and parameter.

It is important to remember that these values intend to be indicators of the overall behaviour of a tridimensional model, it is not possible to make any assumptions of the local behaviour of the structure. The local behaviour will be addressed in the following chapter.

Furthermore, each of the presented values relates to the maximum of each alignment, it is hard to ascertain the section (or sections) that condition that same alignment. The main reason for the definition of these parameters is to allow for a more significant number of situations to be considered which would not be possible if the internal forces were to be compared directly, as were in the previous topic.

i.Case M_A.I

Table 3.12 to Table 3.15 present the values relating to the models **M_A.I**. All these models have 6 floors with a height between them of 3m, spans of 7m and no shear walls.

Table 3.12 – Values of $\alpha_{b,M}$ for the case M_A.I

Transfer Beam		Reg.	X1			X2			YA	YB	YC
Discontinued Column			B1	C1	B1 + D1	B2	C2	B2 + D2	A2	B2	C2
$\alpha_{b,M}$	X1	2.18	0.88	0.89	0.89	1.70	2.00	1.86	2.43	2.30	**2.79**
	X2	1.62	1.56	1.73	1.60	0.85	0.83	0.87	1.26	1.25	1.29
	X3	1.62	1.79	1.81	1.84	1.54	1.72	1.54	1.82	1.83	1.90
	X4	2.18	2.61	2.71	2.69	2.31	2.32	2.47	2.50	2.38	2.46
	YA	2.19	2.48	2.51	2.40	2.42	2.53	2.37	0.88	1.60	2.24
	YB	1.63	1.28	1.83	1.33	1.27	1.85	1.29	1.55	0.85	1.62
	YC	1.67	1.84	1.32	1.77	2.00	1.31	1.84	1.84	1.61	0.86
	YD	1.63	1.82	1.83	1.33	1.80	1.85	1.29	1.90	1.77	1.62
	YE	2.19	2.51	2.51	2.40	2.43	2.53	2.37	2.73	2.71	2.24

Table 3.13 – Values of $\alpha_{b,V}$ for the case M_A.I

Transfer Beam		Reg.	X1			X2			YA	YB	YC
Discontinued Column			B1	C1	B1 + D1	B2	C2	B2 + D2	A2	B2	C2
$\alpha_{b,V}$	X1	1.27	0.85	0.84	0.86	1.20	1.31	1.26	1.55	1.57	1.69
	X2	1.38	1.30	1.35	1.32	0.81	0.82	0.82	1.26	1.05	1.29
	X3	1.38	1.41	1.40	1.42	1.22	1.36	1.30	1.41	1.39	1.44
	X4	1.27	1.65	1.67	1.66	1.52	1.48	1.55	1.58	1.61	1.53
	YA	1.27	1.58	1.58	1.55	1.58	1.58	1.51	0.84	1.17	1.47
	YB	1.38	1.27	1.42	1.32	1.06	1.40	1.08	1.35	0.81	1.28
	YC	1.42	1.42	1.31	1.38	1.41	1.09	1.43	1.39	1.24	0.82
	YD	1.38	1.49	1.42	1.32	1.44	1.40	1.08	1.47	1.42	1.28
	YE	1.27	1.57	1.58	1.55	1.57	1.58	1.51	**1.70**	1.69	1.47

Based on the results presented above, the following consideration may be taken for the beams:

- As concluded from the initial analysis, for the transfer beams the gravity load combination is always more conditioning than the seismic load combination. This conclusion is somehow expected given the fact that the bending moments and shear in a beam with a point load (reaction of the discontinued column) at mid-span are very high and, therefore, the difference between the QPLC and the FLC is higher than the increase due to the seismic action.

- The absolute maximum $\boldsymbol{\alpha_{b,M}}$ occurs for beam X1 in the model **M_A.I_Y-c2** with a value of 2.79. This value is not only the absolute maximum but also the highest difference between the regular and the irregular models.
  From the analysis of the internal forces for the regular model and the model **M_A.I_Y-c2,** the following conclusions could be established:

  - The bending moment for the QPLC is approximately equal in both models.
  - The bending moment due to the seismic action is higher in the irregular model. This may be justified by the analysis of the base shear of each frame.
    For better understanding the situation, the values of the base shear force (F_b) for each model are presented in Table 3.14.

    Table 3.14 – Base shear for the models M_A.I_R and M_A.I_Y-c2

Alignment of the frame	M_A.I_R		M_A.I_Y-c2	
	F_b [kN]	%	F_b [kN]	%
X1	1358.5	16.2	1628.8	19.3
X2	2846.0	33.8	2123.2	25.2
X3	2846.0	33.8	3231.7	38.4
X4	1358.5	16.2	1442.7	17.1

    As can be concluded from these values, there is an increase in the base shear of the frame X1. The reason for this is the reduction in stiffness of the frame X2 as a result of the discontinued column. This reduction goes along with an increase in the other alignments, being the largest in alignment X1.

- Based on the former conclusions, the following result patterns may be identified:

  - For the beams parallel to the transfer beam (TB), the further away the beam is from the TB, the higher is the parameter $\boldsymbol{\alpha_{b,M}}$. Also, in the beams closest to the TB there is a reduction of $\boldsymbol{\alpha_{b,M}}$ in the irregular model when compared with the regular model. The only exception to this is when the discontinued column is a central one.
  - For the beams perpendicular to the TB**,** the values of $\boldsymbol{\alpha_{b,M}}$ are always higher in the irregular model than in the regular one. The only exception for this is in the perpendicular beam which has a discontinued column. This is justified with the reduction in the base shear force for these alignments as shown previously.

- Conclusions taken for the parameter $\boldsymbol{\alpha_{b,M}}$ also apply to the parameter $\boldsymbol{\alpha_{b,V}}$**.**

In Table 3.15 are presented the values regarding the parameter $\boldsymbol{\alpha_c}$ for the case **M_A.I**.

Table 3.15 – Values of α_c for the case M_A.I

Transfer Beam		Reg.	X1			X2			YA	YB	YC
Discontinued Column			B1	C1	B1 + D1	B2	C2	B2 + D2	A2	B2	C2
α_c	X1	0.87	1.07	1.21	0.97	1.06	1.03	1.05	1.11	1.09	1.08
	X2	0.77	0.85	0.84	0.85	0.90	0.98	0.85	0.87	0.86	0.87
	X3	0.77	0.86	0.86	0.86	0.85	0.84	0.85	0.87	0.86	0.85
	X4	0.87	1.10	1.09	1.09	1.08	1.03	1.07	**1.22**	1.08	1.08
	YA	0.87	1.10	1.21	1.09	1.08	1.03	1.07	**1.22**	1.04	1.08
	YB	0.77	0.87	0.88	0.87	0.87	0.85	0.87	0.85	1.03	0.85
	YC	0.78	0.92	0.87	0.90	0.86	0.86	0.87	0.87	0.86	1.08
	YD	0.77	0.86	0.88	0.87	0.85	0.85	0.87	0.87	0.87	0.85
	YE	0.87	1.08	1.21	1.09	1.04	1.03	1.07	1.11	1.09	1.08

Based on the results presented above, the following consideration may be established for the columns:

- Regarding the alignments with transfer beams, the peripheral ones are more conditioning than the interior ones, which is directly related with the area of influence of each alignment. Analysing the three cases with the transfer beam in the X1 alignment or in the X2 alignment the following was concluded:
    - The case where the centre column (C) is discontinued, corresponds to the higher value of $\boldsymbol{\alpha_c}$
    - The case where the two columns are discontinued (B+D) corresponds to the lower value of $\boldsymbol{\alpha_c}$

    This may be explained based on the influence lines of the reactions on the beam, for the columns in which the reaction of the discontinued column induces a reduction in the compression of the columns, the seismic load combination is prevalent over the fundamental load combination. Although, in the cases where either the B1 or the B2 column is discontinued this does not occur.

ii.<u>Case M_A.II</u>

Table 3.16 to Table 3.18 present the values relating to the models **M_A.II**. All these models have 2 floors with a height between them of 3m, spans of 7m and no shear walls.

Table 3.16 – Values of $\alpha_{b,M}$ for the case M_A.II

Transfer Beam		Reg.	X1			X2			YA	YB	YC
Discontinued Column			B1	C1	B1 + D1	B2	C2	B2 + D2	A2	B2	C2
$\alpha_{b,M}$	X1	1.22	0.83	0.83	0.84	1.21	1.28	1.19	1.86	1.99	2.06
	X2	1.28	1.35	1.44	1.36	0.84	0.88	0.88	1.12	1.14	1.14
	X3	1.28	1.44	1.45	1.46	1.32	1.43	1.30	1.43	1.67	1.59
	X4	1.22	1.38	1.38	1.38	1.37	1.36	1.39	1.76	1.71	1.56
	YA	1.24	2.00	1.84	1.90	**2.10**	1.93	1.99	0.83	1.20	1.38
	YB	1.28	1.13	1.43	1.18	1.14	1.70	1.18	1.35	0.84	1.33
	YC	1.33	1.48	1.19	1.47	1.77	1.23	1.98	1.50	1.34	0.88
	YD	1.28	1.39	1.43	1.18	1.36	1.70	1.18	1.45	1.45	1.33
	YE	1.24	1.71	1.84	1.90	1.74	1.93	1.99	1.40	1.48	1.38

Table 3.17 – Values of $\alpha_{b,V}$ for the case M_A.II

Transfer Beam		Reg.	X1			X2			YA	YB	YC
Discontinued Column			B1	C1	B1 + D1	B2	C2	B2 + D2	A2	B2	C2
$\alpha_{b,V}$	X1	1.04	0.79	0.78	0.80	1.04	1.09	1.04	1.49	1.47	1.51
	X2	1.15	1.20	1.29	1.21	0.79	0.80	0.81	1.12	1.13	1.14
	X3	1.15	1.28	1.28	1.29	1.17	1.31	1.15	1.27	1.40	1.35
	X4	1.04	1.20	1.18	1.18	1.17	1.18	1.20	1.38	1.15	1.06
	YA	1.05	1.53	1.42	1.48	1.52	1.22	1.46	0.79	1.03	1.15
	YB	1.15	1.13	1.26	1.16	1.15	1.42	1.18	1.20	0.79	1.18
	YC	1.18	1.30	1.17	1.53	1.57	1.23	**1.73**	1.32	1.18	0.80
	YD	1.15	1.24	1.26	1.16	1.18	1.42	1.18	1.28	1.28	1.18
	YE	1.05	1.36	1.42	1.48	1.16	1.22	1.46	1.20	1.27	1.15

Given that most of the conclusions taken for the previous case are valid for this one, whenever the considerations are identical they will only be mentioned but not addressed in detail. Based on the results presented above, the following consideration may be taken for the beams:

- In this case it is also confirmed that for the transfer beams the gravity loads are conditioning over the horizontal loads with overall values of the same magnitude as in case **A.I**.

- The maximum absolute value of $\boldsymbol{\alpha_{b,M}}$ occurs for the model **M_A.II_X-b2** in beam YA and with a value of 2.10, lower than in the in models **M_A.I**, in fact, the overall values for this case study are lower than those of case **M_A.I**. Again the maximum occurs for a peripheral beam perpendicular to the transfer beam, in an alignment right next to the one with the discontinuity.
- Comparing with the case M**_A.I,** the values of $\boldsymbol{\alpha_{b,M}}$ are, in average, 31% lower in this case for the regular situation but only 20% lower for the irregular situations. The same relations for the values of $\boldsymbol{\alpha_{b,V}}$ are respectively 17% and 9%. Both are indicators that the presence of the irregularity in the models **M_A.II** leads to an increased aggravation from the regular to the irregular situations than in the case **M_A.I**.

Table 3.18 – Values of α_c for the case M_A.II

Transfer Beam		Reg.	X1			X2			YA	YB	YC
Discontinued Column			B1	C1	B1 + D1	B2	C2	B2 + D2	A2	B2	C2
α_c	X1	1.43	1.93	2.81	1.44	1.77	1.54	1.60	1.71	1.74	1.68
	X2	0.92	1.07	1.02	1.03	1.24	1.68	1.07	1.03	1.03	1.04
	X3	0.92	1.05	1.02	1.03	1.05	0.99	0.99	1.03	1.02	1.00
	X4	1.43	1.74	1.68	1.70	1.76	1.56	1.64	**3.12**	1.81	1.94
	YA	1.43	1.74	2.81	1.70	1.77	1.68	1.64	**3.12**	1.70	1.68
	YB	0.91	1.02	1.01	1.02	1.06	0.98	1.02	1.04	1.81	1.01
	YC	0.96	1.06	1.06	1.07	1.04	1.05	1.04	1.08	1.07	1.94
	YD	0.91	1.34	1.01	1.02	1.06	0.98	1.02	1.02	1.03	1.01
	YE	1.43	1.93	2.81	1.70	1.53	1.68	1.64	1.71	1.74	1.68

Based on the results presented above, the following consideration may be established for the columns:

- It is possible to verify that the conclusion taken for the case **M_A.I**, which mentioned that the columns in peripheral alignments are more conditioning, is valid for this case. It is also possible to conclude that the discontinuity of central columns (C1 or C2) is more severe than the other situations (considering only the TB in the x direction).
- The situation corresponding to the higher value of $\boldsymbol{\alpha_c}$ is the one where the column **A2** is removed with the TB in the y direction, as was for the previous case (**M_A.I**).
- The values of $\boldsymbol{\alpha_c}$ are, in average 39% higher in the models of the case **M_A.II** for the regular situations and 45% higher for the irregular situations. This is a clear indication that the present case is more conditioning than the **M_A.I** and that the variation from regular to the irregular situations is globally higher in this case.

iii.Case M_A.III

Table 3.19 to Table 3.21 present the values relating to the models **M_A.III**. All these models have 10 floors with a height between them of 3m, spans of 7m and no shear walls.

Table 3.19 – Values of $\alpha_{b,M}$ for the case M_A.III

Transfer Beam		Reg.	X1			X2			YA	YB	YC
Discontinued Column			B1	C1	B1 + D1	B2	C2	B2 + D2	A2	B2	C2
$\alpha_{b,M}$	X1	1.97	0.84	0.85	0.86	1.39	1.65	1.46	2.20	2.26	2.38
	X2	1.58	1.50	1.64	1.51	0.78	0.78	0.80	1.18	1.10	1.23
	X3	1.58	1.74	1.73	1.77	1.35	1.59	1.39	1.59	1.78	1.82
	X4	1.97	2.32	2.41	2.40	2.02	2.03	2.09	2.21	2.39	2.21
	YA	1.97	2.20	2.23	2.15	2.20	2.28	2.18	0.84	1.34	1.85
	YB	1.58	1.19	1.60	1.24	1.11	1.78	1.13	1.46	0.78	1.42
	YC	1.62	1.62	1.23	1.51	1.77	1.16	1.61	1.75	1.46	0.83
	YD	1.58	1.77	1.60	1.24	1.75	1.78	1.13	1.84	1.69	1.42
	YE	1.97	2.24	2.23	2.15	2.26	2.28	2.18	**2.49**	2.41	1.85

Table 3.20 – Values of $\alpha_{b,V}$ for the case M_A.III

Transfer Beam		Reg.	X1			X2			YA	YB	YC
Discontinued Column			B1	C1	B1 + D1	B2	C2	B2 + D2	A2	B2	C2
$\alpha_{b,V}$	X1	1.34	0.82	0.82	0.83	1.07	1.17	1.08	1.48	1.49	1.55
	X2	1.19	1.17	1.21	1.17	0.77	0.80	0.77	1.18	1.01	1.23
	X3	1.19	1.29	1.28	1.29	1.10	1.19	1.11	1.28	1.29	1.32
	X4	1.34	1.56	1.59	1.58	1.41	1.39	1.42	1.48	1.56	1.47
	YA	1.35	1.49	1.49	1.46	1.48	1.52	1.46	0.82	1.03	1.30
	YB	1.19	1.20	1.28	1.23	1.02	1.29	1.03	1.15	0.78	1.11
	YC	1.21	1.29	1.22	1.22	1.32	1.04	1.25	1.29	1.13	0.81
	YD	1.19	1.34	1.28	1.23	1.32	1.29	1.03	1.34	1.27	1.11
	YE	1.35	1.48	1.49	1.46	1.51	1.52	1.46	**1.64**	1.60	1.30

Given that most of the conclusions taken for the first case are valid for this one, whenever the considerations are identical, they will only be mentioned but not addressed in detail. Based on the results presented above, the following consideration may be taken for the beams:

- In this case it is again verified that for the transfer beams the gravity loads are conditioning over the horizontal loads with overall values lower than the ones obtained for the cases **M_A.I** and **M_A.II**.

- The maximum absolute value of $\boldsymbol{\alpha_{b,M}}$ and $\boldsymbol{\alpha_{b,V}}$ occurs for the model **M_A.III_Y-a2** in beam YE and with values of 2.49 and 1.64, both lower than in the in models **M_A.I**. Also, for the present case study the overall values are lower than those of case **M_A.I**. In this case the maximum value relates to a peripheral, as for previous cases, but the beam is not perpendicular to the transfer beam. Instead it is in the further alignment parallel to the transfer beam.
- In this case study the values of $\boldsymbol{\alpha_{b,M}}$ are, in average, 6% lower for the regular situation than in case **M_A.I** but only 9% lower for the irregular situation. The same relations for the values of $\boldsymbol{\alpha_{b,V}}$ are respectively 5% and 7%. On the contrary to the case **M_A.II**, the reduction in the present case to the **M_A.I** is more noticeable in the irregular models. This means that, in the case M_**A.III,** the aggravation from the regular to the irregular situation is lower than in the previous cases.

Table 3.21 – Values of α_c for the case M_A.III

Transfer Beam		Reg.	X1			X2			YA	YB	YC
Discontinued Column			B1	C1	B1 + D1	B2	C2	B2 + D2	A2	B2	C2
α_c	X1	0.93	1.02	1.09	0.93	0.99	0.99	0.98	1.02	1.01	0.99
	X2	0.80	0.83	0.83	0.83	0.86	0.89	0.82	0.85	0.84	0.84
	X3	0.80	0.84	0.84	0.84	0.83	0.83	0.83	0.85	0.84	0.83
	X4	0.93	1.01	1.01	1.01	1.01	0.98	1.00	**1.09**	1.01	0.99
	YA	0.93	1.01	1.09	1.01	1.01	0.99	1.00	**1.09**	0.99	0.99
	YB	0.80	0.85	0.86	0.85	0.85	0.84	0.84	0.83	0.91	0.83
	YC	0.80	0.86	0.85	0.85	0.84	0.84	0.84	0.84	0.84	0.94
	YD	0.80	0.84	0.86	0.85	0.84	0.84	0.84	0.85	0.85	0.83
	YE	0.93	1.02	1.09	1.01	0.99	0.99	1.00	1.02	1.01	0.99

Based on the results presented above, the following considerations may be established for the columns:

- The conclusion, taken for the cases **M_A.I** and **M_A.II**, that the columns in peripheral alignments are more conditioning remains valid for this case too. It is also possible to conclude that the discontinuity of central columns (C1 or C2) is more severe than the other considered situations in the x direction.
- The situation corresponding to the higher value of $\boldsymbol{\alpha_c}$ is the one where the column **A2** is removed with the TB in the y direction, as was for the previously presented cases.
- The values of $\boldsymbol{\alpha_c}$ are, in average, 5% higher in the case **M_A.III** for the regular situation and 5% lower for the irregular situations. This is an indication that, in absolute value, the present case is similar to the **M_A.I** but that the variation from regular to the irregular situations is globally lower in this case.

iv.Case M_B.I

Table 3.22 to Table 3.24 present the values relating to the models **M_B.I**. All these models have 6 floors with a height between them of 3m, spans of 7m and shear walls.

Table 3.22 – Values of $\alpha_{b,M}$ for the case M_B.I

Transfer Beam		Reg.	X1			X2			YA	YB	YC
Discontinued Column			B1	C1	B1 + D1	B2	C2	B2 + D2	A2	B2	C2
$\alpha_{b,M}$	X1	1.36	0.90	0.84	0.89	1.66	1.62	1.84	1.58	1.75	1.45
	X2	0.94	1.00	1.00	1.03	0.78	0.78	0.79	0.93	0.86	0.86
	X3	0.94	1.00	1.00	1.02	0.95	1.03	0.96	1.00	1.02	1.03
	X4	1.36	1.61	1.59	1.61	1.57	1.61	1.60	1.63	1.56	1.99
	YA	1.90	2.22	2.21	2.24	2.15	**2.52**	2.15	0.94	2.28	2.20
	YB	1.11	1.09	1.22	1.11	0.95	1.23	0.98	1.17	0.80	1.14
	YC	1.10	1.21	0.95	1.21	1.23	0.97	1.15	1.17	1.12	0.79
	YD	1.11	1.23	1.22	1.11	1.22	1.23	0.98	1.19	1.20	1.14
	YE	1.90	2.24	2.21	2.24	2.37	**2.52**	2.15	2.19	2.19	2.20

Table 3.23 – Values of $\alpha_{b,V}$ for the case M_B.I

Transfer Beam		Reg.	X1			X2			YA	YB	YC
Discontinued Column			B1	C1	B1 + D1	B2	C2	B2 + D2	A2	B2	C2
$\alpha_{b,V}$	X1	1.37	0.85	0.99	0.85	1.66	1.41	1.67	1.52	1.46	1.27
	X2	0.82	0.88	0.85	0.89	0.77	0.78	0.77	0.89	0.80	0.86
	X3	0.82	0.86	0.86	0.87	0.87	0.92	0.88	0.88	0.86	0.87
	X4	1.37	1.56	1.54	1.56	1.50	1.56	1.53	1.60	1.44	**1.72**
	YA	1.41	1.59	1.58	1.60	1.47	1.56	1.48	0.83	1.42	1.57
	YB	0.93	1.04	0.99	1.05	0.86	0.99	0.87	1.05	0.79	1.00
	YC	0.93	1.02	0.95	1.02	0.99	0.88	0.97	0.98	0.96	0.78
	YD	0.93	1.01	0.99	1.05	1.02	0.99	0.87	1.00	1.02	1.00
	YE	1.41	1.58	1.58	1.60	1.58	1.56	1.48	1.54	1.55	1.57

Given that most of the conclusions taken for the first case are valid for this one, whenever the considerations are identical they will only be mentioned but not addressed in detail. Based on the results presented above, the following consideration may be taken for the beams:

- In the present case the conclusion that, for the transfer beams, the gravity loads are conditioning over the horizontal loads is also verified, although there is a relevant increase in the values of $\boldsymbol{\alpha_{b,M}}$ and $\boldsymbol{\alpha_{b,V}}$ comparing with the other models.

The reason for this is related with the fact that, under horizontal loads, the shear walls impose very high values of internal forces in the connection with the beams which does not occur in such magnitude for gravity loads.

- The maximum absolute value of $\boldsymbol{\alpha_{b,M}}$ occurs for the model **M_B.I_X-c2** in beam YA and with values of 2.52 which is lower than the maximum for the models **M_A.I**. Also, for this case study, the overall values are lower than for case **M_A.I**. In this case study, the maximum relates to a peripheral alignment perpendicular and right next to the transfer beam, as in the cases **M_A.I** and **M_A.II**.

  The values of $\boldsymbol{\alpha_{b,M}}$ are, in average, 31% lower in this case study for the regular situation but only 23% lower for the irregular situation. The same relations for the values of $\boldsymbol{\alpha_{b,V}}$ are, respectively, 16% and 14%. As for the case **M_A.II**, the reduction of the present case (to case **M_A.I**) is lower in the irregular models than in the regular one, which means that there is an aggravation from the regular to the irregular situation in the case **M_B.I**. Although this aggravation is smaller than in the case the **M_A.II**.

Table 3.24 – Values of α_c for the case M_B.I

Transfer Beam		Reg.	X1			X2			YA	YB	YC
Discontinued Column			B1	C1	B1 + D1	B2	C2	B2 + D2	A2	B2	C2
α_c	X1	4.21	2.85	**5.75**	3.57	4.38	5.13	4.82	3.78	4.83	5.17
	X2	0.86	0.94	0.93	0.94	0.93	1.00	0.84	0.93	0.93	0.94
	X3	0.86	0.93	0.93	0.92	0.93	0.93	0.92	0.93	0.93	0.93
	X4	4.21	4.63	5.15	5.05	4.76	5.04	5.17	4.54	5.19	5.06
	YA	4.21	4.63	**5.75**	5.05	4.76	5.13	5.17	4.54	5.19	5.17
	YB	0.93	1.00	1.01	1.00	1.02	1.00	1.02	1.02	1.13	1.01
	YC	0.74	0.83	0.80	0.82	0.80	0.80	0.81	0.80	0.80	0.87
	YD	0.93	1.27	1.01	1.00	1.01	1.00	1.02	1.00	1.01	1.01
	YE	4.21	4.35	**5.75**	5.05	4.75	5.13	5.17	4.27	4.96	5.17

Based on the results presented above, the following considerations may be established for the columns:

- The conclusion taken for the models with plan A (the columns in peripheral alignments are the conditioning) is valid for this case too. For this case, the discontinuity of central columns (C1 or C2) is more severe than the other considered situations for transfer beams oriented in the x direction.
- The situation corresponding to the higher value of $\boldsymbol{\alpha_c}$ is the **X-c1**, which does not occur for the other cases. On all the other cases the situation with higher $\boldsymbol{\alpha_c}$ was the **Y-a2**.
- In the case **M_B.I**, $\boldsymbol{\alpha_c}$ is in average, 178% higher than in case **M_A.I** for the regular situation and 158% higher for the irregular situations. This is an indication that the present case has, by far, the highest values of $\boldsymbol{\alpha_c}$, on the other hand the presented values regard the shear walls and not only the columns, which is in the base of these high values.

v.Case M_C.I

Table 3.25 to Table 3.27 present the values relating to the models **M_C.I**. All these models have 6 floors with a height between them of 3m, spans of 4m and no shear walls.

Table 3.25 – Values of $\alpha_{b,M}$ for the case M_C.I

Transfer Beam		Reg.	X1			X2			YA	YB	YC
Discontinued Column			B1	C1	B1 + D1	B2	C2	B2 + D2	A2	B2	C2
$\alpha_{b,M}$	X1	3.18	0.94	0.93	0.95	3.26	3.03	3.34	4.44	3.60	4.03
	X2	2.44	2.50	2.92	2.57	0.83	0.81	0.89	1.63	1.64	1.67
	X3	2.44	2.89	2.87	2.92	2.49	2.82	2.48	2.79	3.25	3.44
	X4	3.18	3.88	3.97	3.95	3.59	3.64	3.89	**4.57**	3.60	3.74
	YA	3.22	4.51	4.54	4.47	3.75	3.93	3.79	0.93	3.10	3.45
	YB	2.44	1.67	2.77	1.81	1.66	3.22	1.76	2.46	0.82	2.54
	YC	2.52	2.84	1.72	3.01	3.25	1.79	3.08	2.97	2.58	0.88
	YD	2.44	2.77	2.77	1.81	2.75	3.22	1.76	2.95	2.79	2.54
	YE	3.22	4.55	4.54	4.47	3.80	3.93	3.79	4.00	4.11	3.45

Table 3.26 – Values of $\alpha_{b,V}$ for the case M_C.I

Transfer Beam		Reg.	X1			X2			YA	YB	YC
Discontinued Column			B1	C1	B1 + D1	B2	C2	B2 + D2	A2	B2	C2
$\alpha_{b,V}$	X1	1.81	0.86	0.84	0.87	1.72	1.78	1.81	2.39	2.01	2.13
	X2	1.68	1.72	2.02	1.74	0.82	0.84	0.82	1.47	1.48	1.48
	X3	1.68	1.93	1.93	1.95	1.65	1.90	1.68	1.94	2.15	2.25
	X4	1.81	2.15	2.16	2.15	2.01	2.01	2.13	2.34	2.06	1.95
	YA	1.82	**2.41**	2.36	2.38	2.05	2.08	2.06	0.86	1.65	1.92
	YB	1.68	1.48	1.92	1.55	1.49	2.16	1.56	1.70	0.83	1.66
	YC	1.72	2.00	1.52	2.17	2.16	1.58	2.03	1.97	1.67	0.86
	YD	1.68	1.91	1.92	1.55	1.86	2.16	1.56	1.96	1.89	1.66
	YE	1.82	2.32	2.36	2.38	2.08	2.08	2.06	2.19	2.23	1.92

Given that most of the conclusions taken for the first case are valid for this one, whenever the considerations are identical they will only be mentioned but not addressed in detail. Based on the results presented above, the following consideration may be taken for the beams:

- In this case it may also be verified that for the transfer beams the gravity loads are conditioning over the horizontal loads with overall values higher than the ones obtained for the cases with plan A but lower than the ones obtained for the case with plan B.

- The maximum absolute value of $\boldsymbol{\alpha_{b,M}}$ occurs for the model **M_C.I_Y-a2** in beam YE and with values of 4.57, much higher than in the in other cases. Furthermore, for this case the overall values are higher than those of **M_A.I**. Again, for this case the maximum occurs for a peripheral beam, perpendicular to the transfer beam, in an alignment right next to the one with the discontinuity.
- The values of $\boldsymbol{\alpha_{b,M}}$ are, in average, 48% higher in the present case study for the regular situation than in case **M_A.I** and 52% higher for the irregular situation. The same relations for the values of $\boldsymbol{\alpha_{b,V}}$ are, respectively, 31% and 33%. On the contrary to the others, in this case there is an increase in the values of $\boldsymbol{\alpha_{b,M}}$ and $\boldsymbol{\alpha_{b,V}}$ comparing to the case **M_A.I**. Also, the values for the irregular models are higher than in the regular one, which means that in the case M_**C.I** there is an aggravation from the regular to the irregular situation. Although lower than in the case **M_A.II**, which had the more significant variation.

Table 3.27 – Values of α_c for the case M_C.I

Transfer Beam		Reg.	X1			X2			YA	YB	YC
Discontinued Column			B1	C1	B1 + D1	B2	C2	B2 + D2	A2	B2	C2
α_c	X1	1.18	1.43	1.64	1.19	1.29	1.31	1.31	1.34	1.33	1.33
	X2	0.90	0.97	0.97	0.96	1.01	1.14	0.90	0.98	0.98	0.99
	X3	0.90	0.98	0.97	0.98	0.96	0.96	0.96	0.98	0.97	0.96
	X4	1.18	1.34	1.32	1.34	1.34	1.28	1.34	**1.64**	1.32	1.29
	YA	1.18	1.34	1.64	1.34	1.34	1.31	1.34	**1.64**	1.32	1.33
	YB	0.90	0.99	0.98	0.98	1.00	0.97	1.00	0.97	1.18	0.97
	YC	0.91	0.98	0.98	0.99	0.98	0.98	1.00	0.99	0.98	1.21
	YD	0.90	1.05	0.98	0.98	0.96	0.97	1.00	0.98	0.99	0.97
	YE	1.18	1.43	1.64	1.34	1.29	1.31	1.34	1.34	1.33	1.33

Based on the results presented above, the following consideration may be established for the columns:

- Is possible to verify that the conclusion taken for the case **M_A.I** that the columns in peripheral alignments are more conditioning, stays valid for this case study. It is also possible to conclude that, for transfer beams oriented in the x direction, the discontinuity of central columns (C1 or C2) is more severe than the other considered situations.
- The situation corresponding to the higher value of $\boldsymbol{\alpha_c}$ is the one where the column **A2** is removed with the transfer beams in the y direction, as was for all cases but the **M_B.I**.
- Comparing with the case **M_A.I**, the values of $\boldsymbol{\alpha_c}$ are, in average, 25% higher in the case **M_C.I** for the regular situations and 19% higher for the irregular situations. This is an indication that the present case is more conditioning than the **M_A.I** but also that the variation from regular to the irregular situations is globally lower in this case.

3.3. Final Considerations

In this section, the main conclusions of the parametric study are presented as a series of tables that synthesise the results previously presented, allowing for a better interpretation of those results.

3.3.1. Displacements

Analysing the displacements for the various cases, Figure 3.22 to Figure 3.26 present the variation in height of the horizontal displacements in both the x and y direction. In these figures only the displacements of the regular model and of the models with higher and lower displacements for each direction are presented. In Annex C are presented the tables with the displacements of all the cases.

The reason for the emphasis given to the internal forces, rather than to the displacements, has to do with the fact that the irregularity under study has mostly a local the effect. Therefore, as shown in the following figures, the differences obtained for the displacements are not as significant as for the internal forces.

It should be noted that, if the cross-sections had not been redesigned, the effect of the irregularity in the displacements would have been more significant, as seen in the literature review.

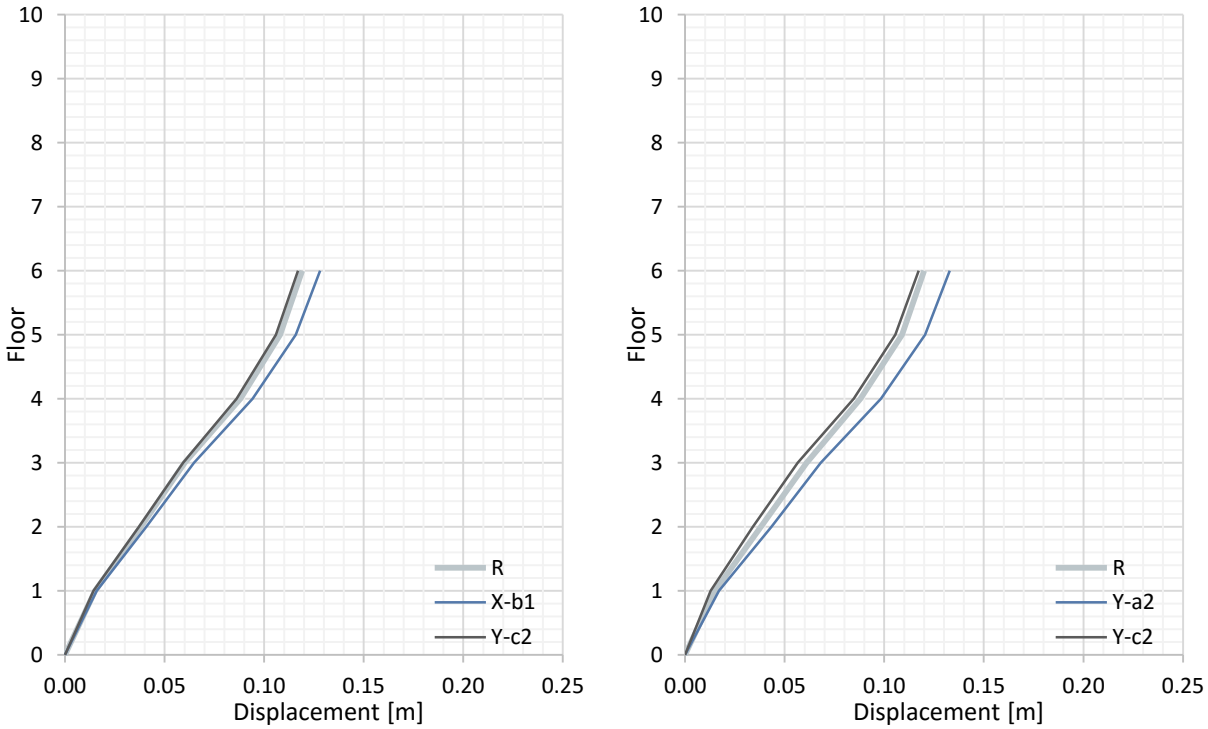

Figure 3.22 – Displacements in the models M_A.I for the x direction (right) and y direction (left)

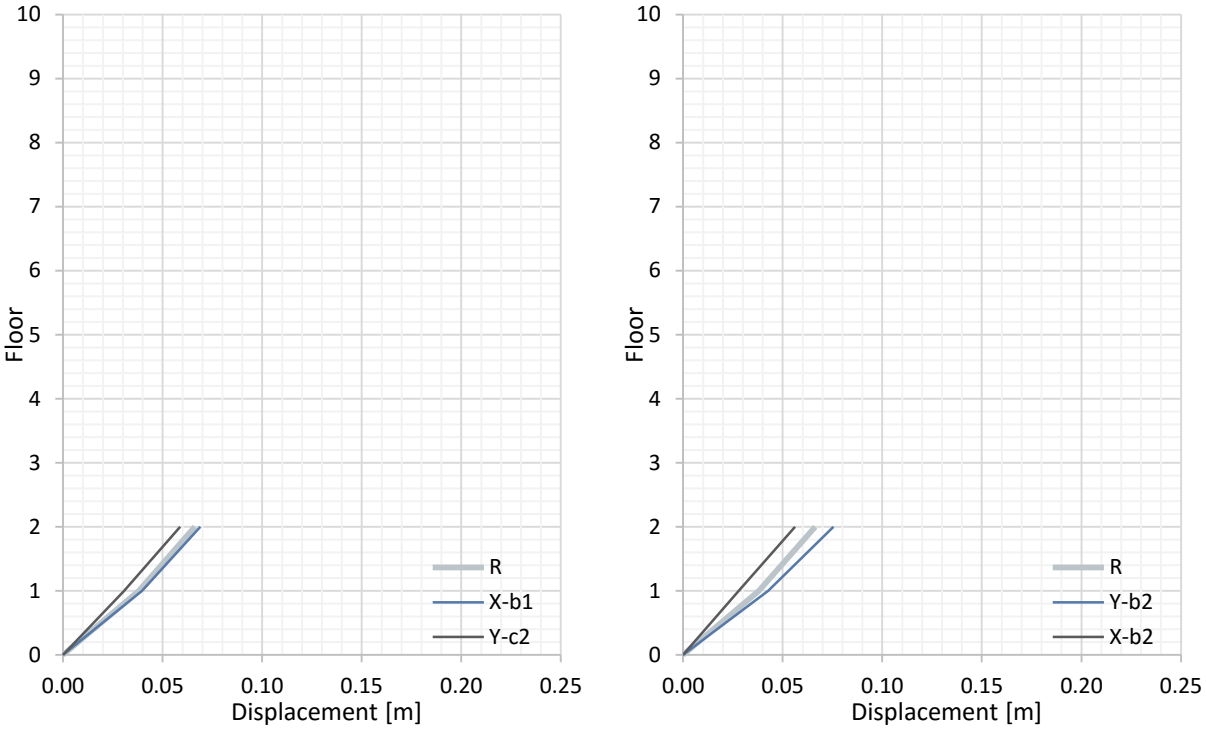

Figure 3.23 – Displacements in the models M_A.II for the x direction (right) and y direction (left)

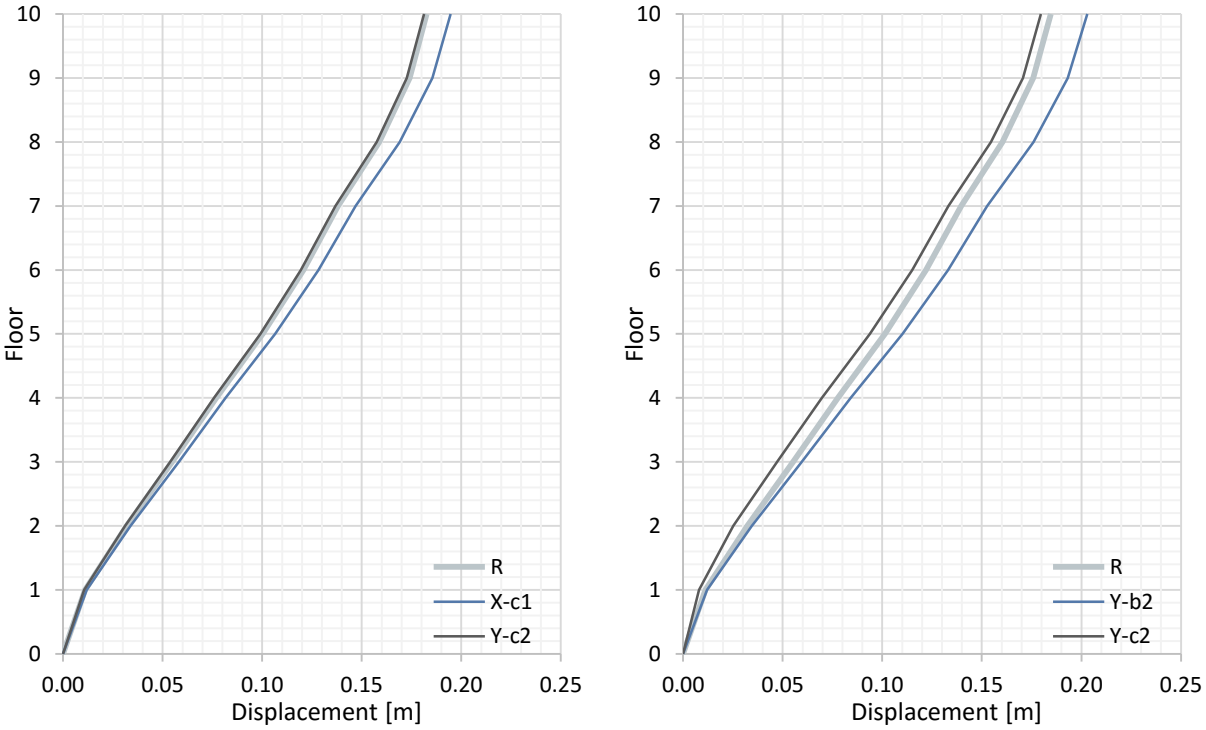

Figure 3.24 – Displacements in the models M_A.III for the x direction (right) and y direction (left)

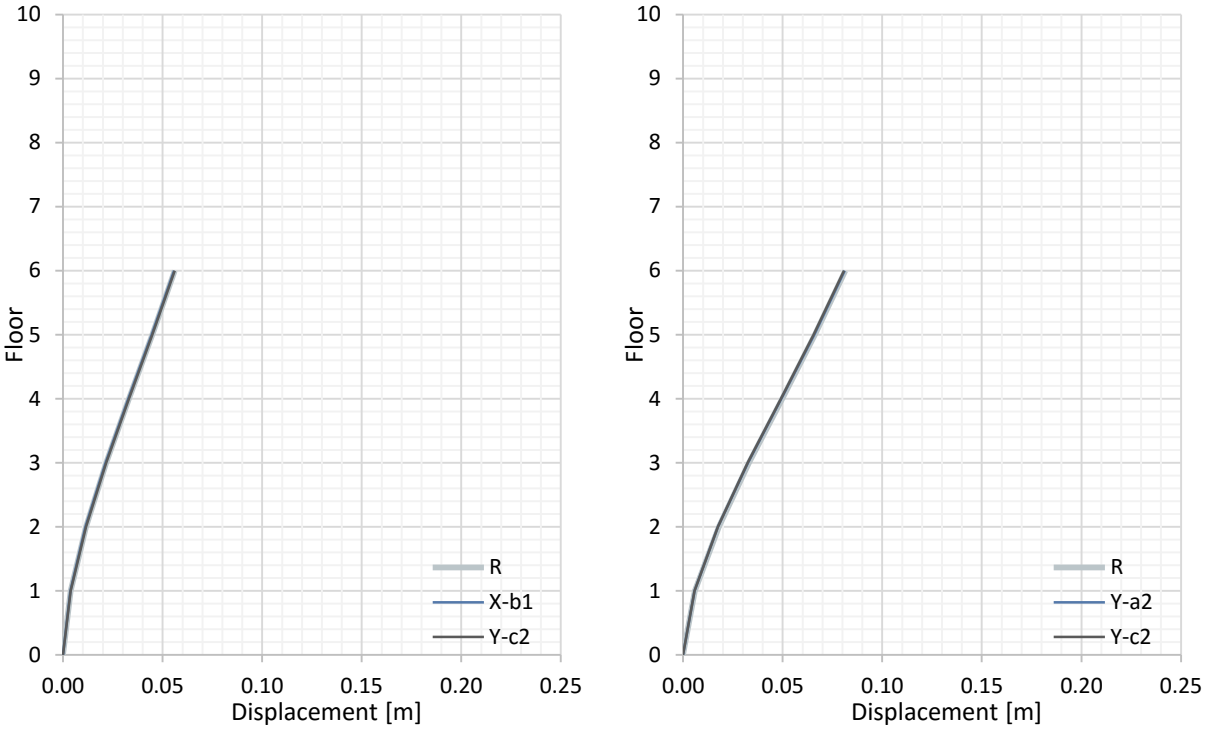

Figure 3.25 – Displacements in the models M_B.I for the x direction (right) and y direction (left)

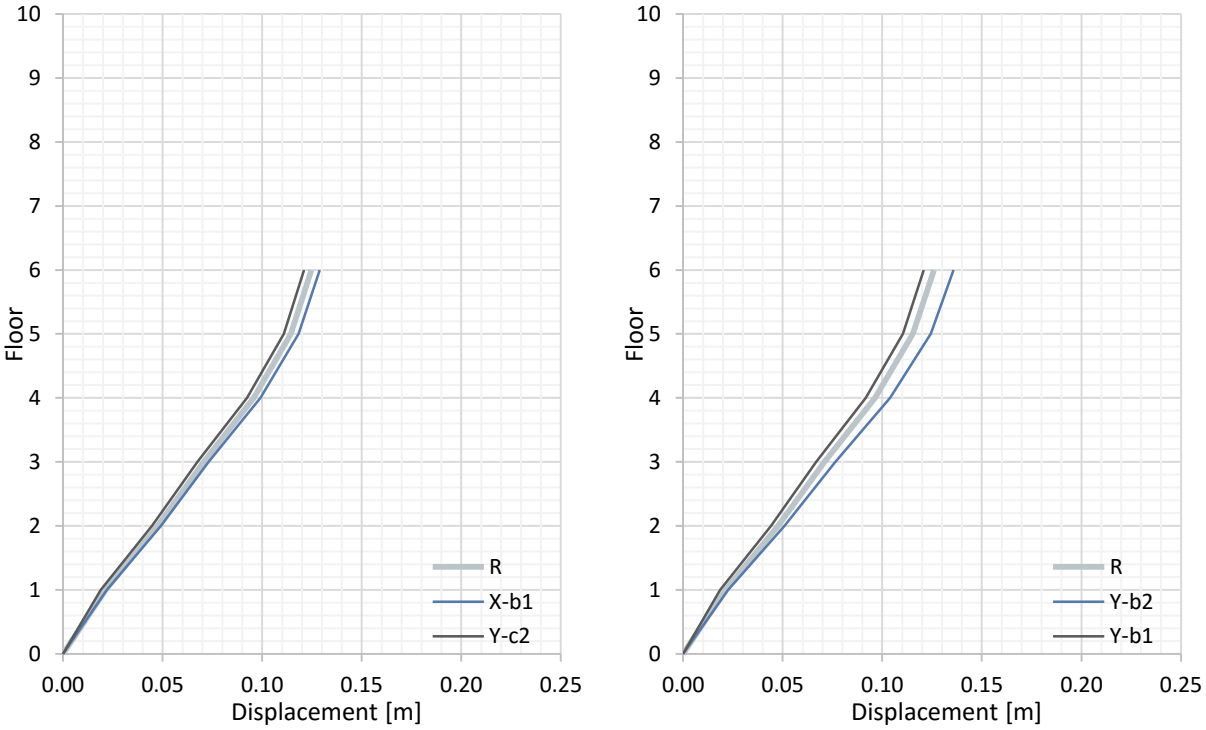

Figure 3.26 – Displacements in the models M_C.I for the x direction (right) and y direction (left)

Based on the results presented the following may be concluded:

- For all the cases and for both directions there is always an irregular situation that is more conditioning than the regular one. The larger differences are registered in the y direction and for irregular cases in which the transfer beam is oriented in the y direction.
- The largest relative variation between regular and irregular models is approximately 14% and occurs for case **M_A.II**. But the highest absolute difference is of 0.018m and occurs in case **M_A.III**. This suggests that the case with fewer floors is more affected by this type of irregularity.
- In case **M_B.I** the presence of the irregularity does not affect the structure in what regards the horizontal displacements. This happens due to the fact that the displacements of structure are controlled by the shear walls, hence having a displacement typical of a cantilever. This could lead to the conclusion that, in structures with predominant wall behaviour, the effect of discontinued columns is not as severe as in other cases. Although, the considered position of shear walls is a very specific and favourable case.
- There are cases in which the presence of the studied irregularity tends to reduce the displacements, this is not due to the irregularity itself, but instead due to the alterations made in the structure that are result of the irregularity, for example, larger columns and beams.

Analysing the results for all the considered cases (present in the tables in Annex C) is possible to validate the thesis that the irregularity under study is more conditioning when present in peripheral alignments.

For the cases in which the transfer beam is oriented in the x direction, the results show that the structural displacements are larger in the models with the discontinued column in the alignment 1 (rather than in alignment 2). The same occurs in the y direction, the models with discontinued columns in the A and B alignments have higher displacements than the other case.

3.3.2. Internal Forces

Table 3.28 to Table 3.30 summarize the values of the parameters α_b and α_c for the regular situations of each case study (i.e. without considering the irregular situations).

Table 3.28 – Values of $\alpha_{b,M}$ for the regular model of every case study

	M_A.I	M_A.II	M_A.III	M_B.I	M_C.I
X1	2.18	1.22	1.97	1.36	3.18
X2	1.62	1.28	1.58	0.94	2.44
X3	1.62	1.28	1.58	0.94	2.44
X4	2.18	1.22	1.97	1.36	3.18
YA	2.19	1.24	1.97	1.90	3.22
YB	1.63	1.28	1.58	1.11	2.44
YC	1.67	1.33	1.62	1.10	2.52
YD	1.63	1.28	1.58	1.11	2.44
YE	2.19	1.24	1.97	1.90	3.22

Table 3.29 – Values of $\alpha_{b,V}$ for the regular model of every case study

	M_A.I	M_A.II	M_A.III	M_B.I	M_C.I
X1	1.27	1.04	1.34	1.37	1.81
X2	1.38	1.15	1.19	0.82	1.68
X3	1.38	1.15	1.19	0.82	1.68
X4	1.27	1.04	1.34	1.37	1.81
YA	1.27	1.05	1.35	1.41	1.82
YB	1.38	1.15	1.19	0.93	1.68
YC	1.42	1.18	1.21	0.93	1.72
YD	1.38	1.15	1.19	0.93	1.68
YE	1.27	1.05	1.35	1.41	1.82

Table 3.30 – Values of α_c for the regular model of every case study

	M_A.I	M_A.II	M_A.III	M_B.I	M_C.I
X1	0.87	1.43	0.93	4.21 (0.93)[i]	1.18
X2	0.77	0.92	0.80	0.86	0.90
X3	0.77	0.92	0.80	0.86	0.90
X4	0.87	1.43	0.93	4.21 (0.93)	1.18
YA	0.87	1.43	0.93	4.21 (0.86)	1.18
YB	0.77	0.91	0.80	0.93	0.90
YC	0.78	0.96	0.80	0.74	0.91
YD	0.77	0.91	0.80	0.93	0.90
YE	0.87	1.43	0.93	4.21 (0.86)	1.18

Analysing the values presented in the previous tables it is possible to conclude that for the regular models, the conditioning case study is the **C.I** for the beams (both for bending moment and shear force) and the **A.II** for the columns. It is important to notice that the case study **B.I** has higher values of α_c although these are related to the shear walls; if comparing the values in the columns the conditioning case is the **A.II**.

Comparing the case studies with floor plan A it is possible to conclude that with the increase of the number of floors there is a generalized reduction in the value of α_c. This is to be expected due to the fact that a structure with more floors is more flexible and therefore in the zone of the response spectrum associated with lower values of acceleration leading to lower values of the seismic coefficient (β, computed as the ratio between the base shear force and the total weight of the above ground structure).

[i] The value in brackets corresponds to the maximum α_c in the columns the value of 4.21 relates to the shear walls

On the other hand, for the values of $\alpha_{b,M}$ and $\alpha_{b,V}$ the same cannot be concluded; this is likely related to the fact that for structures with a higher number of floors the columns cross-sections are larger, hence stiffer, and therefore imposing a higher rotation constraint on the floor beams, leading to an increase in the negative bending moments in the beams.

Comparing now the case studies with elevation I the conclusion is that for both cases **B.I** and **C.I** the values of $\alpha_{b,V}$ and α_c are higher than in the case **A.I**. The reason for this is related to the fact that both plan B and plan C correspond to stiffer structures leading to higher values of the seismic coefficient (defined previously). Although case **B.I** is stiffer than **C.I** the values of the parameter are higher in the case **C.I**; the reason for this is that in the **C.I** cases the span is shorter which gives relevance to the SLC comparing with the FLC.

In Table 3.31 to Table 3.33 are presented, for the regular beams and columns, the maximum absolute value of the parameters $\alpha_{b,M}$, $\alpha_{b,V}$ and α_c per alignment and for each case study, among the nine irregular situations.

Also, in each of those tables are presented the obtained results for the relative values (RV), which is the relative variation to the regular model as defined in equation (3.3).

$$RV = \frac{\alpha_I - \alpha_R}{\alpha_R} \tag{3.3}$$

where α_I regards the irregular models and α_R the regular ones. This ratio represent the variation between the values present in Table 3.28 to Table 3.30 and the absolute values present in Table 3.31 to Table 3.33.

To be noted that for the columns all the values are considered even those in the same alignments of those of the transfer beams.

Table 3.31 – Maximum per alignment of the values of $\alpha_{b,M}$ for each case study

	Absolute values					Relative values (RV)				
	A.I	A.II	A.III	B.I	C.I	A.I	A.II	A.III	B.I	C.I
X1	2.79	2.06	2.38	1.84	**4.44**	0.28	**0.69**	0.21	0.35	0.40
X2	1.73	1.44	1.64	1.03	**2.92**	0.06	0.13	0.03	0.09	**0.20**
X3	1.90	1.67	1.82	1.03	**3.44**	0.17	0.30	0.15	0.09	**0.41**
X4	2.71	1.76	2.41	1.99	**4.57**	0.24	**0.45**	0.23	0.46	0.44
YA	2.53	2.10	2.28	2.52	**4.54**	0.15	**0.70**	0.16	0.32	0.41
YB	1.85	1.70	1.78	1.23	**3.22**	0.14	**0.33**	0.13	0.11	0.32
YC	2.00	1.98	1.77	1.23	**3.25**	0.20	**0.49**	0.10	0.12	0.29
YD	1.90	1.70	1.84	1.23	**3.22**	0.17	**0.33**	0.16	0.11	0.32
YE	2.73	1.99	2.49	2.52	**4.55**	0.25	**0.61**	0.26	0.32	0.41

Table 3.32 – Maximum per alignment of the values of $\alpha_{b,V}$ for each case study

	Absolute values					Relative values (RV)				
	A.I	A.II	A.III	B.I	C.I	A.I	A.II	A.III	B.I	C.I
X1	1.69	1.51	1.55	1.67	**2.39**	0.33	**0.46**	0.15	0.22	0.33
X2	1.38	1.29	1.23	0.89	**2.02**	0.00	0.12	0.03	0.09	**0.20**
X3	1.44	1.40	1.32	0.92	**2.25**	0.04	0.22	0.11	0.12	**0.34**
X4	1.67	1.38	1.59	1.72	**2.34**	0.32	**0.33**	0.19	0.26	0.30
YA	1.58	1.53	1.52	1.60	**2.41**	0.24	**0.46**	0.13	0.14	0.33
YB	1.42	1.42	1.29	1.05	**2.16**	0.03	0.24	0.09	0.13	**0.29**
YC	1.43	1.73	1.32	1.02	**2.17**	0.01	**0.47**	0.09	0.10	0.26
YD	1.49	1.42	1.34	1.05	**2.16**	0.08	0.24	0.13	0.12	**0.29**
YE	1.70	1.48	1.64	1.60	**2.38**	0.34	**0.41**	0.22	0.14	0.31

Table 3.33 – Maximum per alignment of the values of α_c for each case study

	Absolute values					Relative values (RV)				
	A.I	A.II	A.III	B.I	C.I	A.I	A.II	A.III	B.I	C.I
X1	1.21	2.81	1.09	**5.75**	1.64	0.40	**0.97**	0.17	0.37	0.39
X2	0.98	**1.68**	0.89	1.00	1.14	0.26	**0.83**	0.12	0.16	0.26
X3	0.87	**1.05**	0.85	0.93	0.98	0.13	**0.14**	0.07	0.08	0.09
X4	1.22	3.12	1.09	**5.19**	1.64	0.41	**1.19**	0.17	0.23	0.39
YA	1.22	3.12	1.09	**5.75**	1.64	0.41	**1.19**	0.17	0.37	0.39
YB	1.03	**1.81**	0.91	1.13	1.18	0.33	**0.98**	0.14	0.22	0.31
YC	1.08	**1.94**	0.94	0.87	1.21	0.38	**1.03**	0.17	0.17	0.34
YD	0.88	**1.34**	0.86	1.27	1.05	0.13	**0.47**	0.07	0.37	0.17
YE	1.21	2.81	1.09	**5.75**	1.64	0.40	**0.97**	0.17	0.37	0.39

To provide for a better interpretation of the results the values in bold relate to the maximum value per alignment of the five case studies and the highlighted values to the maximum value of each parameter. Analysing the absolute values it is possible to conclude that the case study **C.I** is the conditioning one for both of the internal forces in the beams (bending moment and shear force). For the columns, the maximum values relate to the shear walls. If these are not taken in consideration the conditioning situation is the **A.II**.

Comparing now the results of the relative values is possible to conclude that, regarding the beams, the case study in which the variation between the regular and irregular models is higher is mainly the **A.II**. This is also true for the columns as could be expected, given the stiffness of that model.

From these results is possible to conclude that the case study in which the occurrence of the studied irregularity is more severe to the regular beams and for the columns, when compared with a regular model, is for the case **A.II**.

The major conclusions for the regular beams and for the columns, taken from this parametrical analysis, are the following:

- In structures with lower number of floors and therefore stiffer, the effect of discontinuing a column is more severe than in structures with more floors (more flexible);
- In situations with shorter spans the seismic loads gain relevance when compared with the gravity loads, as expected;
- The presence of shear walls, by controlling the overall behaviour of the structure under horizontal loading, reduces the negative effect of the discontinued column in softer elements, concentrating them in the stiffer ones.

Finally, Table 3.34 presents the maximum values of $\alpha_{b,M}$ and $\alpha_{b,V}$, per alignment and for the transfer beams for each of the models in terms of absolute and relative values. The values of α_c are not presented given that they were already analysed previously.

Table 3.34 – Maximum per alignment of the values of $\alpha_{b,M}$ and $\alpha_{b,V}$ for each case study and for the transfer beam

		Absolute values					Relative values				
		A.I	A.II	A.III	B.I	C.I	A.I	A.II	A.III	B.I	C.I
$\alpha_{b,M}$	X1	0.89	0.84	0.86	0.90	**0.95**	-0.59	**-0.31**	-0.56	-0.34	-0.70
	X2	0.87	0.88	0.80	0.79	**0.89**	-0.47	-0.31	-0.49	**-0.16**	-0.64
	YA	0.88	0.83	0.84	**0.94**	0.93	-0.60	**-0.33**	-0.57	-0.50	-0.71
	YB	**0.85**	0.84	0.78	0.80	0.82	-0.48	-0.34	-0.51	**-0.28**	-0.66
	YC	0.86	0.88	0.83	0.79	**0.88**	-0.49	-0.34	-0.48	**-0.28**	-0.65
$\alpha_{b,V}$	X1	0.86	0.80	0.83	**0.99**	0.87	-0.33	**-0.22**	-0.38	-0.27	-0.52
	X2	0.82	0.81	0.80	0.78	**0.84**	-0.41	-0.29	-0.33	**-0.05**	-0.50
	YA	0.84	0.79	0.82	0.83	**0.86**	-0.34	**-0.25**	-0.39	-0.41	-0.53
	YB	0.81	0.79	0.78	0.79	**0.83**	-0.41	-0.31	-0.35	**-0.15**	-0.51
	YC	0.82	0.80	0.81	0.78	**0.86**	-0.42	-0.32	-0.33	**-0.16**	-0.50

In addition to the values in bold (maximum per alignment) there are values with red font that indicate the minimum values per alignment.

From the analysis of the absolute values it is possible to conclude that in most of the cases the conditioning case is the **C.I**. Again, as concluded for the regular beams, the reason for this is related with the span. For shorter spans the internal forces due to vertical loads are reduced and the seismic action gains relevance.

Analysing now the relative values the conclusions are different. The case that presents higher values of α_b for the peripheral alignments is the **A.II** and for the interior ones is the **B.I**. This is as expected given that these models are stiffer and, therefore, the seismic action is more conditioning.

Another important conclusion is that **C.I** is the case with the highest reduction. The reason for this is connected mostly with the seismic action, given that in this model the irregular span (longer span of the TB) is shorter than in the other models, leading to a reduction in the oscillating mass. Thus, the overall internal forces due to the seismic loading is lower in this case, leading also to a lower value of the α_b parameters.

The major conclusions for the transfer beams, taken from this parametrical analysis, are the following:

- For the transfer beams the fundamental load combination is always more conditioning than seismic load combination;
- For stiffer structures seismic load combination gains more relevance. For the case with shear walls (**B.I**) there is a situation in which the SLC is almost equal to the FLC, but lower nonetheless;
- As a rough approximation it is possible to assume for the TB:

$$\frac{SLC}{FLC} \approx 0.80 \; to \; 0.90$$

These values are meant to be seen as an indication and not as an absolute rule because there are many factors that influence these values. Not only have the considered variables but others like the behaviour factor, the complexity of the structure and the value of the vertical loads.

Chapter 4

Non-Linear Inelastic Analysis

The previous chapter led to the conclusion that in all of the wide range of cases considered, the gravity loads are the conditioning load combination for the design of the transfer beam. In this part of the dissertation non-linear seismic analyses are carried out for one of the situation deemed to be more severe for the structure, regarding not only the transfer beam behaviour but specially the global response.

The difficulties inherent to non-linear modelling, analysis and result interpretation led to the decision to focus this part of the study on a single irregular (and a matching regular) model. These non-linear analyses were intended to assess the detrimental effects due to the presence of this irregularity as well as, if so confirmed, to what extent the seismic performance is affected. It is also important to verify if further non-linear studies are necessary for better understanding the effect of irregularities due to the discontinuity of a column.

In this chapter the non-linear analyses were carried out using the program SeismoStruct [40] which is a program specially developed for non-linear seismic analyses, including different material constitutive relationships, elements classes, loadings, etc. To generate the artificial accelerograms considered in the analyses the program SeismoArtif [39] was used.

The case study considered for the development of the non-linear analyses was the **M_A.II**, this model has 2 floors with a height between them of 3m. The 4 spans in the x direction and the 3 spans in the y direction are all 7m long and no shear walls were considered. The choice of this model is based on the results of the parametric study that show that this case generally has the highest relative values for the parameters regarding both the regular beams and the columns (Table 3.31 to Table 3.33). Regarding the transfer beam, the considered model also presents high relative values in the peripheral alignments (Table 3.34).

Given the fact that, for the chosen model, the most severe situation occurs when the irregularity is present in peripheral alignments, the discontinued column considered for this study was **B1.** This situation is among those that had the highest difference between the regular and irregular models.

4.1. Methodologies

4.1.1. Definition of the Non-Linear Models

Before defining the models it is important to refer that in the process of computation of the steel reinforcements it was concluded that the cross-sections of the columns should have been larger and therefore there was the need of redesign the cross-sections. The new cross-sections adopted for the non-linear analysis are presented in Table 4.1. This change was not reflected in the parametric analysis.

Table 4.1 – Dimensions of the cross-sections adopted for the non-linear analysis

Element	Position	H [m]	B [m]
V_0.6x0.3	Regular beams	0.60	0.30
V_1.1x0.4	Transfer beam	1.10	0.40
P_0.4x0.4	Peripheral columns	0.40	0.40
P_0.5x0.5	Internal columns	0.50	0.50

It is also important to mention that for the design of the steel reinforcement the behaviour factors considered were, for the horizontal response spectrum of the regular model, 3.0 and, for the horizontal and vertical response spectrum of the irregular model, 2.4 and 1.5, respectively.

i.<u>Design of the Pre-Stress Tendon</u>

For the pre-stress tendon considered in the irregular model it was assumed to follow the pre-design criterion that the vertical displacement in the zone of the discontinued column should be approximately 0 for the Quasi-Permanent Load Combination.

The considered layout of the tendon is as presented in Figure 4.1.

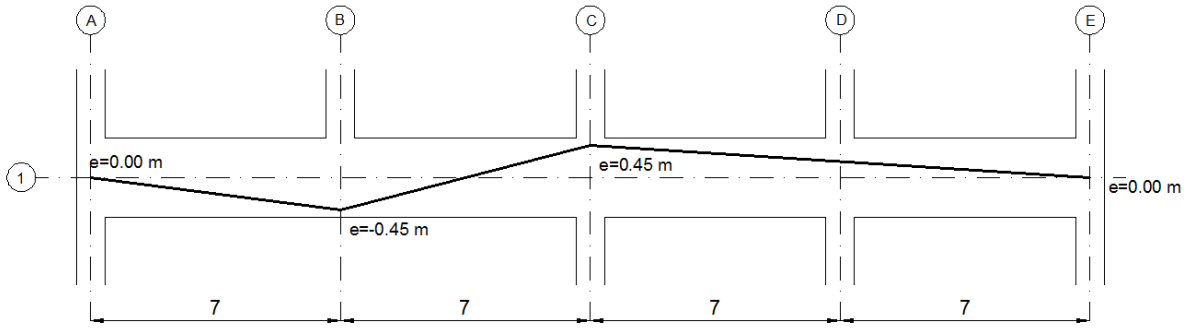

Figure 4.1 – Layout of pre-stress tendon [m]

For a pre-stress pushing force (P) of 1000 kN the forces equivalent to the effect of the pre-stress are those presented in Figure 4.2.

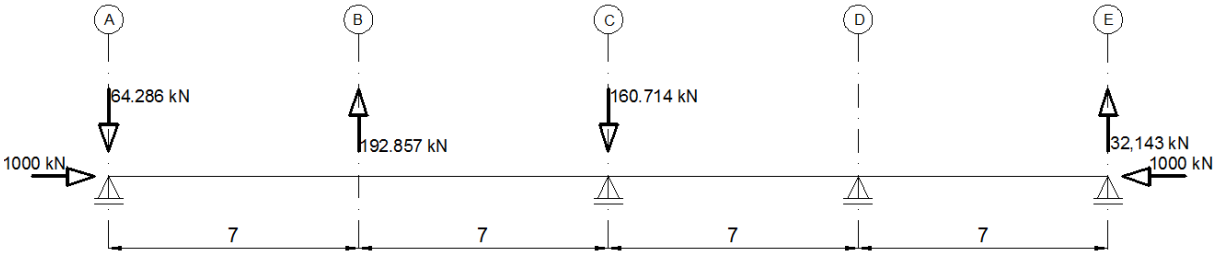

Figure 4.2 – Loads equivalent to the effect of the pre-stress

Finally, Table 4.2 summarizes the vertical displacement for the quasi-permanent load combination and for three solutions for the post-tension pre-stress tendon.

Table 4.2 – Vertical displacement for $t = \infty$

Load Type	Vertical Displacement [m]
QPLC	-0.0291
Pre-Stress [P=1000kN]	+0.0102
4 tendons 6/4 Super [P=2560 kN]	+0.0259
3 tendons 6/7 Normal [P=3150 kN]	+0.0322
1 tendon 6/19 Normal [P=2850 kN]	+0.0291

The adopted solution is the one termed *1 tendon 6/19 Normal* with a pushing force at infinite time (P_∞) of 2850 kN. This choice is based on the fact that this solution is the one that best meets the imposed pre-design criterion. Apart from this, being this a study case, the construction viability of the solution itself is not as relevant as if this was a practical case. Even so, the adopted solution is perfectly feasible.

ii.Design of the Ordinary Reinforcement

For the design of the ordinary reinforcement of the various elements the following criteria were considered:

- Elements with equal cross-section should have the same reinforcement;
- The reinforcement is constant along the length, this means that the curtailment of rebar is not considered;
- In the case of the beams, the reinforcement of the top and bottom faces is defined based on the maximum negative and positive bending moments, respectively;
- For the columns, the reinforcement along the four faces of the cross-section should be the same.
- To take into consideration the bi-directional bending only 70% of the resistant moment in the predominant direction is considered.
- The effect equivalent to the pre-stress is considered on the side of the actions.

a) Beams V_0.6x0.3 (Regular Beams)

Table 4.3 presents the maximum values of the bending moments for each cross-section for the envelope of the Ultimate Limit State (ULS) for both the regular and the irregular models.

Table 4.3 – Design reinforcement for the beams V_0.6x0.3

		M_{ED} [kNm]	μ	ω	$A_{s,d}$ [cm²]	$A_{s,min}$ [cm²]
Regular	+	131.3	0.072	0.076	5.75	9.53
	-	296.5	0.163	0.184	13.94	9.53
Irregular	+	139.8	0.077	0.081	6.15	9.53
	-	346.7	0.191	0.220	16.72	9.53

Based on the values of the previous table the adopted reinforcements for both the regular and the irregular models are presented in Table 4.4.

Table 4.4 – Adopted reinforcement for the beams V_0.6x0.3

		$A_{s,a}$		M_{RD} [kNm]
V_0.6x0.3	Bottom face	$4\phi 20$	12.57 cm²	270.5
	Top face	$4\phi 25$	19.63 cm²	396.2

The design of the transverse reinforcement is based on the principle of capacity design according to the EN1998-1 [15]. The most relevant results are those presented in the Table 4.5.

Table 4.5 – Design shear force for the beams V_0.6x0.3

	Regular Model		Irregular Model	
End-section	i	j	i	j
L [m]	7.0		7.0	
M_{RD} [kNm]	270.5	-396.2	270.5	-396.2
V_{QPLC} [kN]	99.99	-122.60	98.07	-121.37
V_{CD} [kN]	$\pm$95.24		$\pm$95.24	
V_{FLC} [kN]	155.84	-190.83	141.17	200.29
V_{ED} [kN]	195.23	-217.84	193.31	216.61

With the maximum value of the shear force obtained, the stirrups may be determined according to:

$$V_{zcot\theta} \approx 200\ kN \rightarrow \frac{A_{sw}}{s} = 9.29\ cm^2/m$$

Finally, and keeping in mind the limit imposed by the EN1998-1 [15] for the spacing of the stirrups in the zones next to the columns the following transverse reinforcement was adopted:

Stirrups $\phi 10//0.15m$ with 2 legs (10.48 cm^2/m)

b) Beam V_1.1x0.4 (Transfer Beam)

The design values of the envelope for the flexural ULS are presented in Table 4.6.

To be noted that for serviceability limit state (SLS) the pre-stress (PS) tendon has a mean tensile stress of 1070MPa therefore allowing the simplifying assumption that the pre-stress steel presents a $\sigma - \varepsilon$ diagram similar to that of the ordinary steel reinforcement.

Besides, is important to refer that $A_{s,PE}$ is the area of the PS tendon and $\Delta A_{s,d} = A_{s,d} - A_{s,PE}$.

Table 4.6 – Design reinforcement for the beam V_1.1x0.4

	M_{ED} [kNm]	μ	ω	$A_{s,d}$ [cm²]	$A_{s,PE}$ [cm²]	$\Delta A_{s,d}$ [cm²]	$A_{s,min}$ [cm²]
+	315.1	0.039	0.040	7.43	26.60	-19.17	17.33
-	450.0	0.056	0.058	10.72	26.60	-15.88	17.33

Based on the values of the previous table the adopted reinforcements for the transfer beam (on the irregular model) is presented in Table 4.7.

Table 4.7 – Adopted reinforcement ($A_{s,a}$) for the beam V_1.1x0.4

V_1.1x0.4	Bottom face	$4\phi 25$	19.63 cm²
	Top face	$4\phi 25$	19.63 cm²

For the computation of the transverse reinforcement according with the rules of the capacity design imposed in the EN1998-1 [15], it is necessary to determine the resistant bending moment which varies with the position of the PS tendon. Therefore Table 4.8 presents the values for the resistant bending moment and shear force due to the QPLC, the FLC and the capacity design for the sections over the columns.

Table 4.8 – Design shear force for the beams V_1.1x0.4

	A-right	B-left	B-right	C-left	C-right	D-left	D-right	E-left
M_{RD}^{+} [kNm]	1333.9	1854.6	1854.6	813.2	813.2	1073.5	1073.5	1333.9
M_{RD}^{-} [kNm]	-1333.9	-813.2	-813.2	-1854.6	-1854.6	-1594.2	-1594.2	-1333.9
V_{CD}^{+} [kN]	455.5		232.3		418.3		418.3	
V_{CD}^{-} [kN]	-306.7		-529.9		-343.9		-343.9	
V_{QPLC} [kN]	-69.1	111.1	-97.6	60.9	-67.9	90.6	-103.2	77.0
$V_{QPLC} + V_{CD}$ [kN]	-375.8	566.6	-627.5	293.3	-411.8	508.9	-447.1	495.3
V_{ELU} [kN]	-193.4	74.7	-19.2	214.4	-149.8	83.8	-142.7	125.4
V_{ED} [kN]	-375.8	566.6	-627.5	293.3	-411.8	508.9	-447.1	495.3

With the maximum value of the shear force obtained, the stirrups may be determined according to:

$$V_{zcot\theta} \approx 586.7\ kN \rightarrow \frac{A_{sw}}{s} = 7.49\ cm^2/m$$

Based on this value the adopted solution for the transverse reinforcement was:

Stirrups $\phi 10//0.15m$ with 2 legs (10.48 cm^2/m)

c) Columns

Table 4.9 presents the values for bending with axial force that determine the design of the columns P_0.4x0.4, for both the regular and irregular models.

Table 4.9 – Design reinforcement for the columns

		N_{ED} [kN]	M_{ED} [kNm]	ν	μ	$\mu/0.7$	ω	$A_{s,a}$ [cm^2]
P_0.4x0.4	Regular	-258.2	128.2	-0.081	0.100	0.143	0.285	20.97
	Irregular	-177.9	187.9	-0.056	0.147	0.210	0.480	35.31
P_0.5x0.5	Regular	-1093.9	304.2	-0.219	0.122	0.174	0.240	27.59
	Irregular	-1190.1	418.6	-0.238	0.167	0.239	0.380	43.68

Based on the presented results the most detrimental model is irregular. Although, to allow for a better comparison between the regular and the irregular model the same steel reinforcement is considered for both models, keeping in mind that that steel reinforcement relates to a value between those two models. Considering this, the adopted steel reinforcement is the following:

Steel reinforcement $3\phi 25$ in each face of the column (29.45 cm^2) for column P_0.4x0.4

Steel reinforcement $4\phi 25$ in each face of the column (39.27 cm^2) for column P_0.5x0.5

In order to ensure a ductile behaviour of the concrete, an adequate confinement is needed. To guarantee this, the columns stirrups must be designed according to the EN1998-1 [15], based on the principles of the capacity design. This process is iterative therefore only the final solution results are presented. The adopted solution for the transverse reinforcement is.

Stirrups $\phi 10//0.15m$ (10.48 cm^2/m) with 4 legs (and a perimeter of 2.0m) for column P_0.4x0.4

Stirrups $\phi 10//0.15m$ (10.48 cm^2/m) with4 legs (and a perimeter of 2.3m) for column P_0.5x0.5

The parameters defined in the paragraph 5.4.3.2.2 (8) of the EN1998-1 [15] are presented in Table 4.10. These are based on the longitudinal and transversal reinforcement adopted.

Table 4.10 – Parameters for the verification 5.4.3.2.2 (8) of the EN1998-1 [15]

	μ_ϕ	α	$\varepsilon_{sy,d}$	$b_c = h_c$	$b_0 = h_0$	$\omega_{wd,adop}$
P_0.4x0.4	5.0	0.44	0.00218	0.40	0.33	0.143
P_0.5x0.5	5.0	0.60	0.00218	0.50	0.43	0.106

The values regarding the conditioning element for each model is presented in Table 4.11.

Table 4.11 – Design value of the transverse reinforcement for the columns

		N_{ED} [kN]	M_{RD} [kNm]	V_{ED} [kN]	$A_{sw,d}/s$ [cm^2/m]	$\omega_{wd,calc}$
P_0.4x0.4	Regular	-526.2	173.4	126.8	4.63	0.069
	Irregular	-987.9	215.5	157.6	5.75	0.165
P_0.5x0.5	Regular	-1191.9	355.8	260.2	7.38	0.093
	Irregular	-1226.1	359.8	263.0	7.47	0.098

To be noted that the value of $\omega_{wd,calc}$ of the irregular model for the column **P_0.4x0.4** is higher than the adopted value (due to the effect of the pre-stress). This only occurs in a single element, for all others the adopted reinforcement assures that the EN1998-1 [15] is respected.

4.1.2. Modelling of the Structures in SeismoStruct

i.Constitutive Relationship of the Materials

a) Concrete

The concrete fibres were modelled with the constitutive relationship proposed by Mander *et al.* [26] (non-linear concrete model). As stated in the user guide of SeismoStruct [40], "this is a uniaxial nonlinear constant confinement model, initially programmed by Mandas [25], that follows the constitutive relationship proposed by Mander *et al.* [26] and the cyclic rules proposed by Martinez-Rueda and Elnashai [27]. The confinement effects provided by the lateral transverse reinforcement are incorporated through the rules proposed by Mander *et al.* [26] whereby constant confining pressure is assumed throughout the entire stress-strain range."

The constitutive relationship defined by Mander *et al.* [26] for the monotonic loading of concrete is presented in Figure 4.3.

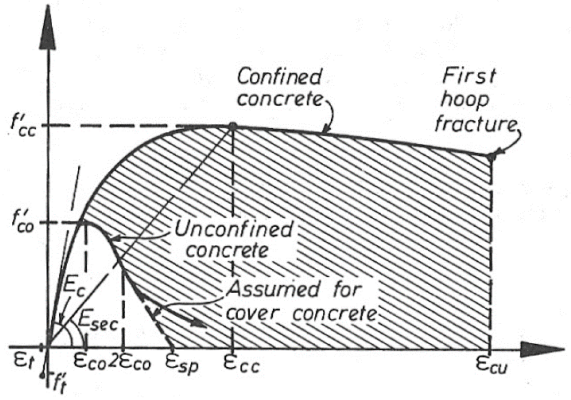

Figure 4.3 – Constitutive relationship of the concrete under monotonic loading [26]

Where f'_{cc} and f'_{c0} are, respectively, the confined and unconfined concrete compressive strength and f'_t the concrete tensile strength. The corresponding strains to the previously defined strength values are, in the same order, ε_{cc}, ε_{c0} and ε_t. The ultimate strain for the confined and unconfined concrete are represented by ε_{cu} and ε_{sp}, respectively.

E_c represents the initial modulus of elasticity of the concrete and E_{sec} the secant modulus of elasticity at peak stress, both defined according to equations (4.1) and (4.2).

$$E_c{}^{ii} = 5000\sqrt{f'_{c0}}\,MPa \tag{4.1}$$

$$E_{sec} = \frac{f'_{cc}}{\varepsilon_{cc}} \tag{4.2}$$

The constitutive relationship presented in Figure 4.3 is described by equation (4.3).

$$f_c = \frac{f'_{cc} \cdot \frac{\varepsilon_c}{\varepsilon_{cc}} \cdot r}{r - 1 + \left(\frac{\varepsilon_c}{\varepsilon_{cc}}\right)^r} \tag{4.3}$$

Where f_c, ε_c are the compressive concrete stress and strain, respectively, and with ε_{cc} and r defined by equations (4.4) and (4.5).

$$\varepsilon_{cc} = \varepsilon_{c0}\left(1 + 5\left(\frac{f'_{cc}}{f'_{c0}} - 1\right)\right) \tag{4.4}$$

$$r = \frac{E_c}{E_c - E_{sec}} \tag{4.5}$$

In order to fully define the behaviour of the concrete under cyclic loading a set of analytical expressions were proposed by Mander *et al.* [26] that defined the unloading and reloading branches of the constitutive relationship in compression and tension. These expressions are not presented here given that they are outside the scope of this work.

The values adopted for the different parameters, entered in the program are presented in Table 4.12.

Table 4.12 – Properties adopted for the concrete

Mean compressive strength (f_{cm}) [kPa]	38000
Mean tensile strength (f_{ctm}) [kPa]	3800
Modulus of elasticity (E_c) [kPa]	28 970 000
Strain at peak stress [m/m]	0.002
Specific weight (γ_c) [kN/m^3]	24

b) Steel Reinforcement

The chosen constitutive relationship for modelling the steel reinforcement was the Menegotto and Pinto [28] steel model. As stated in the user guide of SeismoStruct [40], "this is a uniaxial steel model initially programmed by Yassin [43] based on a simple, yet efficient, stress-strain relationship proposed by Menegotto and Pinto [28], coupled with the isotropic hardening rules proposed by Filippou *et al.* [19]. The current implementation follows that carried out by Monti *et al.* [29].

[ii] In SeismoStruct [40], E_c is defined by $E_c = 4700\sqrt{f'_{c0}}\,MPa$

An additional memory rule proposed by Fragiadakis *et al.* [20] is also introduced, for higher numerical stability/accuracy under transient seismic loading. Its employment should be confined to the modelling of reinforced concrete structures, particularly those subjected to complex loading histories, where significant load reversals might occur.

As discussed by Prota *et al.* [35], with the correct calibration, this model, initially developed with ribbed reinforcement bars in mind, can also be employed for the modelling of smooth rebars, often found in existing structures".

The constitutive relationship proposed by Menegotto and Pinto [28] is described in equation (4.6).

$$\sigma^* = b\varepsilon^* + \frac{(1-b)\varepsilon^*}{(1+\varepsilon^{*R})^{1/R}} \tag{4.6}$$

Where:

σ^*, ε^* are the normalized stress and strain given by equation (4.7) and (4.8), respectively.

$$\sigma^* = \frac{\sigma - \sigma_r}{\sigma_0 - \sigma_r} \tag{4.7}$$

$$\varepsilon^* = \frac{\varepsilon - \varepsilon_r}{\varepsilon_0 - \varepsilon_r} \tag{4.8}$$

b is the strain-hardening ratio given by equation (4.9).

$$b = \frac{E_T}{E_0} \tag{4.9}$$

R is a parameter allows for a good representation of the Bauschinger effect by influencing the shape of the transition curve, given by the equation (4.10).

$$R\left(\xi_p^n\right) = R_0 - \frac{a_1 \cdot \xi_p^n}{a_2 + \xi_p^n} \tag{4.10}$$

The parameters used in equations (4.7) to (4.10) are defined according to Figure 4.4.

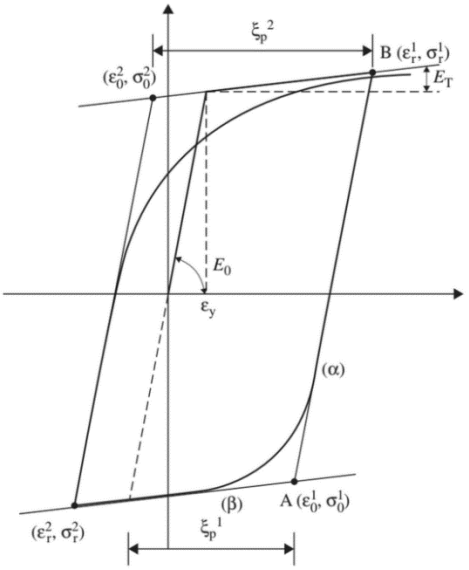

Figure 4.4 – Constitutive relationship of the steel rebar under cyclic loads [20]

Where σ_0 and ε_0 are the coordinates of the point A and σ_r and ε_r are the coordinates of the point B. ξ_p^n is the plastic excursion at the current semicycle defined by $\xi_p^n = \varepsilon_r^n - \varepsilon_y^n$. Furthermore, R_0 is the value of R during the first loading, defined experimentally along with a_1 and a_2.

The isotropic hardening rule proposed by Filippou *et al.* [19] is defined in equation (4.11).

$$\Delta\sigma_I = a_3 \left(\frac{\varepsilon_{max}}{\varepsilon_y} - a_4 \right) \sigma_y \tag{4.11}$$

Where ε_{max} is the maximum strain reached in the direction opposite to the current loading and a_3 and a_4 are parameters determined experimentally.

Based on these principals the values adopted for the different parameters, entered in the program, are presented in Table 4.13.

Table 4.13 – Properties adopted for the steel rebars

Modulus of elasticity (E_s) [GPa]	200
Yield strength (f_y) [MPa]	500
Strain hardening parameter (b) [-]	0.005
Transition curve initial shape parameter (R_0) [-]	20
Transition curve shape calibrating coefficients (a_1) [-]	18.5
Transition curve shape calibrating coefficients (a_2) [-]	0.15
Isotropic hardening calibrating coefficients (a_3) [-]	0
Isotropic hardening calibrating coefficients (a_4) [-]	1
Fracture/buckling strain [-]	0.100
Specific weight (γ_s) [kN/m^3]	78

ii.Sections and Elements of the Model

Developing a model with the software SeismoStruct [40] requires that the cross-sections be previously defined; a different section must be defined whenever there is a variation in the reinforcement (longitudinal or transverse), in the geometry of the section, in the cover thickness or in the materials that composed the section.

In the case of the regular beams and columns there is no variation along the element, therefore only one section is defined for each of these structural elements. For the transfer beam, due to the variation on the position of the pre-stress tendon, various sections must be defined according with the integration sections and the position of the tendon.

Regarding the elements, in all cases the integration method was the force-based. The elements based on the flexibility formulation (force based) approximate the results of the stress field along the element. This strictly satisfies the equilibrium conditions, regardless of the non-linearity of the material, hence leading to a better solution than when displacement-based elements are used. The advantages (and disadvantages) of force-based elements over the displacement-based are comprehensibly explained in the study by Correia *et al.* [9].

For the regular beams the adopted element class was the **inelastic force-based frame element**. The element was divided in 5 integration sections and each section was divided in 150 fibres as presented in the Figure 4.5 on the left. All the integration sections were the same.

The element class adopted for the transfer beam was also the **inelastic force-based frame element** with 5 integration section of 200 fibres each. The integration sections varies accordingly to the layout of the PS tendon. Some of those integration sections may be observed in the right side of Figure 4.5.

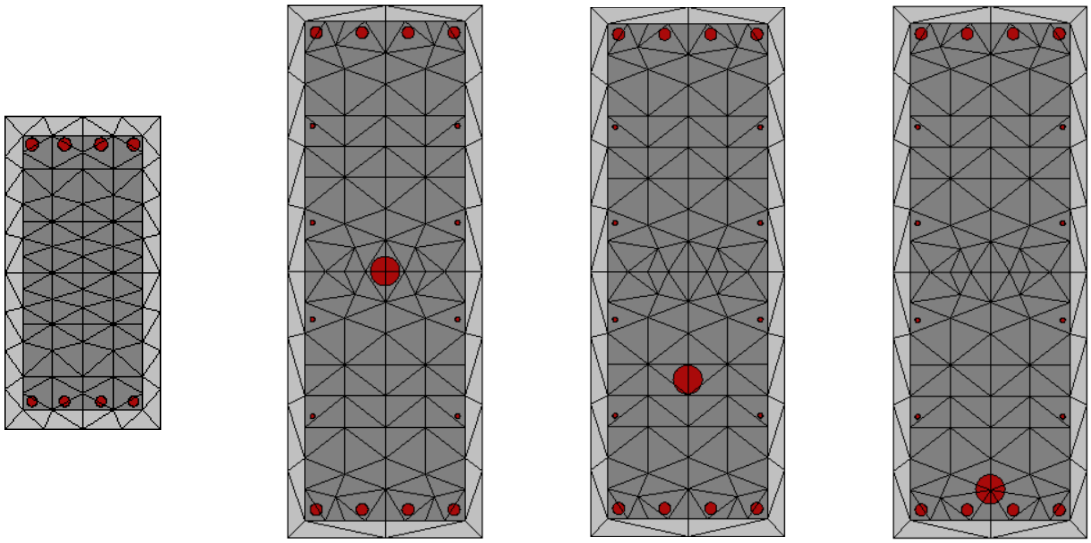

Figure 4.5 – Fibres defined for the regular beam section (right) and for the transfer beam section (left)

As for the columns the chosen element class was the **inelastic plastic-hinge force-based frame element** with 150 fibres per section and a plastic-hinge length equal to the height of the section (around 15% of the element length in each end). The reason for this choice is that in the case of the columns the non-linearity will be concentrated next to the ends of the element and therefore, without losing much accuracy in the results, it is possible to reduce the computation time. Figure 4.6 illustrates the considered subdivision of the column's cross-section into fibres.

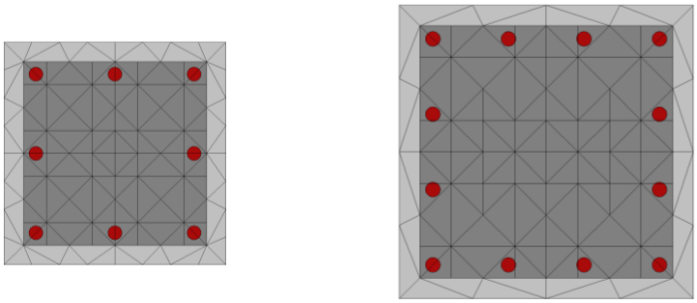

Figure 4.6 – Fibres defined for the columns P_0.4x0.4 (left) and P_0.5x0.5 (right)

To determine the adequate class of elements, number of integration sections, number of fibres and plastic-hinge length various tests were carried out in order to assure that the benefit obtained by reducing the computation time would not give way to a loss in the overall quality of the results.

As defined before, the effect of the pre-stress is partly modelled by the equivalent loads. Although, the part of the effect associated with the variation of the stress in the tendon due to the seismic loads is not accounted by the equivalent loading.
Given the fact that the used software does not allow for the consideration of different constitutive relationships for the steel reinforcement nor the possibility to model directly the pre-stress tendon, the adopted solution was to model the resisting part of the pre-stress as an ordinary reinforcement and use performance criteria to control the stress and strain in the steel rebar that models the pre-stress tendon.

iii.Constraints

In SeismoStruct [40] the slabs are not explicitly modelled which leads to a need for special care of two different aspects of the modelling, one of which is mentioned in the next topic.
One of these aspects is related with the rigid diaphragm effect that is ensured by the slab. Without the presence of the slab, a constraint at the level of each floor must be defined, ensuring that the displacements on the horizontal plan of the nodes of the same floor are related. These constraints are modelled by defining a master node at each floor level and all the other nodes (on that floor) as slave nodes. The master node should be located close to the floor centre.
With the definition of the rigid diaphragm there is also the need to check the properties of the constraints in order to define its type. Normally in linear elastic analysis the constraints are computed by geometrical transformations, although in a geometrically non-linear analysis they might induce problems in numerical convergence. Therefore, SeismoStruct [40] only implements the constraints by penalty functions or by Lagrange multipliers.
By default the software chooses the penalty functions for being easier to compute and by having less convergence problems. On the other hand the penalty functions have an allowable range and must be chosen by the user which might lead to some errors in the results. The adopted methodology was the penalty functions.
Regarding the choice of the rigid diaphragms weights, various values were tested in order to determine which would lead to the desired effect. To be noted that choosing a large number is not sufficient, the value cannot be so high that the beams are not allowed to elongate when under cyclic actions. After some iterations, the adopted value for the rigid diaphragms weight was 10E+7.

iv.Gravity Loads and Mass Source

As mentioned in the previous topic, the absence of the slab implies a certain level of care on the modelling of structures. Beside the need to consider a rigid diaphragm is required that the loads due to the quasi-permanent load combination be assigned as additional mass to the beam elements or as lumped mass. These masses should not include the self-weight of the modelled frames.
The only load that is directly applied to the structure are the ones related to effect of the pre-stress and must not be considered as structural mass.

In SeismoStruct [40] project settings it is possible to alter the definitions of both the mass and loads of the structures. The mass should be defined as “from frame elements (specific weight and additional section mass), and mass elements (lumped or distributed)”. The loads must be defined as “from applied loads and, only in the gravity direction, based on the g (9,81m/seg^2) value”.

v.Damping

In SeismoStruct [40] there are two ways to define the damping of the structure, either is done in the project settings and affects all structural elements or is done individually for each element (which is useful if there are elements with varying damping characteristics). In this work the damping was defined equally for all elements.

The damping matrix (C) may be proportional to either the stiffness matrix (K) or the mass matrix (M), as indicated in equation (4.12) but may also be proportional to both, as indicated in equation (4.13). This latter is denominated Rayleigh damping and was the one considered in this work.

$$C = a_M \cdot M \qquad \text{or} \qquad C = a_K \cdot K \tag{4.12}$$

$$C = a_M \cdot M + a_K \cdot K \tag{4.13}$$

In these equations the proportionality constants a_M and a_K have units of sec^{-1} and sec, respectively, and might be defined, according to Clough and Penzien [7], by equation (4.14).

$$\begin{Bmatrix} a_M \\ a_K \end{Bmatrix} = 2\frac{(\omega_m \omega_n)}{\omega_n^2 - \omega_m^2} \begin{bmatrix} \omega_n & -\omega_m \\ -1/\omega_n & 1/\omega_m \end{bmatrix} \begin{Bmatrix} \xi_m \\ \xi_n \end{Bmatrix} \tag{4.14}$$

Where ω_m and ω_n are the circular frequencies and ξ_m and ξ_n the respective damping ratios, as defined according to Figure 4.7.

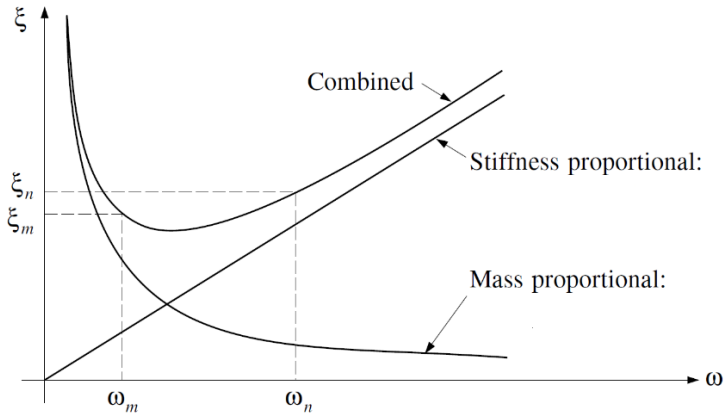

Figure 4.7 – Relation between damping ratio and frequency (for the Rayleigh damping) [7]

Based on the presented, to determine the proportionality constants according to equation (4.14) is necessary to define the two pair of point ($\omega - \xi$). The considered pairs are presented in Table 4.14, and regard the first vibration mode and the sixth vibration mode (last horizontal vibration mode).

Table 4.14 – Values for defining the Rayleigh damping

		Period (T) [s]	Circular Frequency (ω) [rad]	Damping Ratio (ξ) [%]
Regular Model	Mode 1 (n)	0.322	0.494	2
	Mode 2 (m)	0.089	1.788	2
Irregular Model	Mode 1 (n)	0.340	0.468	2
	Mode 2 (m)	0.100	1.592	2

The computed values of a_M and a_K were the presented in Table 4.15.

Table 4.15 – Computed values of the proportionality constants

Model	a_M $[sec^{-1}]$	a_K $[sec]$
Regular	0.6115	0.000444
Irregular	0.5712	0.000492

The damping ratio has a value lower than the usual 5% that concrete structures have because most of the overall structural damping is due to the non-linearity of the materials, which is already taken in consideration in this type of analysis.
Finally, is important to refer that the damping is proportional to the tangent stiffness. If the initial stiffness was considered a much lower value of the damping ratio should have been considered.

4.1.3. Definition of the Analyses

The non-linear study of the structures is carried out in two parts, the first by a **static time-history analysis** in order to compare the response of the structure to a cyclic and a monotonic loading of the regular and irregular models and to determine if there is a global effect on the structure for horizontal loads. The second part regards the study of the structures by a **dynamic time-history analysis** in order to assess if there is an accumulation of inelasticity and damage immediately above the irregularity which is the base for the reduction on the behaviour proposed in the EN1998-1 [15] for structures with vertical irregularities.

i.Non-Linear Static Time-History Analysis

A static time-history analysis, contrarily to the dynamic analysis, does not take in consideration the dissipative forces (inertia and damping). This kind of analysis simply applies loads (forces or displacements) to the structure according to a pre-defined time-history record.
In this analysis a displacement is imposed in the top of the building and the base shear is measured. The considered time-history record of imposed displacements are presented in Figure 4.8 for the cyclic loading. The loading cases are considered in both the x and the y directions.

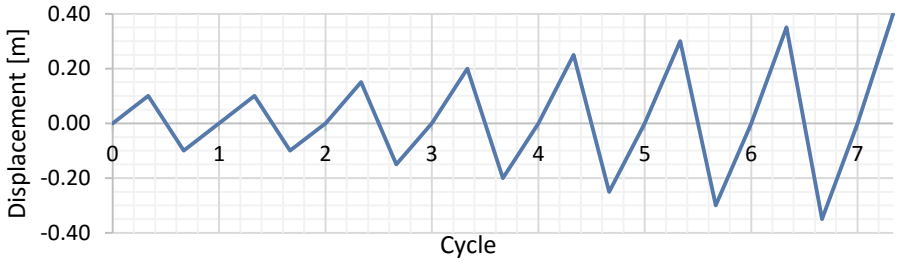

Figure 4.8 – Time-History record of imposed cyclic loading

This type of analysis is much faster to compute. The results of the monotonic loading allow to estimate the maximum base shear of the structure as well as the maximum displacement that is possible to impose, the results of this analysis is similar to attained for a pushover analysis.

ii.Non-Linear Dynamic Time-History Analysis

A non-linear dynamic time-history analysis is one of the types of analysis that better simulates the behaviour of a real structure; the major drawback is the long computation time that make this kind of analysis not very practical in day-to-day design practices. For the present work this analysis was very useful but, due to the reasons presented above, the considered cases were not many and further studies are necessary to fully understand the implications of this irregularity when following this modelling approach.

The time-history records was separated in two groups, the first using a set of artificial accelerograms generated in conformance with the EN1998-1 [15] specifications in order to study in detail the structural behaviour. The second group consisted in a real accelerogram recorded during an earthquake in order to compare the responses of the regular and of the irregular model and to verify if the conclusions taken for the artificial accelerograms remain valid.

a) Artificial Accelerograms

The artificial accelerograms were generated using the program SeismoArtif [39]. In this program, by introducing the data of a given elastic response spectrum, it generates a set of accelerograms compatible with the PGA of the introduced response spectrum. The seismic action type 1 was considered predominant over the seismic action type 2, therefore the response spectrum considered in all the analysis was the one regarding the type 1 for both the vertical and horizontal accelerograms. The considered envelope was a trapezoidal envelope as represented in Figure 4.9.

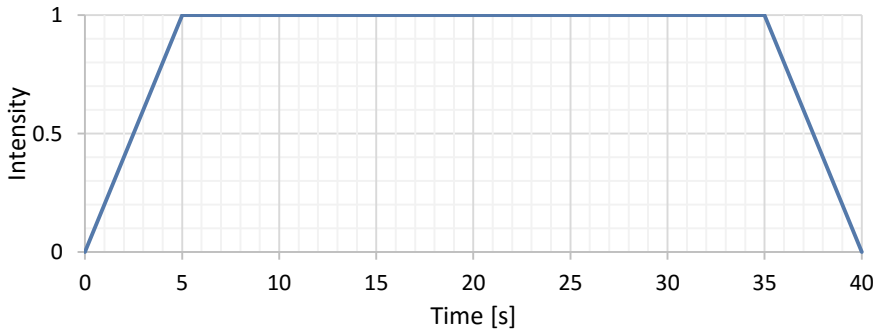

Figure 4.9 – Envelope shape considered for the definition of the artificial accelerograms

The generated accelerograms are presented in Annex D. Three records were generated for each direction (horizontal and vertical). Table 4.16 summarizes some of the more relevant characteristics of these artificial records.

Table 4.16 – Information regarding the artificial accelerograms

	H1	H2	H3	V1	V2	V3
Time step [s]	0.005	0.005	0.005	0.005	0.005	0.005
Total Duration [s]	40	40	40	40	40	40
PGA [g]	0.249	0.274	0.248	0.176	0.216	0.156
Time of the PGA [s]	32.885	11.170	16.395	24.295	17.805	28.905

Figure 4.10 and Figure 4.11 present the elastic response spectrum as defined by the EN1998-1 [15] and by the accelerograms presented previously.

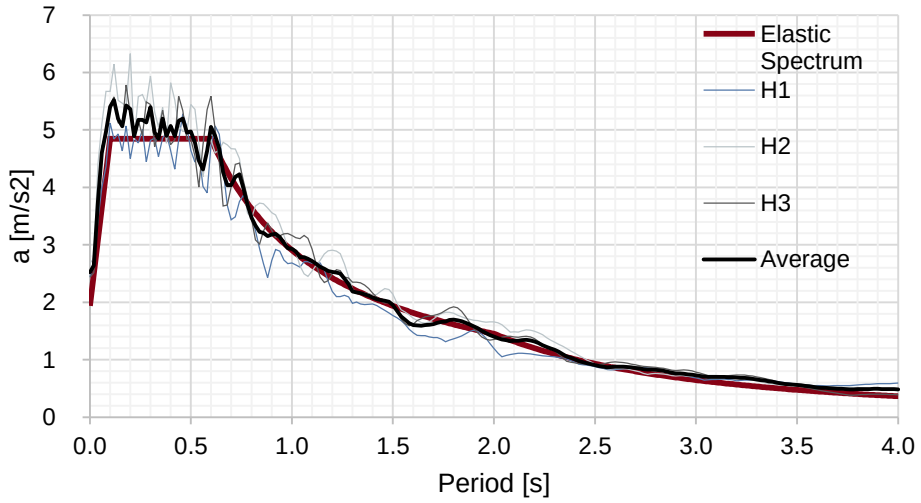

Figure 4.10 – Elastic Response Spectrum for the horizontal component

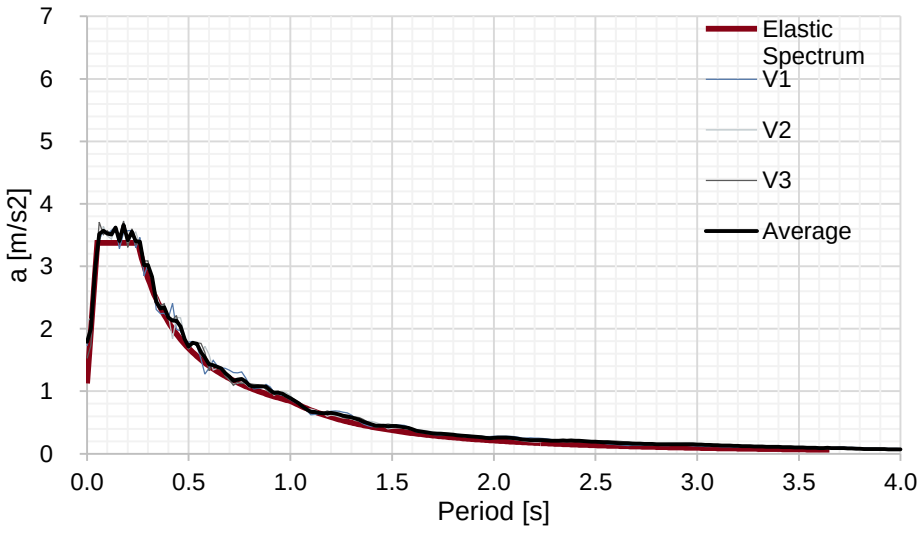

Figure 4.11 – Elastic Response Spectrum for the vertical component

It is possible to conclude, from the presented charts, that in the case of the vertical response spectrum the accelerograms are very close to the one defined by the EN1998-1 [15]. On the other hand, the horizontal accelerograms are not so close to the response spectrum defined according to the EN1998-1 [15].

Based on the presented records, the considered cases (combinations of accelerograms for x, y and z directions) are presented in Table 4.17. To be noted that in paragraph 3.2.3.1.2 of the EN1998-1 [15] are presented specific rules for the generated accelerograms and their combinations.

It should be noted that, according to paragraph 4.3.3.4.3 of the EN1998-1 [15], if less than seven non-linear time-history analyses are considered the design value of the seismic effects should be the most unfavourable of the results obtained for the different analyses. In the present study this was considered too conservative leading to the adoption of the mean value of the maxima results.

Table 4.17 – Considered cases for the analysis

	Accelerograms		
Direction	X	Y	Z
Case A	H1	H2	V1
Case B	H2	H3	V2
Case C	H3	H1	V3

b) Recorded Accelerograms

The recorded accelerograms of a real earthquake were retrieved from the Center for Engineering Strong Motion Data website [5] for the Tohoku earthquake that occurred in Japan on the 11th of March of 2011 at 05:46:24 UTC at the coordinates 38.30N 142.37E and at a depth of 29.0km. The recording station considered was the Tsukidate station (ID MYG004) at 125.9 km to the epicentre.

Figure 4.12, Figure 4.13 and Figure 4.14 present the recorded accelerograms of the mentioned station.

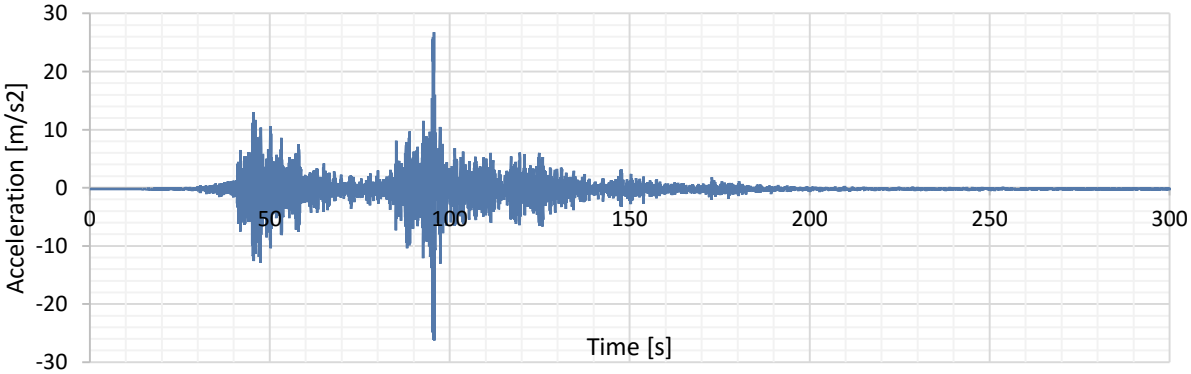

Figure 4.12 – North-South (NS) time-History record for the Tsukidate station for the Tohoku earthquake

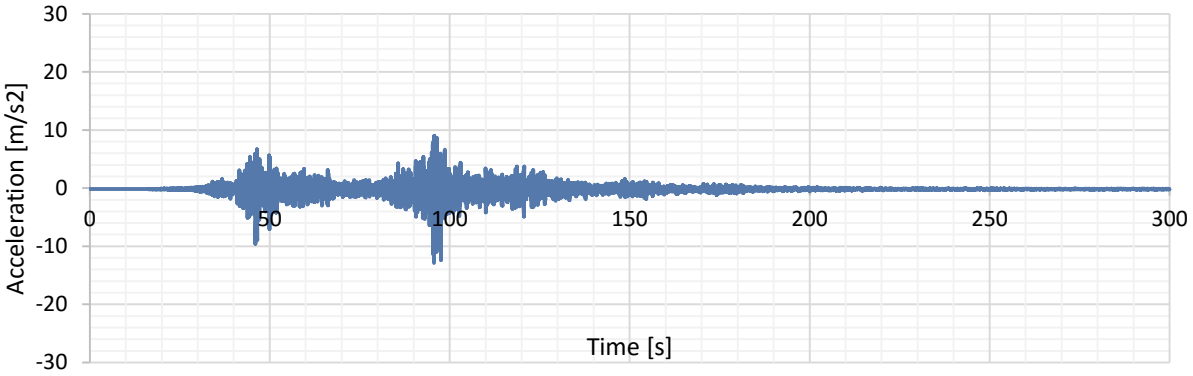

Figure 4.13 – East-West (EW) time-History record for the Tsukidate station for the Tohoku earthquake

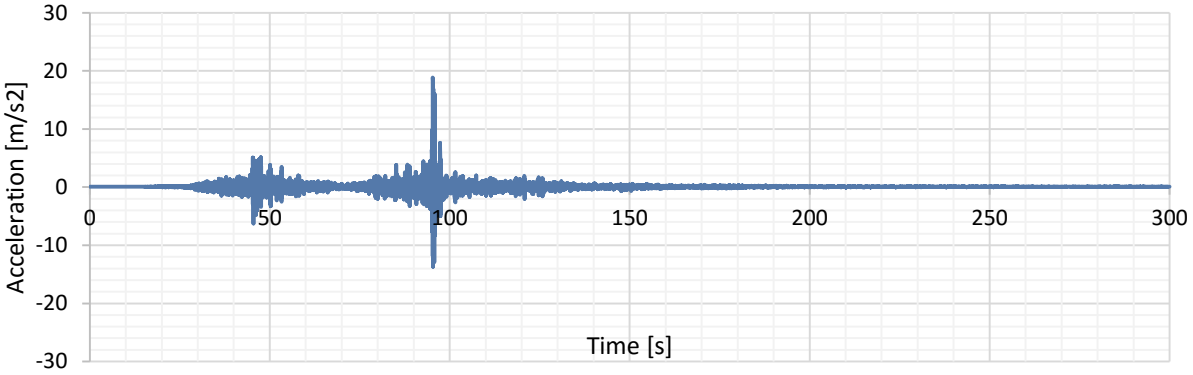

Figure 4.14 – Up-Down (UD) time-History record for the Tsukidate station for the Tohoku earthquake

Similar to the artificial accelerograms in Table 4.18 is presented a synthesis of some aspects of the presented records.

Table 4.18 – Information regarding the recorded accelerograms

	NS	EW	UD
Time step [s]	0.010	0.010	0.010
Total Duration [s]	300	300	300
PGA [g]	2.731	1.310	1.923
Time of the PGA [s]	95.610	95.670	95.320

To conclude the definition of this action is important to indicate that the NS accelerogram will be applied in the x direction, the EW in the y direction and the UD in the z direction.

4.2. Presentation and Discussion of Results

To conclude the non-linear part of the present work the results obtained from the different non-linear analyses are presented in the following, along with some comments and interpretation of the most relevant aspects.

4.2.1. Non-Linear Static Time-History

The results for each of the analyses are presented in Figure 4.15 to Figure 4.18.

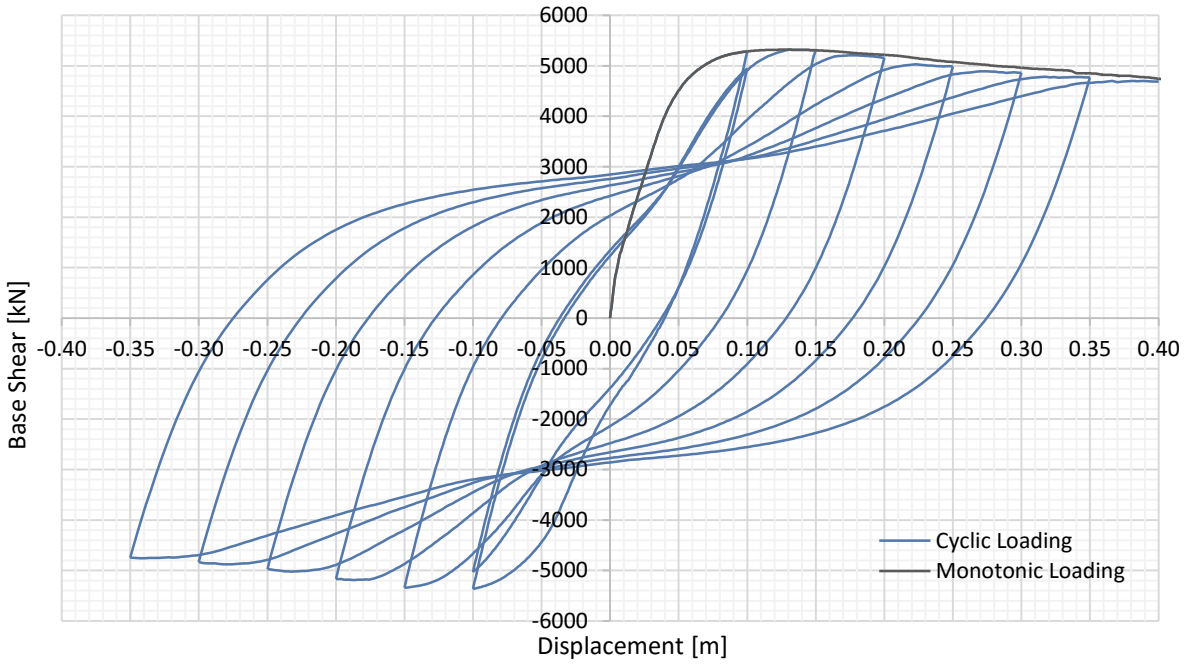

Figure 4.15 – Displacement/base shear chart for the Regular Model loaded in the X direction

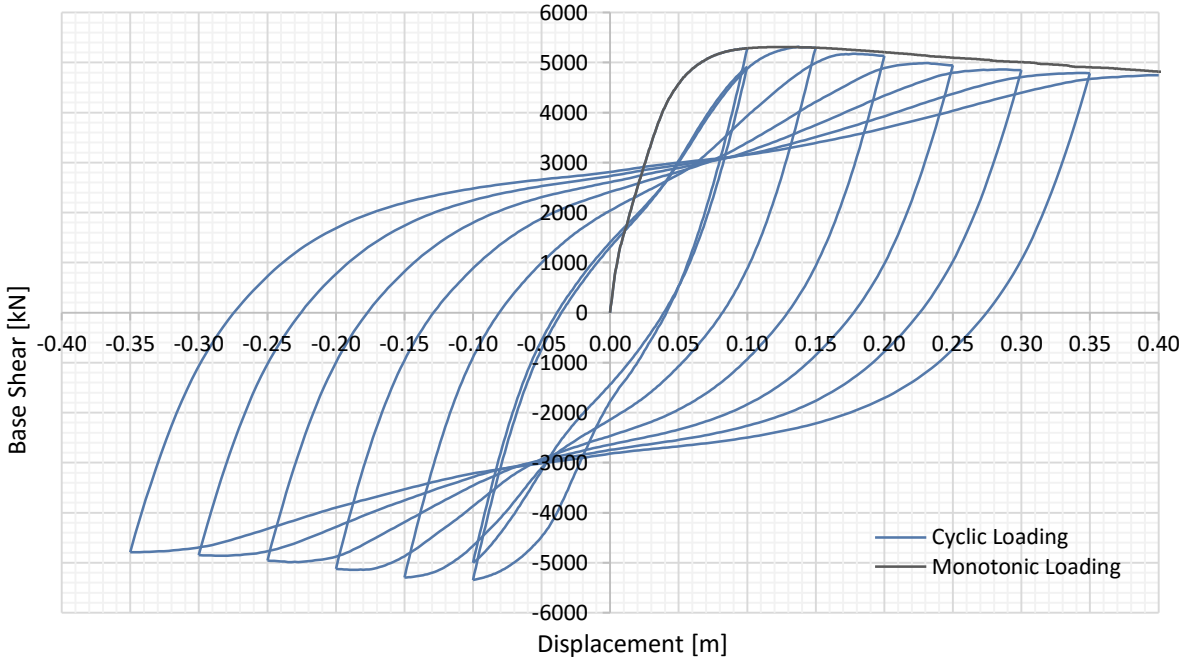

Figure 4.16 – Displacement/base shear chart for the Irregular Model loaded in the X direction

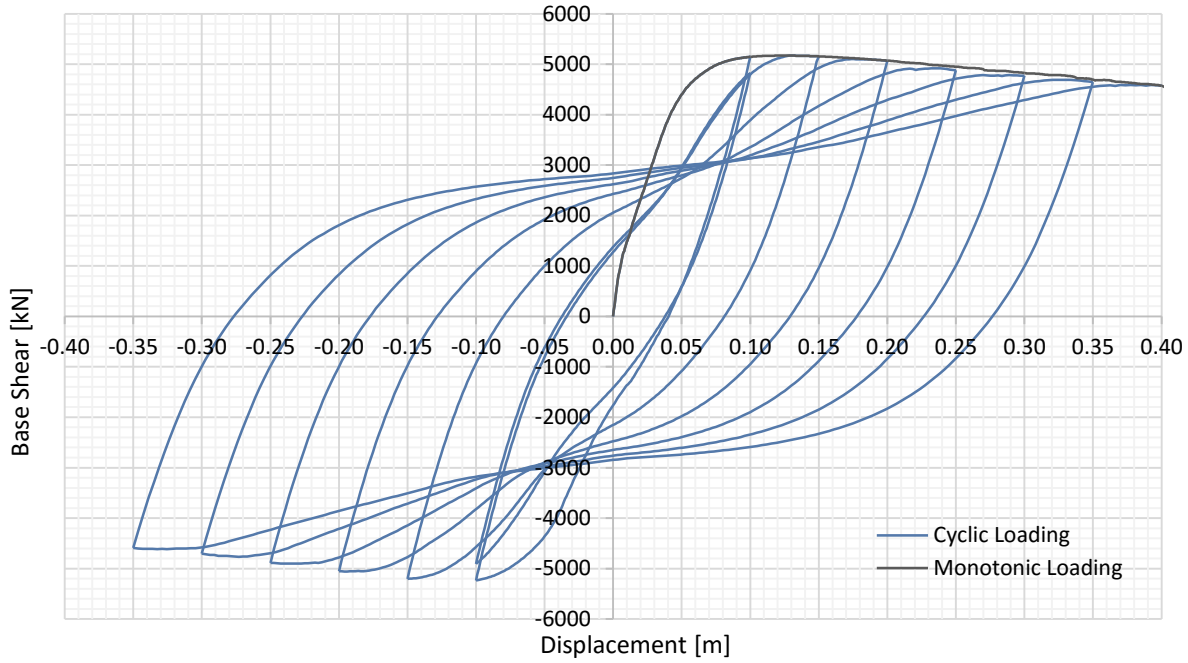

Figure 4.17 – Displacement/base shear chart for the Regular Model loaded in the Y direction

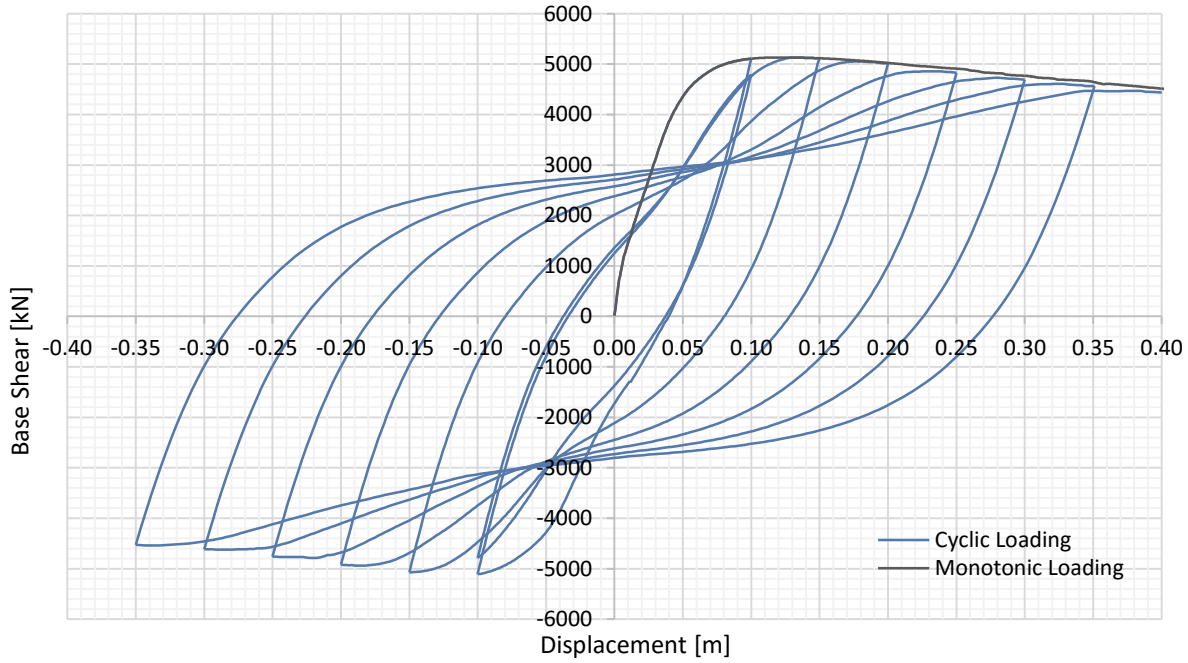

Figure 4.18 – Displacement/base shear chart for the Irregular Model loaded in the Y direction

Comparing the differences between the monotonic loading and the cyclic loading it is possible to observe that there is not a substantial overall difference between the presented cases. Anyhow, the model with the most significant cyclic degradation is the irregular one for the x direction. The reason for this might be related to the presence of the transfer beam that, by being pre-stressed and by having a least effective confinement, may induce a more brittle behaviour.

To better illustrate the cyclic degradation of each model, in Table 4.19 are presented the reduction in base shear for a consecutive cycle of a displacement of 0.1m (first two cycles).

Table 4.19 – Variation in base shear for first two cycles

Direction	Model	Loading	Base Shear	Base Shear Reduction
X	Regular	1st	5285.8	6.4%
		2nd	4946.8	
	Irregular	1st	5286.1	7.0%
		2nd	4916.7	
Y	Regular	1st	5146.2	6.2%
		2nd	4826.3	
	Irregular	1st	5107.2	6.2%
		2nd	4792.2	

Also, in Figure 4.19 are presented the accumulated dissipated energy for each model and for each direction.

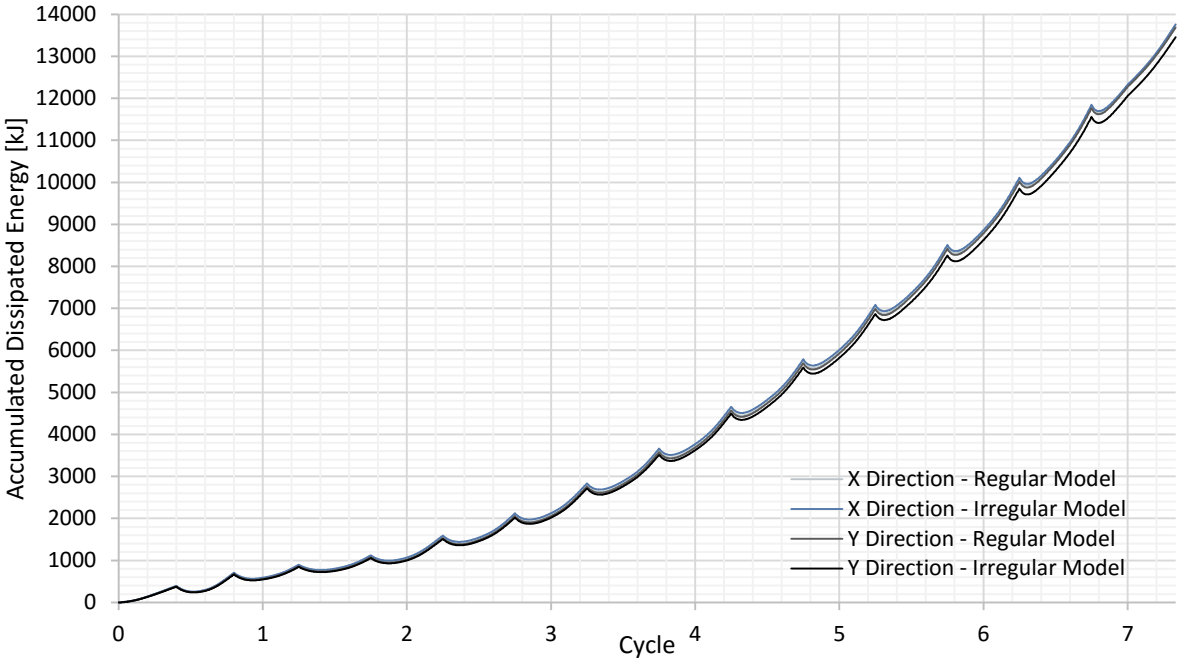

Figure 4.19 – Accumulated Dissipated Energy for the analysed models and for each direction

From the analysis of the presented chart the following may be concluded:

- Both models dissipate more energy in the x direction, presenting similar values;
- The model that dissipated less energy is the irregular one loaded in the y direction. The reason for this is the fact that the removal of the column was not compensated by a stiffer beam (as is the case along the x direction);
- The larger the imposed displacement the higher is the dissipated energy.

In Figure 4.20 is presented the displacement/base shear for the monotonic loading for all the cases.

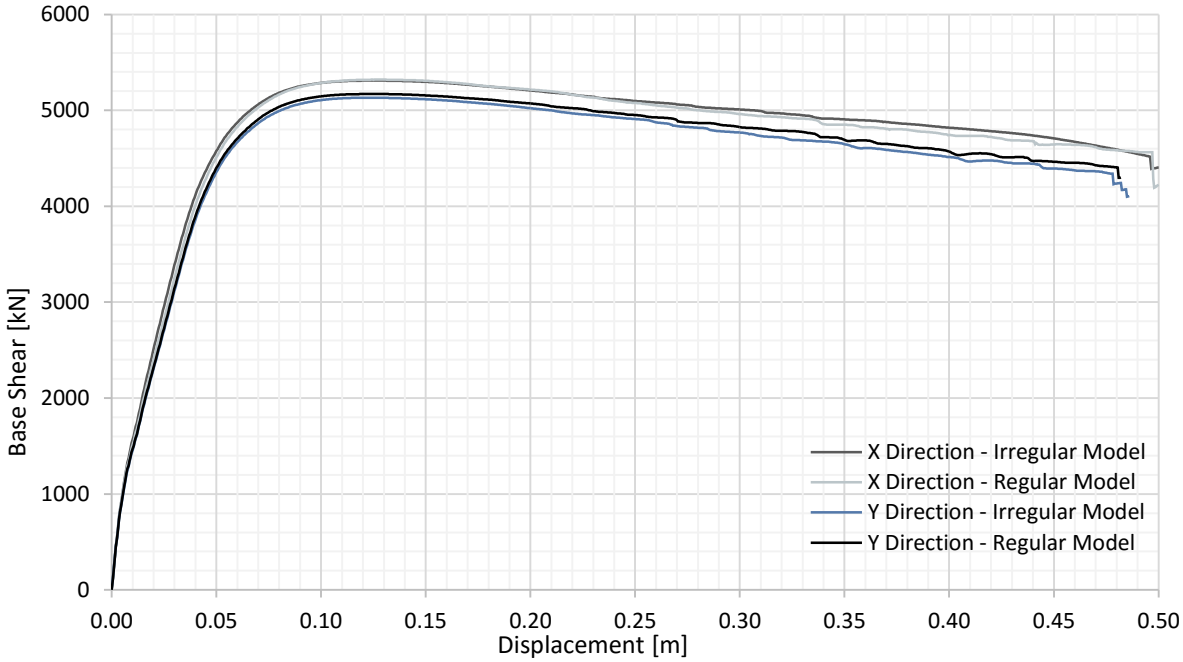

Figure 4.20 – Displacement/Base Shear for the monotonic loading of the 4 cases

From the presented chart it is possible to conclude that for both models, the y direction is less resistant and has a lower ultimate displacement. The reason for the lower value of base shear in the y direction might be related to various factors, one is the effectiveness of the resistant frames that, in this direction, are more numerous but have a lower number of spans than in the x direction. The other reason could be related to the stiffness provided by the floor diaphragm.

From this analysis was possible to take the fallowing conclusions:

- All models have similar behaviour under horizontal static loads;
- None of the models shows a significant reduction in resistance under cyclic loads, being the irregular model in the x direction the one with the higher loss;
- The structures are less resistant and stiff in the y direction;
- From this analysis the effect of the vertical component of the seismic action is not taken in consideration, which has a significant influence in the results.

4.2.2. Non-Linear Dynamic Time-History – Artificial Accelerograms

In order to assess if the presence of the discontinuous column leads to an accumulation of inelasticity (and therefore damage) immediately above the irregularity, the chord rotation, structural displacement and base shear are computed and compared. The structural displacements and base shear are presented in order to compare the global behaviour of the structure. On the other hand the chord rotations are determined to allow for a better understanding of the local behaviour of some parts of the structure.

In this study not only the regular and irregular models are compared but also the values obtained for the non-linear analysis are compared with the obtained from a linear response spectrum analysis (RSA) for a unitary behaviour factor. The three components of the seismic excitation are considered simultaneously for both non-linear and linear analysis, in which the directional combination was performed using the square root of sum of squares (SRRS) rule.

i.Displacements

Firstly are presented the values for the horizontal displacements in the x and y direction "measured" at the level of the 1st and 2nd floors. Table 4.20 and Table 4.21 present the results regarding these displacements.

Table 4.20 – Displacements [m] obtained for the Regular model

		x direction		y direction	
		1st floor	2nd floor	1st floor	2nd floor
Linear Analysis		0.017	0.032	0.017	0.033
Non Linear Analysis	Case A	0.029	0.048	0.031	0.051
	Case B	0.033	0.054	0.030	0.052
	Case C	0.030	0.053	0.025	0.043

Table 4.21 – Displacements [m] obtained for the Irregular model

		x direction		y direction	
		1st floor	2nd floor	1st floor	2nd floor
Linear Analysis		0.017	0.032	0.018	0.034
Non Linear Analysis	Case A	0.029	0.048	0.033	0.053
	Case B	0.034	0.054	0.032	0.053
	Case C	0.031	0.052	0.024	0.040

It is important to refer that for the linear analysis the Young's Modulus of the concrete was reduced in 50% to account for the cracking of concrete, therefore increasing the displacements. Considering this, it is possible to conclude that the non-linear results present higher values than the linear analysis, approximately 1.8 times on the first floor and 1.6 times on the second.

It is also seen that the displacements in the regular model are very similar to the ones obtained for the irregular model although the displacements for the y direction are slightly larger in the irregular model. The reason for this may be related with the fact that, in the x direction, the removal of a column is compensated by the existence of a stiffer transfer beam but in the y direction there is only the removal of the column and, therefore, an overall reduction in the buildings stiffness for this direction (which is consistent with previous conclusions).

The ratio between the non-linear analysis and the linear analysis results for the regular and the irregular model is presented in Table 4.22 in which the non-linear values used are the average of the values of the three considered cases. This ratio has a meaning similar to that of the displacement behaviour factor q_d.

Table 4.22 – Ratio between the displacements for the non-linear and the linear analysis

	x direction		y direction	
	1st floor	2nd floor	1st floor	2nd floor
Regular Model	1.80	1.61	1.69	1.47
Irregular Model	1.84	1.60	1.65	1.43

The overall values obtained for the ratio between the non-linear and linear analysis are higher than anticipated. It is commonly assumed that the behaviour factor for the displacements is unitary implying that the linear displacements are of the same magnitude as the non-linear, although based on the presented results this is not verified.

According to the EN1998-1 [15], structures with fundamental periods lower than T_C have higher values of non-linear displacements than the ones obtained in a linear analysis, this might be attested by the charts presented in Figure 4.21.

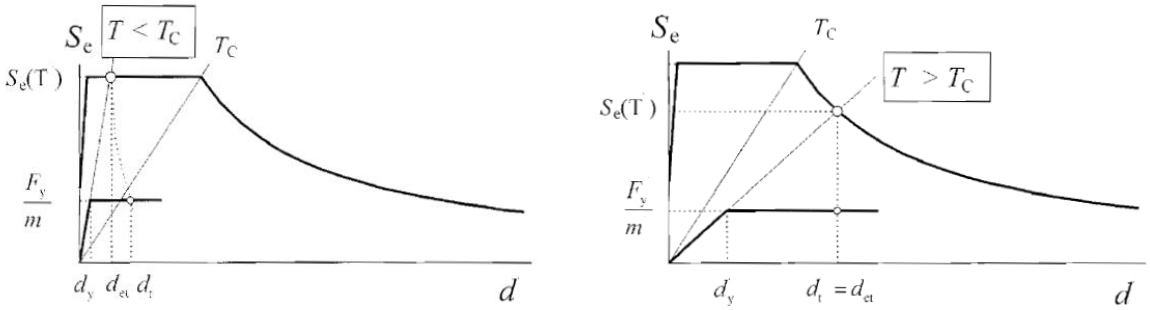

Figure 4.21 – Relation between the elastic displacements (d_{el}) and the target (non-linear) displacements (d_t). Adapted from EN1998-1 [15].

Other aspects that may help to justify the results, although with lower importance, are the reduction in the Young's Modulus of the concrete, which is a very rough approximation that, in most cases, is far from the real reduction in the flexural and shear stiffness due to cracking. Other reason might be linked to the computing of the flexural and shear stiffness in the software which considers the inertia of the steel rebar and it's Young's Modulus.

ii.Base Shear

To complement the analysis of the displacements the values for the total base shear are now presented in Table 4.23 and Table 4.24.

Table 4.23 – Total base shear [kN] obtained for the regular model

		X direction	Y direction	Z direction
Linear Analysis		6448.7	6448.7	16249.9
Non Linear Analysis	Case A	4923.3	5380.8	13953.9
	Case B	5459.1	5042.5	14420.5
	Case C	5063.9	4454.8	13771.0

Table 4.24 – Total base shear [kN] obtained for the irregular model

		X direction	Y direction	Z direction
Linear Analysis		6950.5	6884.1	17561.6
Non Linear Analysis	Case A	4752.7	5292.3	17728.1
	Case B	5333.2	5087.5	17766.3
	Case C	4987.4	4260.4	16796.9

The most significant conclusion taken from the presented values is that for the linear analysis the value of the base shear increases from the irregular to the regular model but in the non-linear analysis the opposite occurs. In the linear analysis, due to the computation method (model combination), the irregular model, being stiffer than the regular one, leads to higher values of base shear. On the other hand, the reduction on the non-linear analysis is mostly influenced by the structural efficiency and the adopted steel reinforcement.

The ratio between the linear analysis and the non-linear analysis results for the regular and the irregular model is presented in Table 4.25 in which the non-linear values used are the average of the values of the three considered cases. This ratio has a meaning similar to that of the behaviour factor q_F.

Table 4.25 – Ratio between the base shear for the linear and the non-linear analysis

	X direction	Y direction	Z direction
Regular Model	1.25	1.30	1.16
Irregular Model	1.38	1.41	1.01

The results presented are far from current values for both the regular and irregular models. Furthermore, the values are not coherent with the assumption that the presence of the irregularity would mean a reduction in the behaviour factor. Although odd, these values might be explained by the following:

- Assuming that F_B^{lin} is the elastic value of the total base shear obtained from a RSA and that q_{EC8} is the behaviour factor defined according with the EN1998-1 [15], the design value of the total base shear ($F_{B,ED}$) is given by equation (4.15).

$$F_{B,ED} = \frac{F_B^{lin}}{q_{EC8}} \tag{4.15}$$

  Considering that the maximum base shear that might be developed in a non-linear analysis (F_B^{Nlin}) is equal to the resisting base shear ($F_{B,RD}$), q_F is given by the equation (4.16).

$$q_F = \frac{F_B^{lin}}{F_B^{Nlin}} \cong \frac{F_B^{lin}}{F_{B,RD}} \tag{4.16}$$

Based on the equations (4.15) and (4.16) is possible to establish the relations between q_F and q_{EC8}, as shown in equation (4.17).

$$\begin{cases} if\ F_{B,RD} < F_{B,ED} \leftrightarrow \dfrac{F_B^{lin}}{q_F} < \dfrac{F_B^{lin}}{q_{EC8}} \leftrightarrow q_F > q_{EC8} \\ if\ F_{B,RD} = F_{B,ED} \leftrightarrow \dfrac{F_B^{lin}}{q_F} = \dfrac{F_B^{lin}}{q_{EC8}} \leftrightarrow q_F = q_{EC8} \\ if\ F_{B,RD} > F_{B,ED} \leftrightarrow \dfrac{F_B^{lin}}{q_F} > \dfrac{F_B^{lin}}{q_{EC8}} \leftrightarrow q_F < q_{EC8} \end{cases} \tag{4.17}$$

- As mentioned in the design of the steel reinforcement, it was considered that all elements with equal cross-section would have the same reinforcement and that only the conditioning section was considered for its determination. Also, by adopting a certain reinforcement defined by standard rebars, the adopted reinforcement is larger than the needed from the design. These assumption lead to a significant enlarging of $F_{B,RD}$ and therefore reduction in the value of q_F.

  This affects in similar way the two models and justifies the overall low values presented in Table 4.25 but doesn't account for the fact that the regular model have lower values than the irregular one.
- To justify that, it is important to recall that in the linear elastic analysis, used to design the steel reinforcements, the behaviour factor used for the irregular model was reduced relatively to the used for the regular model in 20%, leading to higher design values for the internal forces. Although in the definition of the reinforcement, it was considered the same for both models with the purpose of better comparing the results obtained. This assumption led to more reinforcement then the strictly needed in the regular model and fewer reinforcement in the irregular model. This leads to a reduction in the $F_{B,RD}$ of the irregular model, hence an increase in q_F, and an increase in $F_{B,RD}$ on the regular model leading to lower values of q_F.

These conclusions justify the obtained results but compromise their quality. It is not possible to separate, with confidence, the reductions in the behaviour factors due to the presence of the irregularity or due to the overdesign of the structure. In order to better understand the level of overdesign Table 4.26 presents the scale factors by which the considered accelerograms had to be multiplied to reach total collapse.

Table 4.26 – Overdesign factor of the regular and irregular model

	Regular Model	Irregular Model
Case A	4.67	4.13
Case B	4.62	4.09
Case C	4.63	4.05
Average	4.64	4.09

Although there are more effects that may influence the values presented previously, it is safe to assume that, in fact, the regular model is more overdesigned than the irregular one, corroborating the mentioned justifications for the obtained values.

iii.Chord Rotation

The results presented so far regard an overall behaviour of the structures which does not show a significant difference between the regular and the irregular models, influenced by the choice of considering equal reinforcements in both models. In order to study the local behaviour of the structures, the chord rotation is computed for the end-sections of all the frames in both x and y direction.

Only the results for the alignments 1, 2, B and C, accordingly with Figure 4.22, are presented, being the results for the rest of the structure present in Annex E. Given that the steel reinforcement is equal in both models it is possible to compare the results of the regular and irregular models with the assurance that the results are indeed comparable.

In this comparison only the results for the non-linear analysis were considered.

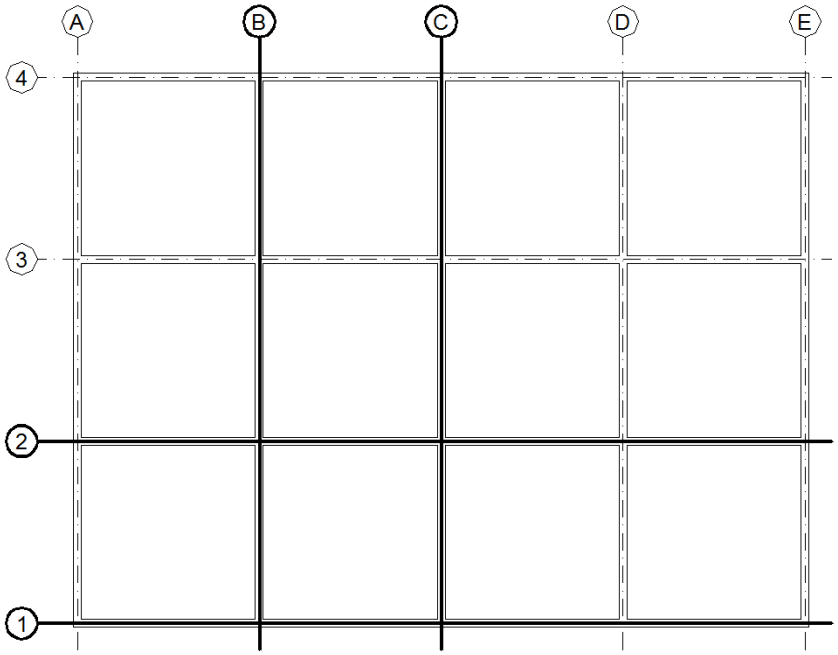

Figure 4.22 – Alignments considered for the comparison of the chord rotation (bold)

The nomenclature given to the nodes of the frames is presented in Figure 4.23 and Figure 4.24. The notation of each end-section, in which the chord rotation is computed, is composed by the node name followed by the relative position of the end-section to the respective node (right, left, up and down).

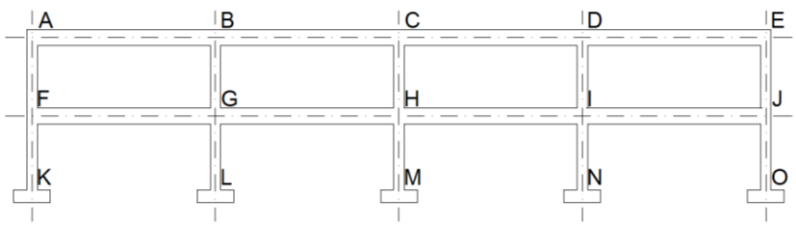

Figure 4.23 – Notation of the nodes of the frames oriented in the x direction

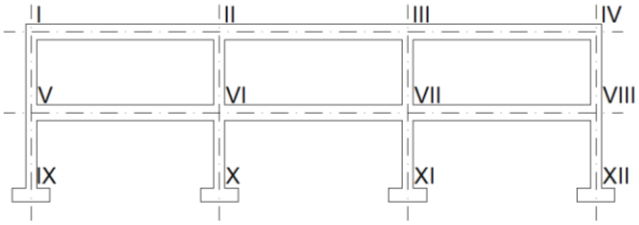

Figure 4.24 – Notation of the nodes of the frames oriented in the y direction

Table 4.27 to Table 4.30 present the values of the chord rotation for the alignment 1 (alignment of the TB) in both the regular and irregular models, these values relate to the absolute maximum value for each section. The values in bold are, in Table 4.28, the ratio between the irregular and regular model in the transfer beam and, in Table 4.29, the same ratio but for the sections right above the transfer beam.

Table 4.27 – Chord rotation on the end-sections of the beams of the 2nd floor of the alignment 1

	Chord Rotation on the Irregular Model [mrad]			Chord Rotation on the Regular Model [mrad]			Average Chord Rotation [mrad]		Irr/ Reg
	Case A	Case B	Case C	Case A	Case B	Case C	Irregular Model	Regular Model	
A_{right}	3.09	3.92	3.76	4.59	5.06	5.36	3.59	5.00	0.72
B_{left}	1.85	1.73	1.82	1.19	1.37	1.31	1.80	1.29	1.39
B_{right}	2.01	2.14	2.05	1.21	1.34	1.28	2.07	1.28	1.62
C_{left}	1.63	1.97	1.64	1.30	1.42	1.42	1.75	1.38	1.27
C_{right}	1.25	1.47	1.22	1.30	1.42	1.42	1.31	1.38	0.95
D_{left}	1.12	1.16	1.20	1.21	1.30	1.32	1.16	1.28	0.91
D_{right}	1.05	1.07	1.12	1.21	1.29	1.29	1.08	1.26	0.86
E_{left}	3.72	4.09	3.63	4.81	5.19	4.47	3.81	4.82	0.79

Table 4.28 – Chord rotation on the end-sections of the beams of the 1st floor of the alignment 1

	Chord Rotation on the Irregular Model [mrad]			Chord Rotation on the Regular Model [mrad]			Average Chord Rotation [mrad]		Irr/ Reg
	Case A	Case B	Case C	Case A	Case B	Case C	Irregular Model	Regular Model	
F_{right}	0.98	1.14	1.12	6.05	7.22	7.22	1.08	6.83	**0.16**
G_{left}	0.95	1.33	1.30	3.85	4.14	4.18	1.19	4.06	**0.29**
G_{right}	0.66	0.83	0.81	3.83	4.17	4.22	0.77	4.07	**0.19**
H_{left}	0.54	0.56	0.52	3.95	4.22	4.31	0.54	4.16	**0.13**
H_{right}	0.69	0.70	0.76	3.96	4.21	4.30	0.72	4.16	**0.17**
I_{left}	0.31	0.34	0.32	3.90	4.05	4.10	0.32	4.02	**0.08**
I_{right}	0.23	0.23	0.24	3.85	4.00	4.11	0.24	3.99	**0.06**
J_{left}	0.62	0.65	0.65	6.44	6.73	6.11	0.64	6.43	**0.10**

Table 4.29 – Chord rotation on the end-sections of the columns of the 2nd floor of the alignment 1

	Chord Rotation on the Irregular Model [mrad]			Chord Rotation on the Regular Model [mrad]			Average Chord Rotation [mrad]		Irr/ Reg
	Case A	Case B	Case C	Case A	Case B	Case C	Irregular Model	Regular Model	
A_{down}	3.97	4.18	3.98	4.44	4.25	4.27	4.05	4.32	0.94
B_{down}	4.68	5.43	4.79	5.68	6.20	6.80	4.97	6.23	0.80
C_{down}	4.37	5.09	5.03	5.53	5.84	6.28	4.83	5.88	0.82
D_{down}	4.48	5.21	5.47	5.98	6.36	6.05	5.05	6.13	0.82
E_{down}	3.81	4.23	4.44	4.52	4.65	4.61	4.16	4.60	0.91
F_{up}	5.84	6.24	5.92	1.52	1.65	1.39	6.00	1.52	**3.95**
G_{up}	6.23	7.03	6.20	3.30	3.52	3.88	6.48	3.56	**1.82**
H_{up}	5.45	6.47	6.05	3.00	3.08	3.41	5.99	3.17	**1.89**
I_{up}	5.33	6.18	6.39	3.41	3.55	3.28	5.96	3.41	**1.75**
J_{up}	5.73	6.38	6.66	1.50	1.55	1.52	6.26	1.52	**4.11**

Table 4.30 – Chord rotation on the end-sections of the columns of the 1st floor of the alignment 1

	Chord Rotation on the Irregular Model [mrad]			Chord Rotation on the Regular Model [mrad]			Average Chord Rotation [mrad]		Irr/ Reg
	Case A	Case B	Case C	Case A	Case B	Case C	Irregular Model	Regular Model	
F_{down}	7.79	10.40	9.68	5.14	4.48	4.32	9.29	4.64	2.00
G_{down}	-	-	-	6.00	6.71	5.66	-	6.12	-
H_{down}	8.26	11.43	10.29	5.47	7.02	5.94	9.99	6.14	1.63
I_{down}	8.84	10.65	9.68	5.44	7.59	6.49	9.72	6.51	1.49
J_{down}	8.77	9.92	8.88	4.72	6.57	5.29	9.19	5.53	1.66
K_{up}	8.63	12.21	11.24	10.24	10.06	9.26	10.69	9.85	1.09
L_{up}	-	-	-	9.77	10.76	9.82	-	10.12	-
M_{up}	8.60	11.28	10.30	9.40	11.15	10.20	10.06	10.25	0.98
N_{up}	9.05	10.80	9.83	9.06	11.51	10.55	9.89	10.37	0.95
O_{up}	9.50	10.33	9.35	9.52	11.98	11.04	9.73	10.85	0.90

Only the values relating the peripheral alignment (alignment 1) are presented, the results for the rest of the structure are presented in Annex E. In order to allow for a better visualization of the results the ratio between the irregular and regular models are presented in Figure 4.25 to Figure 4.28, for the alignments indicated in Figure 4.22. Values higher than one represent that the chord rotation in the irregular model is higher than in the regular model.

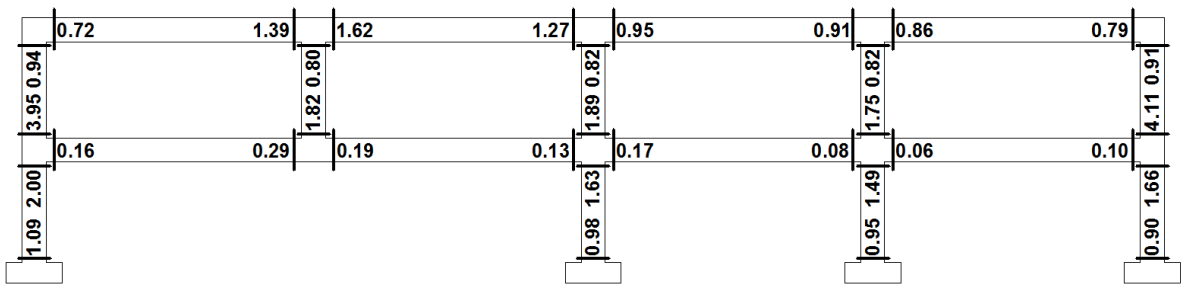

Figure 4.25 – Ratio between the chord rotation in the irregular and regular model in alignment 1

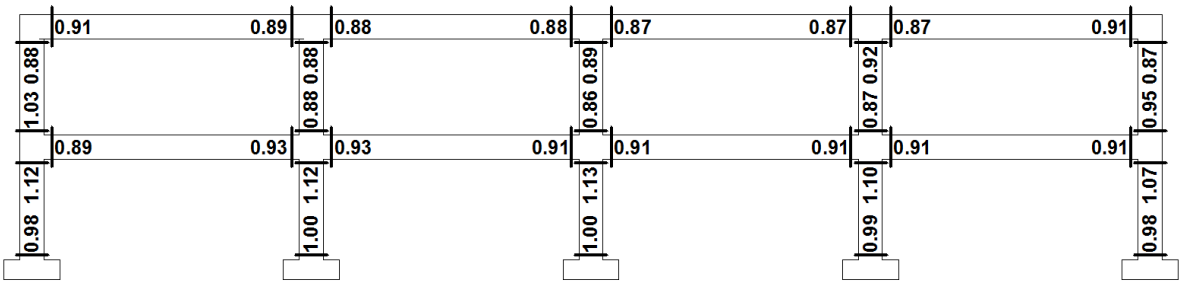

Figure 4.26 – Ratio between the chord rotation in the irregular and regular model in alignment 2

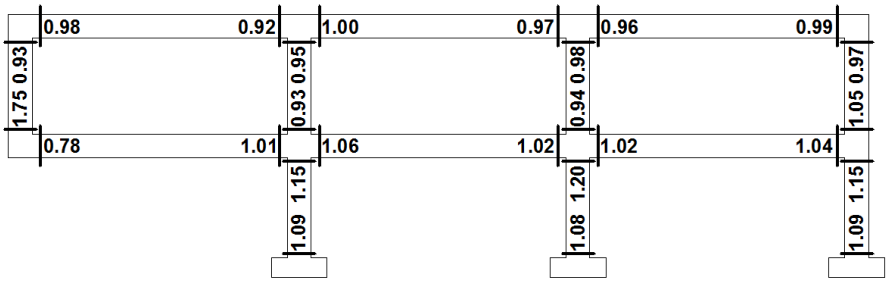

Figure 4.27 – Ratio between the chord rotation in the irregular and regular model in alignment B

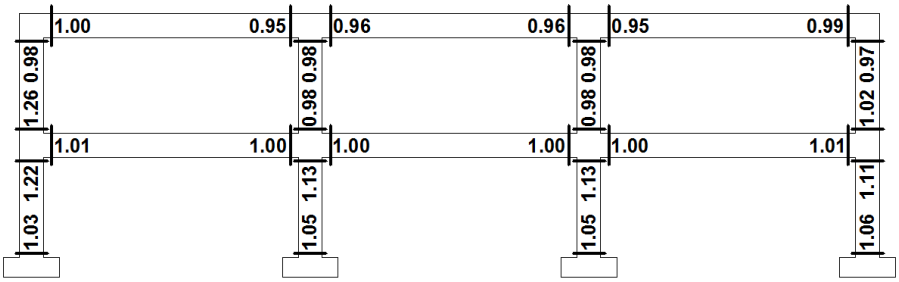

Figure 4.28 – Ratio between the chord rotation in the irregular and regular model in alignment C

Based on the values obtained for the chord rotations (CR) the following was concluded for the beams:

- Considering all the alignments but the one with the irregularity it was concluded that, in general, the CR were of the same magnitude in the two models. This led to the conclusion that the presence of the irregularity did not significantly affect the regular beams chord rotations.
- Considering now the alignment 1 (Figure 4.25) it was concluded that, in the transfer beam, the chord rotations were particularly low comparing to the same beam in the regular model. Although the geometry of both beams is different, which makes the comparison between them harder, it was assumed that the results were within the expected considering the higher stiffness of the transfer beam.
- In the beams right above the transfer beam and next to the discontinued column there was a significant increase in the CR, likely due to the local effect of the vertical component of the seismic action.

- The beam perpendicular to the transfer beam which is indirectly supported in the TB (alignment B) had a lower chord rotation in the irregular model. This was attributed to do the fact that, by removing a column, this beam becomes more flexible, leading to a lesser concentration of internal forces, hence reducing the CR. This was in accordance with the conclusions taken in the parametric study.

Considering now the results for the columns, the following conclusions may be taken:

- Considering the sections at the connection with the foundations, no significant variations between the regular and irregular models were observed apart from a reduction in the chord rotation on the alignment 1. This likely had to do with the increase in CR that occurs in the other end of those columns, imposed by the transfer beam.
- In the column sections connected to the beams of the first floor, there was an overall increase in the chord rotation (of about 10%) in the sections bellow the mentioned beams, especially in the connection to the TB (with an average increase of 70%) due to its higher stiffness.

  In the sections of the columns, above the 1st floor the results were different, apart from the columns in the alignment 1, there was an overall reduction in chord rotation. Nevertheless, in the columns above the transfer beam, there was a significant increase in the CR for both directions. This is a relevant conclusion that can be taken from the presented results as it is an indirect indicator that there is an accumulation of damage and inelasticity in the zones above the irregularity, which is in the base of the reduction in the behaviour factor indicated in the EN1998-1 [15].

iv.Axial Force

In order to study the variation in axial force, are presented now the results obtained for the column of the 2nd floor, right above the discontinued column. It was intended to determine if there is a significant variation due to the effect of the seismic action between the two cases. In Figure 4.29 and Figure 4.30 is presented the evolution of the axial force along the time for the regular and irregular models, respectively.

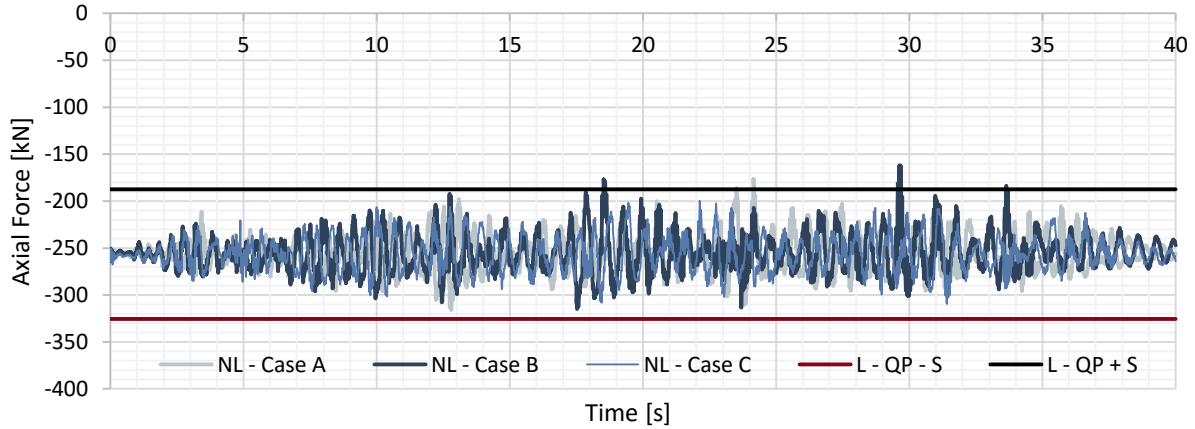

Figure 4.29 – Axial Force on the column above the discontinuity for the regular model

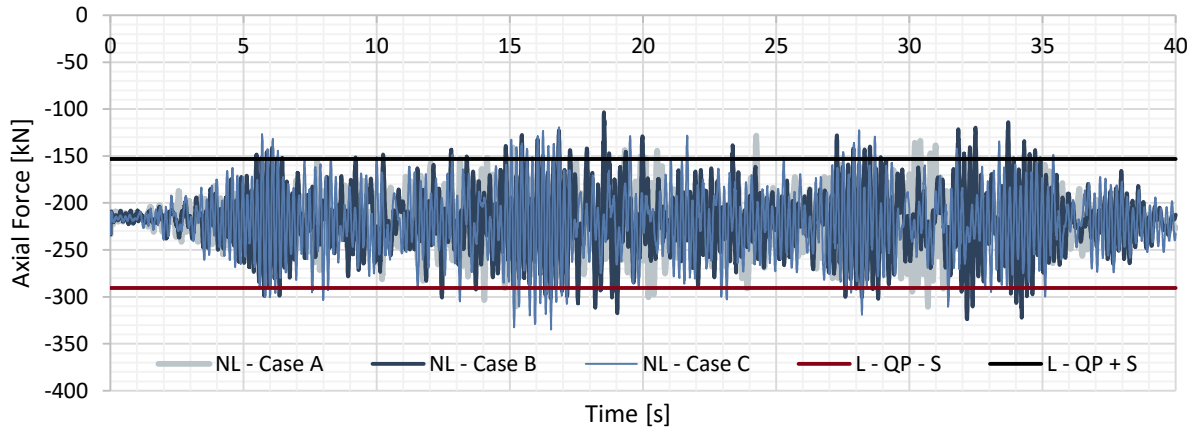

Figure 4.30 – Axial Force on the column above the discontinuity for the irregular model

From the results presented the following was concluded:

- The amplitude of the axial force in the irregular model was far greater than in the regular one. The first had an amplitude, due to the vertical component of the seismic action, of 206 kN and the latter of 134 kN.
- Although it's not very conclusive from the figures, a careful examination shows that the frequency of vibration of the regular model is far higher than in the irregular model, as was expected, given that the irregular model resisting mechanism (to vertical loading) is more flexible than the regular model.
- The results for the non-linear analysis for the regular model are lower than the obtained for the linear analysis, considering the maximum absolute values. The same did not occur for the irregular model in which, in certain points, the non-linear values are higher than the linear ones. This is an indication that for this column the behaviour factor is lower than one, which is unconventional and might lead to an undervaluation of the bending moments is the transfer beam when a RSA is considered in the design.

v.Near Collapse Situation

Although the results obtained by comparing the chord rotations for the regular and the irregular models are very relevant, the absolute values are not as significant, in part due to the overdesign of the structures as shown in Table 4.26. In order to study the response of the structures in a situation near the collapse is defined a factor by which the base accelerations should be multiplied to take in consideration the Limit State of Near Collapse (LSNC) as defined in the EN1998-3 [16].

The Limit State of Significant Damage (LSSD), defined in the EN1998-1 [15] and used to compute the accelerograms adopted for that study, considers a return period of 475 years. On the other hand, the LSNC considers a probability of exceedance of 2% in 50 years which is equivalent to a return period of 2475 years. To take into consideration the different return period, the importance factor (γ_I) that was considered unitary in the definition of the elastic and design response spectrum should now be computed according with equation (4.18).

$$\gamma_I = \left(\frac{T_{LSSD}}{T_{LSNC}}\right)^{-1/k} = 3.00 \quad (4.18)$$

Being T_{LSSD} the return period for the LSSD (T_{LSSD}=457y), T_{LSNC} the return period for the LSNC (T_{LSNC}=2457y) and exponent *k* dependant of seismic action (for seismic action type 1 k=1.5).
To simplify the process, the new importance factor was considered by multiplying both the accelerograms and the response spectrum by the factor. The structures were analysed again for the new scale factor regarding its displacements, base shear and chord rotation.

Table 4.31 presents the average displacements of the three cases considered in the non-linear analysis, the linear displacements obtained in the RSA and the displacements behaviour factor.

Table 4.31 – Displacements for the Limit State of Near Collapse

Model	Analysis	x direction		y direction	
		1st floor	2nd floor	1st floor	2nd floor
Regular	Non-linear	0.123	0.149	0.122	0.152
	Linear	0.050	0.095	0.051	0.098
	q_d	2.46	1.57	2.39	1.55
Irregular	Non-linear	0.127	0.150	0.130	0.156
	Linear	0.051	0.097	0.053	0.101
	q_d	2.49	1.55	2.45	1.54

From the presented results it was concluded the following:

- The displacements in the LSNC obtained for the linear analysis were exactly three times higher than in the LSSD as was supposed. For the non-linear analysis the displacements on the second floor were also 3 times higher in the LSNC, although for the first floor they were 4 times higher. This is an evidence that the linear analysis underestimates the displacements.
- Comparing the displacements for the 1st and 2nd floors was concluded that the displacements were 1.2 and 1.9 times higher on the second floor then in the first for the non-linear and linear analysis, respectively. This is a strong indication that the collapse occurs by formation of soft-storey mechanism, furthermore, using a linear RSA the possibility of formation of this mechanism is undetectable.
- Comparing the results q_d of the LSNC with the ones for the LSSD it was concluded that the results for the second floor are identical and for the first floor there was an increase of approximately 40% which was associated with the formation of the collapse mechanism.

Table 4.32 presents the same results as for the displacements but for the total base shear on the regular and irregular models. Again, for the response spectrum analysis the model combination was made considering the CQC and the directional combination was made based on the SRSS.

Table 4.32 – Base shear for the Limit State of Near Collapse

Model	Analysis	x direction	y direction	z direction
Regular	Linear	19345.8	19345.8	22458.9
	Non-Linear	5429.8	5360.0	15039.8
	q_F	3.56	3.61	1.49
Irregular	Linear	20847.3	20600.3	25184.1
	Non-Linear	5353.0	5254.6	25330.1
	q_F	3.89	3.92	0.99

Based on the results presented the following was concluded regarding the base shear:

- There is an inevitable increase in the values of the behaviour factor due to the fact that the growth in base shear for the linear analysis is directly proportional to the action (which was 3 times higher) but the increase in the non-linear analysis has an upper limit that is the maximum resisting force of the structure; i.e. the base shear in the linear model increases 3 times when in the non-linear the increase is very low (approx. 1.1 times),
- The fact that values of the q_F are higher for the LSNC confirms the reason given for the overall low values obtained for the LSSD due to the overdesign of the structure. Nevertheless, the values for the irregular model are still higher than the ones for the regular model, also due to the reason presented for the results presented in the LSSD.

Table 4.33 to Table 4.36 present the results for the chord rotation for alignment 1 (alignment with irregularity). Only the results for this alignment are shown, given that this is the one that presented the higher values of CR and is the one that matters the most in this study. The values in bold are, in Table 4.34, the ratio between the irregular and regular model in the transfer beam and, in Table 4.35, the same ratio but for the sections right above the transfer beam.

Table 4.33 – Chord rotation on the end-sections of the beams of the 2nd floor of the alignment 1 for the LSNC

	Chord Rotation on the Irregular Model [mrad]			Chord Rotation on the Regular Model [mrad]			Average Chord Rotation [mrad]		Irr/ Reg
	Case A	Case B	Case C	Case A	Case B	Case C	Irregular Model	Regular Model	
A_{right}	4.90	5.39	5.42	5.65	6.08	6.67	5.24	6.13	0.85
B_{left}	4.02	3.30	3.10	1.49	1.65	2.02	3.47	1.72	2.02
B_{right}	2.84	3.41	3.21	1.39	1.67	1.94	3.15	1.67	1.89
C_{left}	2.44	2.31	2.27	1.42	1.46	1.51	2.34	1.46	1.60
C_{right}	2.16	2.97	2.44	1.43	1.45	1.50	2.52	1.46	1.73
D_{left}	1.31	1.23	1.35	1.29	1.63	1.91	1.30	1.61	0.80
D_{right}	1.22	1.22	1.49	1.24	1.70	1.88	1.31	1.61	0.82
E_{left}	4.58	4.58	4.59	5.34	6.06	6.65	4.58	6.02	0.76

Table 4.34 – Chord rotation on the end-sections of the beams of the 1st floor of the alignment 1 for the LSNC

	Chord Rotation on the Irregular Model [mrad]			Chord Rotation on the Regular Model [mrad]			Average Chord Rotation [mrad]		Irr/ Reg
	Case A	Case B	Case C	Case A	Case B	Case C	Irregular Model	Regular Model	
F_{right}	1.46	1.73	1.55	9.27	12.23	10.30	1.58	10.60	**0.15**
G_{left}	2.94	2.76	2.65	4.29	4.53	4.91	2.78	4.58	**0.61**
G_{right}	2.13	1.98	1.85	4.32	4.96	4.75	1.99	4.68	**0.43**
H_{left}	1.05	0.90	0.86	4.44	4.88	5.18	0.94	4.83	**0.19**
H_{right}	1.46	1.74	1.26	4.43	4.85	5.22	1.49	4.83	**0.31**
I_{left}	0.58	0.63	0.62	4.28	4.43	5.26	0.61	4.66	**0.13**
I_{right}	0.45	0.44	0.42	4.16	4.51	4.95	0.44	4.54	**0.10**
J_{left}	0.81	0.75	0.80	9.05	10.56	13.66	0.79	11.09	**0.07**

Table 4.35 – Chord rotation on the end-sections of the columns of the 2nd floor of the alignment 1 for the LSNC

	Chord Rotation on the Irregular Model [mrad]			Chord Rotation on the Regular Model [mrad]			Average Chord Rotation [mrad]		Irr/ Reg
	Case A	Case B	Case C	Case A	Case B	Case C	Irregular Model	Regular Model	
A_{down}	6.65	5.49	6.62	5.04	5.56	6.70	6.25	5.76	1.08
B_{down}	6.34	5.93	6.38	7.88	8.61	9.45	6.21	8.65	0.72
C_{down}	6.70	7.18	6.79	7.34	8.00	9.22	6.89	8.19	0.84
D_{down}	7.45	8.31	7.89	7.27	8.33	9.96	7.88	8.52	0.93
E_{down}	6.35	7.02	6.48	5.52	5.98	6.29	6.62	5.93	1.12
F_{up}	9.46	8.23	9.31	3.12	3.47	3.31	9.00	3.30	**2.73**
G_{up}	7.81	7.55	8.47	5.29	5.54	6.36	7.94	5.73	**1.39**
H_{up}	8.33	8.55	8.42	4.78	4.87	5.71	8.43	5.12	**1.65**
I_{up}	8.43	9.38	8.98	4.65	5.26	5.95	8.93	5.29	**1.69**
J_{up}	8.74	9.37	9.24	3.57	3.90	4.18	9.11	3.88	**2.35**

Table 4.36 – Chord rotation on the end-sections of the columns of the 1st floor of the alignment 1 for the LSNC

	Chord Rotation on the Irregular Model [mrad]			Chord Rotation on the Regular Model [mrad]			Average Chord Rotation [mrad]		Irr/ Reg
	Case A	Case B	Case C	Case A	Case B	Case C	Irregular Model	Regular Model	
F_{down}	35.67	50.93	45.94	22.14	32.78	37.80	44.18	30.90	1.43
G_{down}	-	-	-	28.71	41.64	38.85	-	36.40	-
H_{down}	36.36	51.19	46.49	29.05	42.30	37.87	44.68	36.41	1.23
I_{down}	36.37	51.11	46.48	29.82	43.28	37.13	44.65	36.74	1.22
J_{down}	35.38	50.05	46.12	29.06	42.01	27.37	43.85	32.81	1.34
K_{up}	37.25	51.93	45.89	31.62	45.30	44.06	45.02	40.33	1.12
L_{up}	-	-	-	32.56	46.55	43.38	-	40.83	-
M_{up}	36.34	51.11	46.97	33.03	47.13	42.81	44.80	40.99	1.09
N_{up}	35.79	50.55	47.35	33.45	47.64	42.19	44.56	41.10	1.08
O_{up}	35.26	50.01	47.70	33.96	48.28	40.84	44.33	41.03	1.08

Based on the results presented regarding the chord rotations the following was concluded:

- The sections on alignment 1 that presented the highest increase in the irregular model (comparing with the regular model) were the ones above the transfer beam, although the difference is lower than in the LSSD.
- The absolute values show that the main damage in the structure is located in the columns of the first floor, which confirms that the collapse mechanism is indeed the formation of a soft-storey.
- Table 4.37 presents the average increase from the results for the LSSD to the LSNC, for both beams and columns and for the regular and irregular models.

Table 4.37 – Average of the ratio between the chord rotations obtained for the LSNC and the LSSD

		Regular Model	Irregular Model
Columns	1st floor	5.00	4.54
	2nd floor	1.63	1.45
Beams	1st floor	1.27	1.90
	2nd floor	1.22	1.46

It was concluded that the increase in chord rotation is more significant in the regular model for the columns and more significant in the irregular model for the beams. It was also observed that the increase in the CR on the columns of the first floor is much higher due to the formation of the collapse mechanism.

In order to assess the suitability of the structure to accommodate the chord rotation imposed by the horizontal actions the value of the ultimate chord rotation capacity (θ_{um}) is computed according with the paragraph 3.2.2 of Annex A of the EN1998-3 [16], given by equation (4.19).

$$\theta_{um} = \frac{1}{\gamma_{cl}} 0.016 \cdot (0.3^{\nu}) \left[\frac{\max(0.01;\omega')}{\max(0.01;\omega)} f_c\right]^{0.225} \left(\min\left(9;\frac{L_V}{h}\right)\right)^{0.35} 25^{\left(\alpha\rho_{sx}\frac{f_{yw}}{f_c}\right)} (1.25^{100\rho_d}) \qquad (4.19)$$

Where:

γ_{cl} is equal to 1.5 for all the elements given that all elements are primary seismic elements;

h is the depth of the of the cross-section;

L_V $= M/V$, is the ratio moment/shear at the end section;

ν $= N/bhf_c$ (b width of compression zone, N axial force positive for compression);

ω, ω' is the mechanical reinforcement of the tension and compression zones;

f_c is the concrete compressive strength (MPa) considered in this study the mean value inputted in the model ($f_c = 38$ MPa);

f_{yw} is the stirrup yield strength (MPa) considered in this study the mean value inputted in the model ($f_{yw} = 500$ MPa);

ρ_{sx} $= A_{sx}/b_w s_h$, is the ratio of transverse steel parallel to the direction x of the loading (s_h = stirrups spacing);

ρ_d is the steel ratio of diagonal reinforcement, which is none in this case;

α confinement effectiveness factor, that may be taken equal to:

$$\alpha = \left(1 - \frac{s_h}{2b_0}\right)\left(1 - \frac{s_h}{2h_0}\right)\left(1 - \frac{\sum b_i^2}{6h_0 b_0}\right) \quad (4.20)$$

Where:

b_0, h_0 is the dimension of the confined core to the centreline of the hoop;

b_i is the centreline spacing of longitudinal bars lately restrained by a stirrup corner or a cross-tie along the perimeter of the cross-section.

Given that all the columns in alignment 1 have the same geometry (square cross-section of 0.4 by 0.4m) it is possible to derive most of the values defined for equations (4.19) and (4.20). In Table 4.38 are presented the geometrical properties according with the defined previously and in Table 4.39 are presented the internal forces in the sections Kup, Fdown and Gup in both models only for the Case B, for being the one that had the higher values of chord rotation.

Table 4.38 – Geometrical properties of the columns cross-section

h [m]	0.400
b [m]	0.400
h_0 [m]	0.330
b_0 [m]	0.330
b_i [m]	0.153
A_{sx} [cm^2]	10.48
s_h [m]	0.150
b_w [m]	0.400

Table 4.39 – Internal forces for the instant *t* with higher chord rotation for Case B

Model	Irregular Model			Regular Model		
Section	Kup	Fdown	Gup	Kup	Fdown	Gup
N [kN]	-389.8	-39.2	-205.6	-82.4	-125.8	-273.9
M [kNm]	280.8	277.8	271.7	270.9	281.9	284.3
V [kN]	-160.4	181.3	-172.5	-179.3	177.6	-187.6

Based on these values is possible to determine the entry parameters of equation (4.19). It was considered the simplification $\omega = \omega'$, which implies $\frac{\max(0.01;\omega')}{\max(0.01;\omega)} f_c = f_c$ is always true and, therefore, the values of ω and ω' are irrelevant and were not calculated. In Table 4.40 are presented the values necessary to determine the ultimate chord rotation capacity (θ_{um}).

Table 4.40 – Entry parameters of equation (4.19)

Model	Irregular Model			Regular Model		
Section	K_{up}	F_{down}	G_{up}	K_{up}	F_{down}	G_{up}
γ_{cl} [-]	1.5	1.5	1.5	1.5	1.5	1.5
h [m]	0.400	0.400	0.400	0.400	0.400	0.400
L_V [m]	1.751	1.532	1.575	1.511	1.588	1.515
ν [-]	0.064	0.006	0.034	0.014	0.021	0.045
f_c [MPa]	38	38	38	38	38	38
f_{yw} [MPa]	500	500	500	500	500	500
ρ_{sx} [-]	0.017	0.017	0.017	0.017	0.017	0.017
α [-]	0.595	0.595	0.595	0.595	0.595	0.595

Defined all parameters, the values for the ultimate chord rotation capacity (θ_{um}) were determined and are presented in Table 4.41, along with the computed chord rotations (θ_d) and the quotient between the two.

Table 4.41 – Values of the ultimate chord rotation capacity (θ_{um})

Model	Irregular Model			Regular Model		
Section	K_{up}	F_{down}	G_{up}	K_{up}	F_{down}	G_{up}
θ_d [mrad]	51.93	50.93	7.55	45.30	32.78	5.54
θ_{um} [mrad]	58.29	59.62	58.26	58.83	59.35	56.70
θ_d/θ_{um} [-]	0.89	0.85	0.13	0.77	0.55	0.10

From the results presented the following is concluded:

- The values of the ultimate chord rotation capacity (θ_{um}) are very similar in both models, as was expected given that the steel reinforcement considered was the same.
- In the irregular model, the section K_{up} has a chord rotation very close to the ultimate capacity, which indicates that the structure is very near the situation of collapse. Section F_{down} is also close to maximum capacity. It's recalled that both the mentioned sections belong to the same column implying that, if both reach their maximum capacity, this column would not contribute further to the overall resistance of the structure.
- The regular model is not as close to reach its maximum capacity, with the conditioning section still having the capacity to accommodate for a rotation of more approximately 14 mrad.
- Regarding the values for section G_{up}, it was concluded that both are far from there maximum capacity. Although, the chord rotation is higher in the irregular model, as was expected based on previous results. The discrepancy between the values for the columns in the first and second floor are due to the formation of a soft-storey collapse mechanism.

- Comparing the values of θ_d/θ_{um} for the irregular and regular models is possible to conclude that, in average the irregular presents values 30% higher than the regular model. This may be considered as an indication that the reduction in the behaviour factor of 20%, which represents an increase on the seismic effect of about 25%, is suitable to this type of vertical irregularity (if not an underestimate).

This concludes the study under artificial accelerograms. Following are briefly presented the results obtained for the displacements of the structure for recorded accelerograms.

4.2.3. Non-Linear Dynamic Time-History – Recorded Accelerograms

Addressed previously in detail the linear and non-linear behaviour of the structure under a dynamic loading, in this part only the non-linear response for the regular and irregular models is compared under a real seismic action, recorded during an earthquake. By using a recorded accelerogram is possible to have the closest proximity to the real behaviour of the structure under a seismic action using computational methods.

The response of the structure regarding the displacement on the first and second floor is presented in Figure 4.31 and Figure 4.32, respectively.

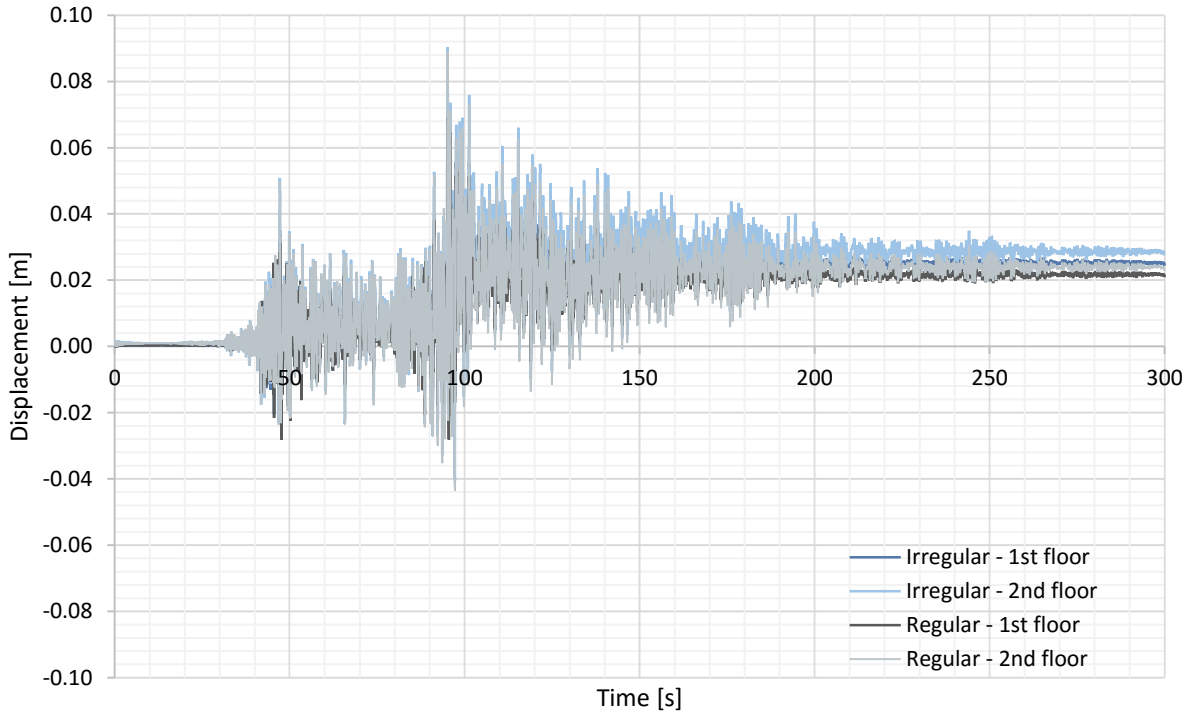

Figure 4.31 – Displacement of the first and second floor of the regular and irregular models in the x direction

Comparing the results obtained for the x direction is possible to conclude that the horizontal displacements in the irregular model are higher and the residual displacement more evident than in the regular model. Furthermore, the residual displacement of the first floor of the irregular model is higher than the one of the second floor of the regular model, suggesting (as for the artificial accelerograms) that the damage in the irregular model is more relevant than in the regular model.

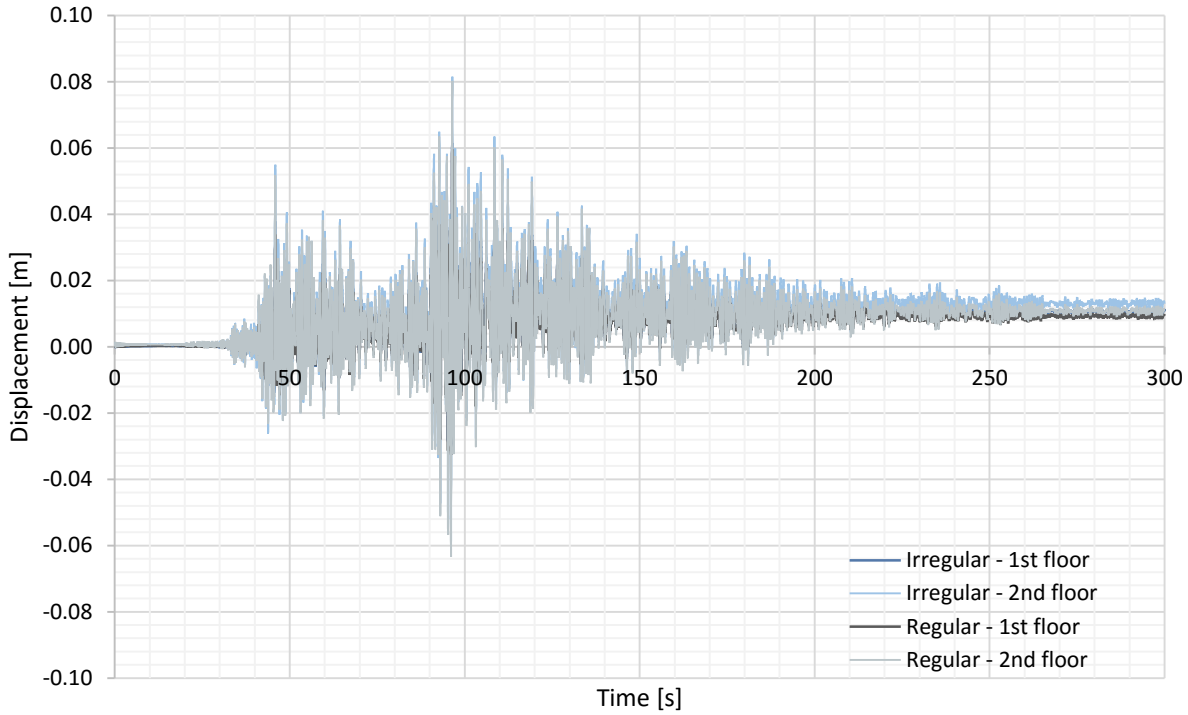

Figure 4.32 – Displacement of the first and second floor of the regular and irregular models in the y direction

Based on the results for the y direction the conclusions are similar to the ones previously taken for the x direction. The major differences are the lower absolute value of residual displacements as well as the differences of those residual displacements between the regular and irregular model.

To allow for a better comparison between the two directions are presented, in Table 4.42, the most relevant values of displacements. The percentage displacement (%d) is given by equation (4.21).

$$\%d = \frac{d_{1st}}{d_{2nd}} \tag{4.21}$$

Where d_{1st} and d_{2nd} are the residual displacements of the first and second floors, respectively.

Table 4.42 – Maximum, minimum and residual displacement for the studied cases

Model	Irregular				Regular			
Direction	X		Y		X		Y	
Floor	1st	2nd	1st	2nd	1st	2nd	1st	2nd
Max Displacement	0.072	0.090	0.062	0.082	0.069	0.089	0.060	0.080
Residual Displacement	0.025	0.029	0.011	0.013	0.022	0.024	0.009	0.011
%d	0.86		0.85		0.91		0.81	

Analysing the results presented it is concluded that the differences between the two models regarding the maximum absolute displacements are low (never superior to 5 mm) and might be considered negligible. On the other hand, regarding the residual displacements, there is a higher difference between the regular and irregular models. In the irregular models the residual displacement is 20% higher than in the regular ones. This is an important indication that the damage in the irregular model is more significant than in a model without this irregularity.

Also, by analysing the percentage displacement is possible to conclude that both structures might have soft-storey problems, being the regular model the one with higher values, contradicting the previously concluded. In this study the collapse also occurs by the formation of a soft-storey mechanism. Further studies need to be made in order to identify if this type of collapse mechanism is aggravated by the presence of the studied irregularity or not.

In Figure 4.33 are presented the results for the accumulated dissipated energy.

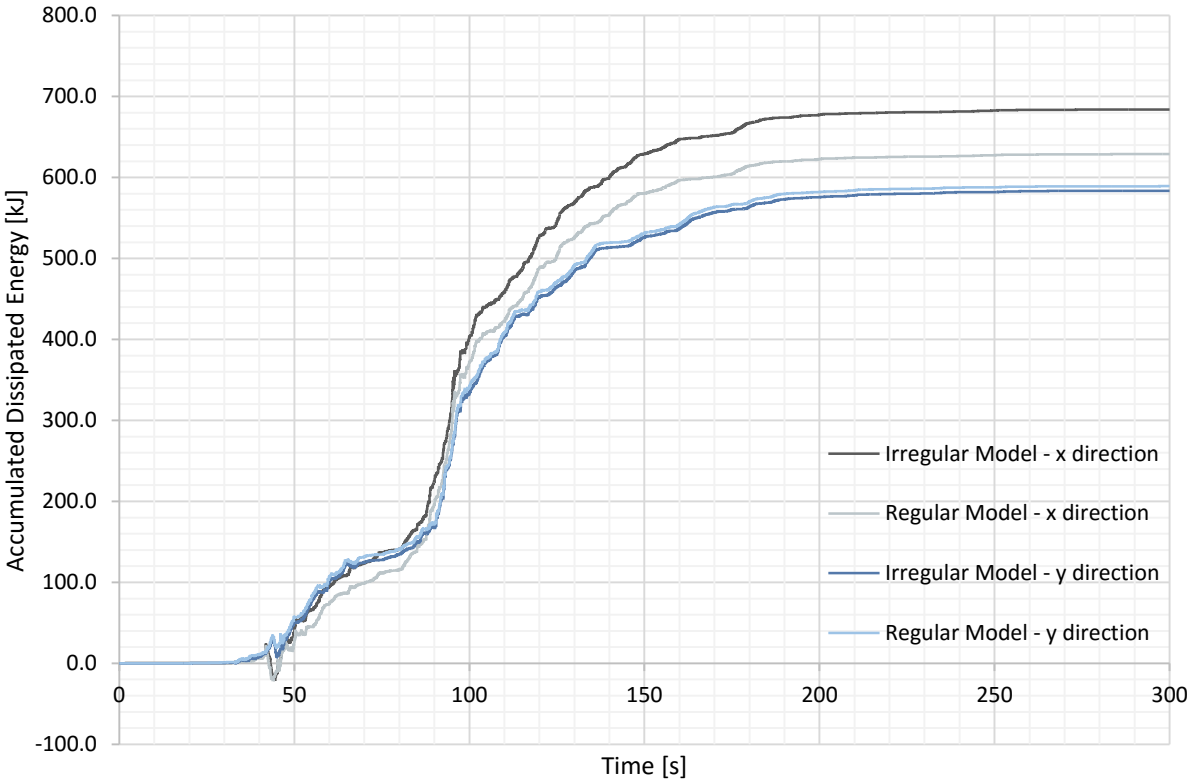

Figure 4.33 – Accumulated dissipated energy for the Tohoku earthquake

From the results presented is possible to conclude that in both the regular and the irregular models the dissipated energy is very similar for the y direction. This is as expected, given the fact that in this direction there is a slight variation in the resisting mechanism (only one column is eliminated). On the other hand, for the x direction there is a more significant variation being the irregular the model that dissipates more energy, the reason for this may be related with the existence of the transfer beam that is much more robust than the regular beams.

4.3. Final Considerations

In this section, the main conclusions of the non-linear studies are presented, synthesising the previous results and allowing for a better interpretation.

Based on the static time-history analysis it was concluded that the presence of the irregularity does not have a very significant effect on the overall behaviour of the structure for static loading (both monotonic and cyclic). This conclusion is based on the fact that there is no significant modification on the resisting mechanism. The discontinuity of the column led to the increase in the size of the transfer beam which stiffens the structure.
From this analysis was also possible to assess the maximum base shear that the structure may develop. This value is directly influenced by the adopted reinforcement for the elements and by the resisting mechanism, the first was considered equal in both models to allow for a better comparison, the latter is slightly different between the models but not enough to lead to significantly different results. This is the reason for the very similar responses for both models.

The dynamic time-history analyses were far more conclusive than those previously commented. It was concluded that the displacements for both structures are very similar, but these differed substantially from the results of the linear analyses; this discrepancy may be attributed to the fact that structures in which $T < T_C$ generally have higher non-linear displacements than the ones obtained from the elastic RSA. Other aspect that might take part in justifying the obtained results is the effect of cracking (that was considered by a reduction in 50% of the Young's modulus) which, in most cases, is a very rough approximation.
Regarding the q_F, the values were much lower than expected. The reason for this had to do with the overdesign of the structure and the decision of adopting equal reinforcements in both structures.
The study of the chord rotations led to the conclusion that there was, in fact, an accumulation of damage in the alignment that had the transfer beam, comparing with the regular model. Furthermore, in other parts of the structure there was a reduction in chord rotation, leading to the conclusion that the basis for the consideration of this situation as a vertical irregularity by the EN1998-1 [15] is adequate.
In order to evaluate the response of the structure in a situation of near collapse an aggravated action was considered and determined in accordance with the LSNC defined in the EN1998-3 [16]. From this analysis was concluded that the collapse mechanism for both models is one of soft-storey at the ground floor. The results also shown that the relations between the regular and irregular models regarding the displacements and the shear base were still valid although the absolute values of total base shear for each model were higher in the LSNC than in the LSSD, as was expected.
Through the comparison of the computed chord rotation (θ_d) with the ultimate capacity (θ_{um}) of each element was possible to strengthen the conclusion that the increase in the internal forces due to the presence of the irregularity of 25% that is in the base for the reduction in the behaviour factor is adequate to this situation, if not insufficient.

Chapter 5

Conclusions and Future Studies

5.1. Conclusions

With the development of this dissertation most of the initial objectives (set forth for the two studies) were achieved. In the parametric linear elastic study, different situations were considered allowing to gather sufficient information to identify the case (layout and irregularity position) in which the existence of a discontinued column would be more severe. The non-linear inelastic study that followed point towards the consideration of the irregularity in a similar manner as other vertical irregularities in the EN1998-1 [15] (i.e., through a reduction of 20% in the behaviour factor). This is a consequence of the accumulation of inelasticity above the irregularity.

5.1.1. Parametric Linear Elastic Study

The development of the parametric study was supported in a reasonable number of cases. Although many other could have been considered, the set of layouts presented and compared proved to be sufficient to conclude the following:

- When a discontinued column is considered in the architectural design, it is imperative for the cross-sections of the transfer beam (TB) and of the columns to be re-dimensioned, in order to endow the structure with a suitable behaviour for the serviceability and ultimate limit states. Regarding the design of the structure, the use of a pre-stress tendon is not the sole solution. A reinforced concrete structure (not pre-stressed) is a viable solution regarding the ULS, although it might prove unfitting in order to ensure an acceptable behaviour for the SLS.

- Bearing the previous conclusion in mind, the existence of this type of irregularity leads to a structure with stiffness comparable with that of the corresponding regular situation. Moreover, in the direction of the TB the structure is somewhat stiffer than in the perpendicular direction.
- It was also concluded that stiffer structures with the same plan layout have a higher aggravation than softer structures in what concerns the internal forces due to the irregularity. The basis for this conclusion is the fact that elevation II (2 floors) has the highest aggravation and elevation III (10 floors) the smallest. On the other hand, considering the in-plan layouts, the case with a shorter span (4m) presents a higher aggravation than the case with a longer span (7m) when considering the regular beams and the columns; however this trend is reversed when the TB is considered. The results for floor plan B, with shear walls being the main load-resisting system (and not the frames), show that the negative effects of the irregularity, in terms of the internal forces, are alleviated for the regular beams and columns at the cost of an aggravation for the transfer beams and shear walls.
- From these results it was also concluded that the design of the TB is determined by the gravity loads. This cannot be interpreted as a sign that there are no seismic implication associated with this irregularity, but that it rather is an indicator that the problem associated with the irregularity is not one of resistance but of ductility. Anyhow the results clearly indicate that, regarding the design of steel reinforcement of the TB, the gravity loads are predominant over the seismic loads.
- The effect of the irregularity is more detrimental to the frames set perpendicularly to the TB; this is related with the fact that, in that direction, the removal of the column is not compensated by the increase of the cross-section in any of the beams set in that direction.
- Another important result of this work is the fact that the seismic loads acting in the direction perpendicular to the TB originates a bending moment on that beam with a magnitude similar to the bending moment originated by the seismic action on the direction of the beam. This is not common in regular structures but, in this particular case, is an important feature that must not be overlooked in the design.

5.1.2. Non-linear Inelastic Study

With the development of the non-linear study, though only considering one irregular situation, the following conclusions were drawn:

- Regarding the global behaviour of the structure, the existence of the discontinued column leads to a structure with similar response to seismic loading (acting in the direction of the TB) as that of the regular case. However, in the perpendicular direction there is a reduction on the efficiency of the resisting mechanism due to the removal of the column. This comes in accordance with the conclusions taken regarding the stiffness of the structure.

- The displacements obtained for the regular and the irregular models are similar for both the linear elastic analysis and the non-linear inelastic analysis. However, the results for each of these analyses are different, leading to values of q_d higher than anticipated. These results are also confirmed by the values presented for the total base shear, for which the q_F values were lower than expected. This outcome (regarding q_F) is mostly due to the decisions considered during the design of the steel reinforcement, as previously explained.
  The fact that in both the regular and irregular cases the results for the displacements and base shear are similar, highlights the conclusion that the effect of the discontinued column is not a global one but a local one. It should be stressed that, in all studies (the parametric and the non-linear), only one (or two) columns were discontinued in each model. If more columns were discontinued the global response of the structure would be more affected.
- The results obtained for the chord rotations confirm this assumption (regarding irregularity local effect) given that there is a clear concentration of inelasticity, mostly in the sections above the TB, but also in the ones below. This indicates that the presence of this irregularity leads to an aggravation of the seismic effects, which must be duly considered in the design.
  It is also possible to conclude that, due to the cross-section redesign of the TB, this element (TB) is not considerably affected by the seismic action. However it leads to a concentration of inelasticity in the columns precipitating the formation of a soft-storey mechanism.
- Analysing the results for the limit state of near collapse it is possible to reaffirm most of the conclusions taken for the chord rotations. Furthermore, it is also concluded that the existence of this irregularity leads to the earlier failure of the structure. Although the collapse mechanism is the same as for the regular model (soft-storey), the existence of the discontinued column leads to higher damage (for the same action) in the irregular model than in the regular model.
  As seen from the obtained results, the existence of the discontinued column affects the chord rotations of the vertical elements, representing an increase of approximately 30%, when compared with the same elements in the regular model.
  These results are very specific and were derived considering one layout under one accelerogram only, further studies are needed to confirm the previous conclusions.
- It is clear from the presented results that a linear elastic response spectrum analysis underestimates the actual axial force in the discontinued column. This means that the behaviour factor should be inferior to 1.0, which is an unusual situation. It is important to mention that in the EN1998-1 [15] the behaviour factor for the design vertical response spectrum is 1.5. The results presented in this work point in the direction that considering a behaviour factor, as proposed in the previously mentioned standard, leads to an underestimation of the bending moment in the TB, which might prove to be a serious problem.

5.1.3. General Conclusions

The major conclusion taken from this dissertation is that the existence of a discontinued column has a negative effect on the structure that should not be overlooked.

Although the EN1998-1 [15] envisages a reduction on the behaviour factor in order to consider this irregularity, this measure globally affects the structure, leading to excessive reinforcement on all the columns (regardless of their position with respect to the discontinued column).
A more rational alternative solution would consist in assuming special rules of detailing in the zones next to the TB, endowing these zones with adequate ductility, ensuring a suitable behaviour under seismic loading. This way, the local concentration of inelasticity would be properly addressed, assuring that the chord rotation capacity is higher in those zones.

5.2. Future Studies

The development of this work leaves a number of other aspects that were not considered and that need to be addressed in order to fully understand the effect of discontinued columns and the correct way to consider them at the design stage. Some of the possible studies that might be developed based on the forwarded results are:

- Regarding the linear studies many other situations could be considered, although one parameter that should be taken in consideration is the number of discontinued columns. As mentioned before, only one or two columns were discontinued in one single alignment, is important to study the effect of the removal of more columns, leading to conclusions regarding the global or local effect of this irregularity.
- Regarding the non-linear behaviour many other studies might be developed:
    - One possible line of research could consist in the study of the adequate values of the behaviour factors (for both horizontal and vertical directions), to be considered at the design stage. Considering the results for the axial force in the discontinued column it is possible that the prescription of a behaviour factor for the vertical response spectrum of 1.5 is not a suitable assumption. This might cause some problems for the TB, even when the fundamental load combination is more detrimental than the seismic load combination for this beam.
    - Complementary to the former approach, the study of special detailing rules for the zones where the accumulation of inelasticity occurs could be a promising line of development. These rules should be focused not only on the columns but also on the connection of these with the TB.
    - The comparison of the two presented lines of research (either separate or joint) in terms of ultimate and serviceability limit states response, structural efficiency and cost, would also be a considerable enrichment to the state of the art.
    - Finally, the study of progressive collapse would be important. Not only regarding a regular structure that had a column failure situation, creating a case similar to the studied in the dissertation, but also the effects of the occurrence of some problems in the pre-stress tendon.

References

[1] AGARWAL, P., THAKKAR, S. K. & DUBEY, R. N. (2002). Seismic Performance of Reinforced Concrete Building During Bhuj Earthquake of January 26, 2001. ISET Journal of Earthquake Technology, 39(3), 195-217.

[2] APPLETON, J. (2013). Estruturas de Betão vol. 1 e 2. Lisboa: Orion. [in Portuguese]

[3] ARLEKAR, J. N., JAIN, S. K. & MURTY, C. V. R. (1997). Seismic Response of RC Frame Building with Soft First Storey. CBRI Golden Jubilee Conference on Natural Hazards in Urban Habitat. New Delhi.

[4] BHENSDADIA, H. & SHAH, S. (2015). Pushover Analysis of RC Frame Structure with Floating Column and Soft Story in Different Earthquake Zones. International Journal of Research in Engineering and Technology, 4(4), 114-121.

[5] CESMD. Center for Engineering Strong Motion Data. Obtido de http://strongmotioncenter.org/

[6] CHINTANAPAKDEE, C. & CHOPRA, A. K. (2014). Seismic Response of Vertically Irregular Frames: Response History and Modal Pushover Analysis. Journal of Structural Engineering, 130(8), 1177-1185.

[7] CLOUGH, R. W. & PENZIEN, J. (2003). Analysis of Dynamic Response - Using Superposition. In Dynamic of Structures (pp. 219 - 257). Berkeley: Computers & Structures, Inc.

[8] CORLEY, W. G. (2002). Application of Seismic Design in Mitigating Progressive Collapse. Skokie, Illinois: Construction Technology Laboratories, Inc.

[9] CORREIA, A. A., ALMEIDA, J. P. & PINHO, R. (2008). Force-based versus displacement-based formulations in the cyclic nonlinear analysis of RC frames. 14th World Conference on Earthquake Engineering. Beijing, China.

[10] DUBAL, R. A., VASANWALA, S. A. & MODHERA, C. D. (2015). Application of Performance based Seismic Design Method to Column Discontinued RC Frame. International Journal of Computed Applications, 119(7).

[11] EARTHQUAKE ENGINEERING RESEARCH INSTITUTE (EERI). Preliminary Observations on the Origin and Effects of the January 26, 2001 Bhuj (Gujarat, India) Earthquake. California: EERI Special Earthquake Report.

[12] EN1990. (2009). Eurocode - Basis of structural design. CEN.

[13] EN1991-1-1. (2009). Eurocode 1: Actions on structures - Part 1-1: General actions - Densities, self-weight, imposed loads for buildings. CEN.

[14] EN1992-1-1. (2010). Eurocode 2: Design of Concrete Structures - Part 1-1: General rules and rules for buildings. CEN.

[15] EN1998-1. (2010). Eurocode 8: Design of structures for earthquake resistance - Part 1: General rules, seismic actions and rules for buildings. CEN.

[16] EN1998-3. (2005). Eurocode 8: Design of structures for earthquake resistance – Part 3: Assessment and retrofitting of buildings. CEN.

[17] FARDIS, M. N. (2009). Seismic Design, Assessment and retrofitting of Concrete Buildings. Springer.

[18] FARDIS, M. N., CARVALHO, E., ELNASHAI, A., FACCIOLI, E., PINTO, P. & PLUMIER, A. (2005). Designers' Guide to EN1998-1 and EN1998-5 Eurocode 8: Design of Structures for Earthquake Resistance. Gulvanessian.

[19] FILIPPOU, F. C., POPOV, E. P. & BERTERO, V. V. (1983). Effects of bond deterioration on hysteretic behaviour of reinforced concrete joints. University of California, Berkeley: Report EERC 83-19, Earthquake Engineering Research Center.

[20] FRAGIADAKIS, M., PINHO, R. & PEREIRA, E. M. (2008). Modelling inelastic buckling of reinforcing bars under earthquake loading. In Progress in Computational Dynamics and Earthquake Engineering, Eds. M. Papadrakakis, D.C. Charmpis, N.D. Lagaros and Y. Tsompanakis, A.A. Balkema. The Netherlands: Taylor & Francis.

[21] GHOSH, S. K. Observations from the Bhuj Earthquake of January 26, 2001. Northbrook, IL: S.K. Ghosh Associates Inc.

[22] GOEL, R. K. Performance of Building During the January 26, 2001 Bhuj Earthquake. California: Earthquake Engineering Research Institute.

[23] HARUGOPPA, R. & MURANAL, S. M. Effect of Floating Columns on Seismic Forces of RC Supporting Flexure Members in a Typical OMRF with and without Infill Masonry.

[24] LOPES, M. (2008). Sismos e Edifícios. Lisboa: Orion. [in Portuguese]

[25] MANDAS, P. (1993). Advanced Modelling of Composite Frames Subjected to Earthquake Loading. Imperial College, University of London, London, UK: PhD Thesis.

[26] MANDER, J., PRIESTLEY, M. & PARK, R. (1988). Theoretical stress-strain model for confined concrete. Journal of Structural Engineering, 114(8), 1804-1826.

[27] MARTINEZ-RUEDA, J. & ELNASHAI, A. (1997). Confined concrete model under cyclic load. Materials and Structures, 30(197), 139-147.

[28] MENEGOTTO, M. & PINTO, P. (1973). Method of analysis for cyclically loaded R.C. plane frames including changes in geometry and non-elastic behaviour of elements under combined normal force and bending. Symposium on the Resistance and Ultimate Deformability of Structures Acted on by Well Defined Repeated Loads. International Association for Bridge and Structural Engineering, Zurich, Switzerland, pp. 15-22.

[29] MONTI, G., NUTI, C. & SANTINI, S. (1996). CYRUS - Cyclic Response of Upgraded Sections, Report No. 96-2. Italy: University of Chieti.

[30] MUNDADA, A. P. & SAWDATKAR, S. G. (2014). Comparative Seismic Analysis of Multistorey Building with and without Floating Column. International Journal of Current Engineering and Technology, 4(5), 3395-3400.

[31] MURTY, C. V. R., GOEL, R. K., GOYAL, A., JAIN, S. K., SINHA, R., RAI, D. C., ARLEKAR, J. N. & METZGER, R. (2012). Reinforced Concrete Structures. Earthquake Spectra, 18(S1), 149-185.

[32] NANABALA, S. G., RAMANCHARLA, P. K. & E, A. (2014). Seismic Analysis of a Normal Building and Floating Column Building. International Journal of Engineering Research & Technology, 3(9), 981-987.

[33] NAUTIYAL, P., AKHTAR, S. & BATHAM, G. (2014). Seismic Response Evaluation of RC Frame Building with Floating Column considering different Soil Conditions. International Journal of Current Engineering & Technology, 4(1), 132-138.

[34] POONAM, KUMAR, A. & GUPTA, A. K. (2012). Study of Response of Structurally Irregular Building Frames to Seismic Excitations. International Journal of Civil, Structural, Environmental and Infrastructure Engineering Research and Development, 2(2), 25-31.

[35] PROTA, A., CICCO, F. & COSENZA, E. (2009). Cyclic behaviour of smooth steel reinforcing bars: experimental analysis and modelling issues. Journal of Earthquake Engineering, 13(4), 500-519.

[36] ROHILLA, I., GUPTA, S. M. & SAINI, B. (2015). Seismic Response of Multi-storey Irregular Building with Floating Column. International Journal of Research in Engineering & Technology, 4(3), 506-518.

[37] SABARI, S. & PRAVEEN, J. V. (2015). Seismic Analysis of Multistorey Building with Floating Column. International Journal of Civil and Structural Research, 2(2), 12-23.

[38] SAP2000. SAP2000 - Integrated software for structural analysis and design. Computers & Structures Inc.

[39] SEISMOSOFT. (2013). SeismoArtif v2.1 – A computer program for generating artificial earthquake accelerograms matched to a specific target response spectrum. Available from http://www.seismosoft.com.

[40] SEISMOSOFT. (2014). SeismoStruct v7.0 – A computer program for static and dynamic nonlinear analysis of framed structures. Available from http://www.seismosoft.com.

[41] SHAH, B. A. & PATODI, S. C. (2011). Performance Based Seismic Evaluation of RC Frames with Floating Columns. Retrieved September 17, 2015, from http://nbmcw.com/articles/miscellaneous/others/25052-performance-based-seismic-evaluation.html

[42] SINGLA, S. & RAHMAN, A. (2015). Effect of Floating Columns on Seismic Response of Multi-Storeyed RC Framed Buildings. International Journal of Engineering Research & Technology, 4(6), 1131-1136.

[43] YASSIN, M. H. (1994). Nonlinear analysis of prestressed concrete structures under monotonic and cyclic loads. University of California, Berkeley, USA: PhD Thesis.

Annex

Annex A

Model Assignments

In this annex are presented the cross-section assigned for each element of the models of the parametric study. It's important to stress that the alterations from the regular to the irregular models was made by only altering the frame in which the column was discontinued, therefore only the assignments of those (irregular) frames are presented, the rest of the elements are considered the same as defined for the regular model. Also, the regular models are bisymmetrical meaning that only half of the frames are defined and the other half is the same.

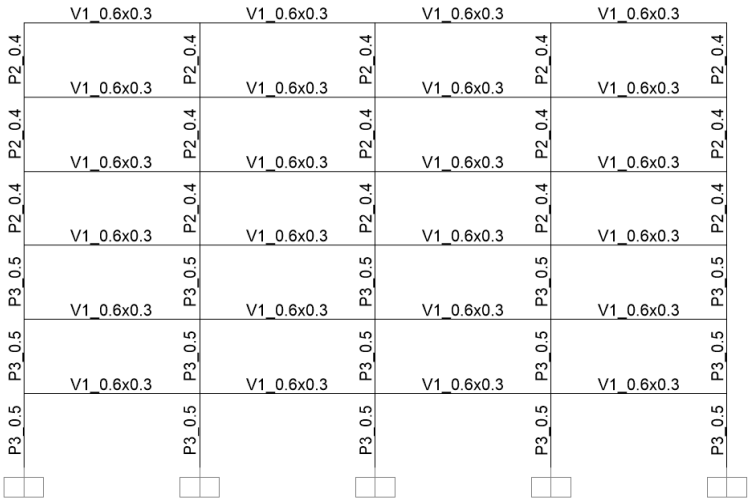

Figure A.1 – Model M_A.I_R for y=0m and y=21m

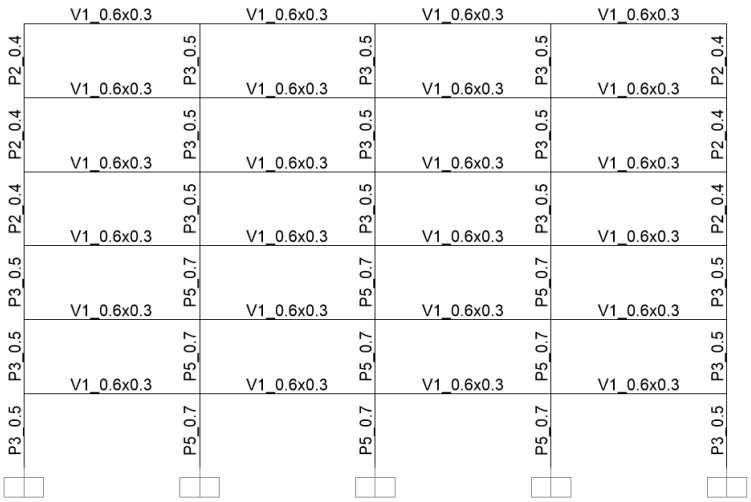

Figure A.2 – Model M_A.I_R for y=7m and y=14m

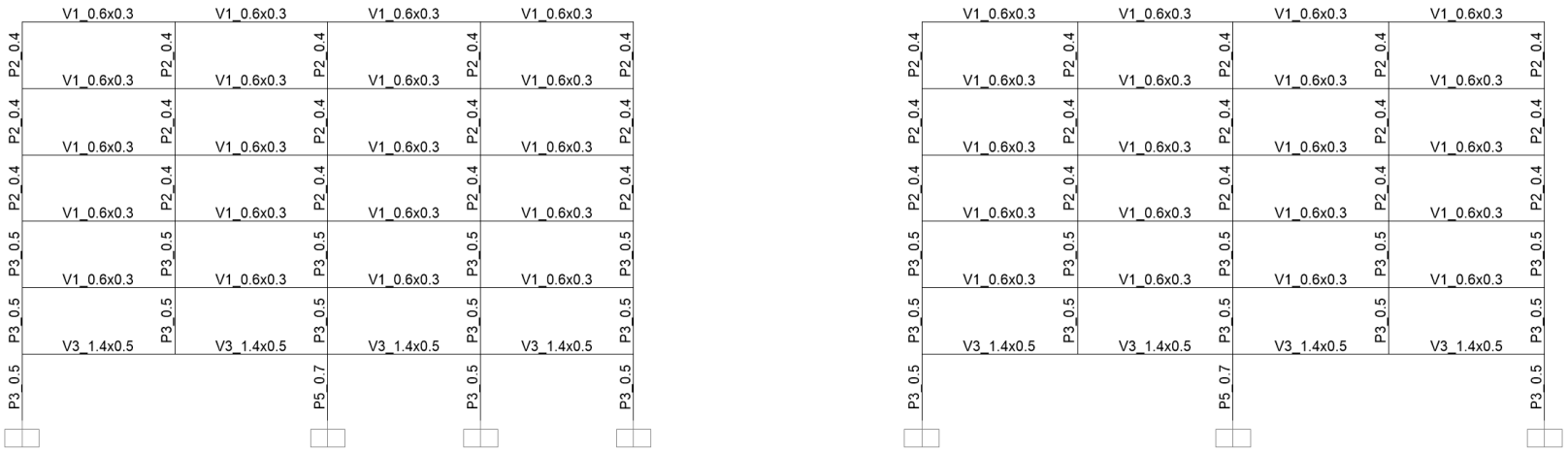

Figure A.3 – Model M_A.I_X-b1 (left) and Model M_A.I_X-bd1 (right) for y=0m

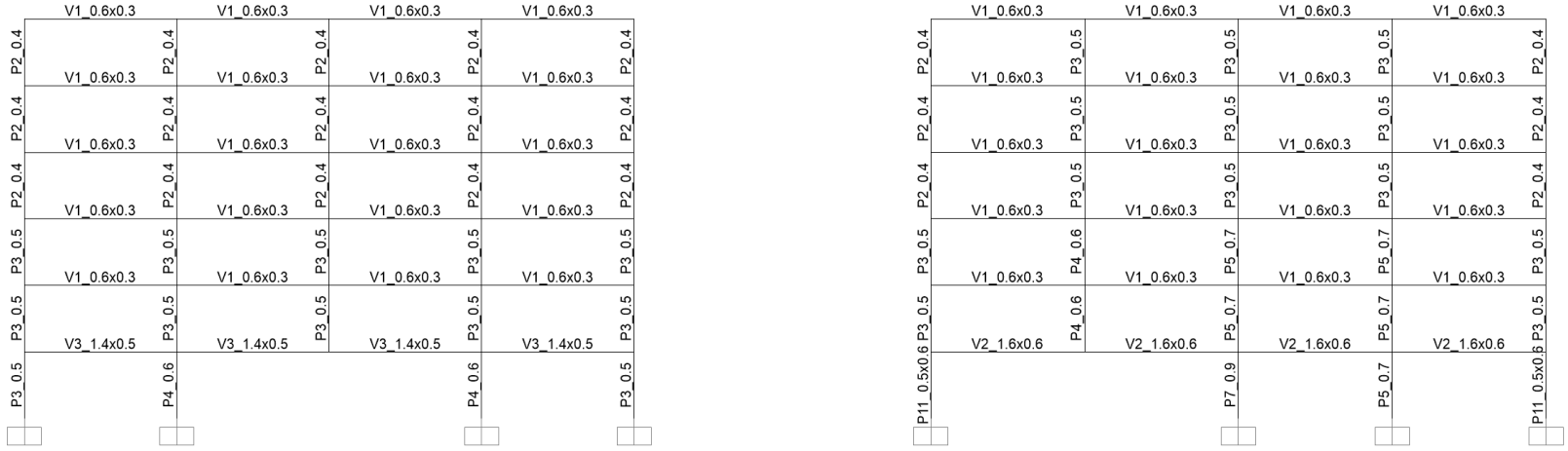

Figure A.4 – Model M_A.I_X-c1 for y=0m (left) and Model M_A.I_X-b2 for y=7m (right)

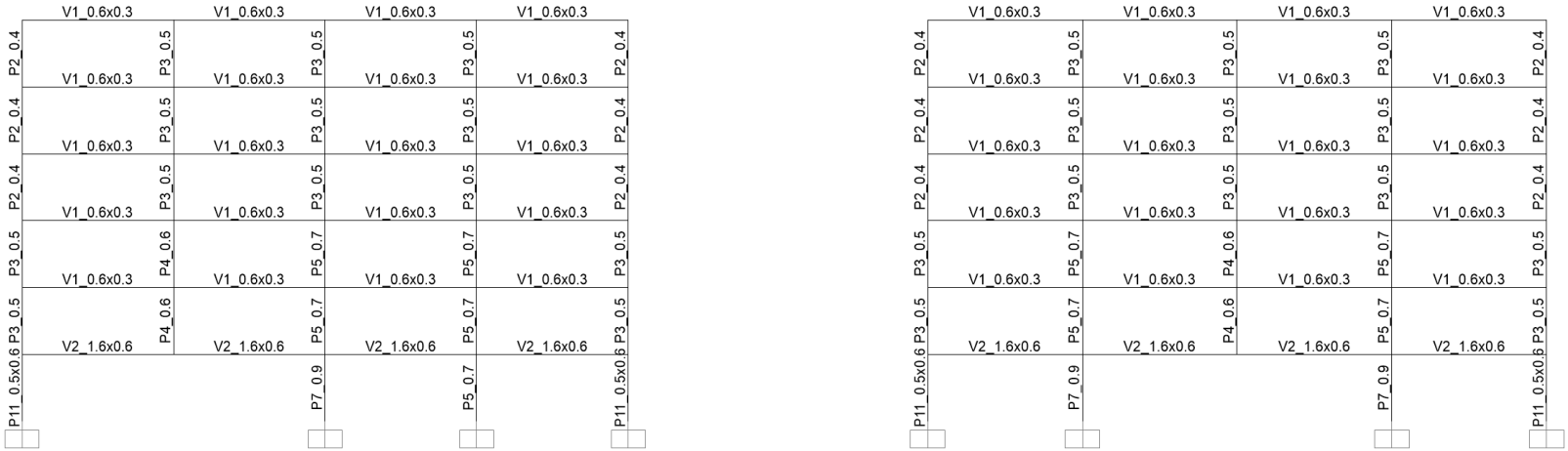

Figure A.5 – Model M_A.I_X-bd2 (left) and Model M_A.I_X-c2 (right) for y=7m

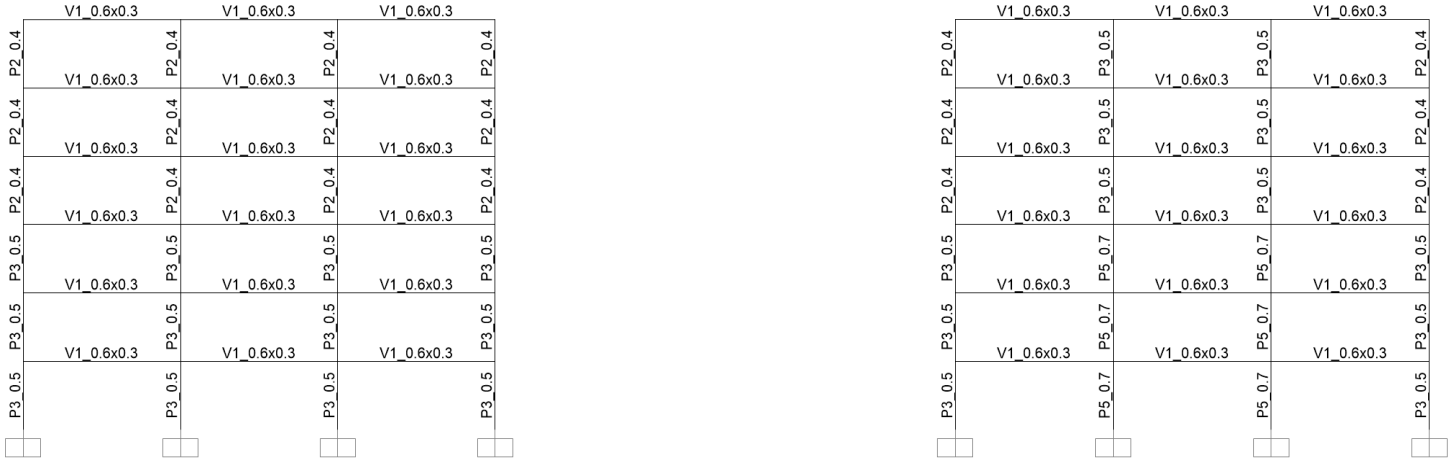

Figure A.6 – Model M_A.I_R for x=0m and x =28m (left) and for x=7m, x=14m and x=21m (right)

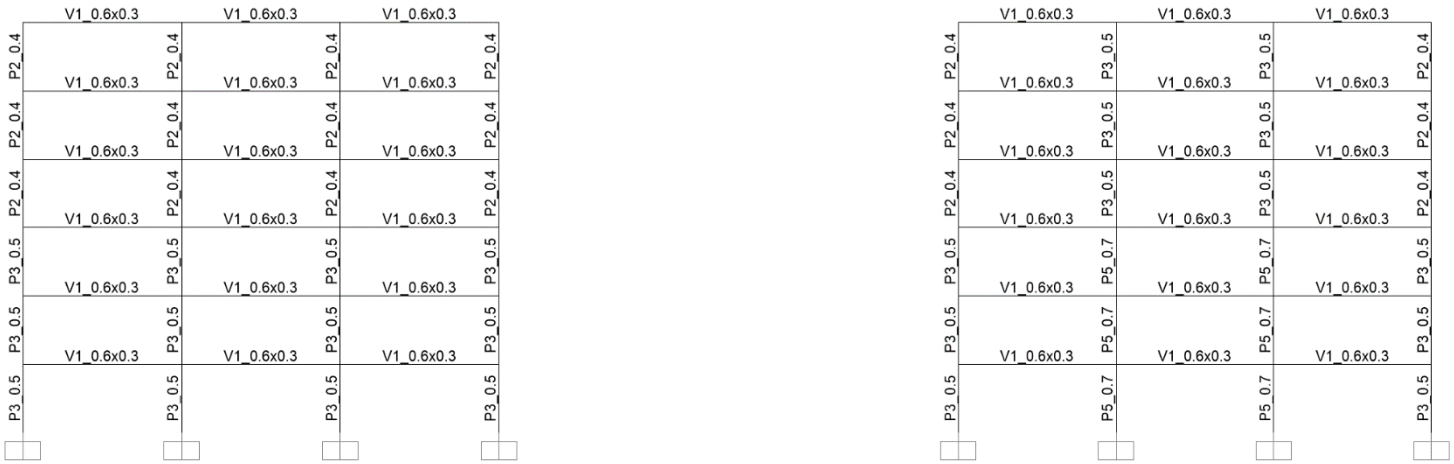

Figure A.7 – Model M_A.I_Y-a2 for x=0m (left), M_A.I_Y-b2 for x=7m and M_A.I_Y-c2 for x=14m (right)

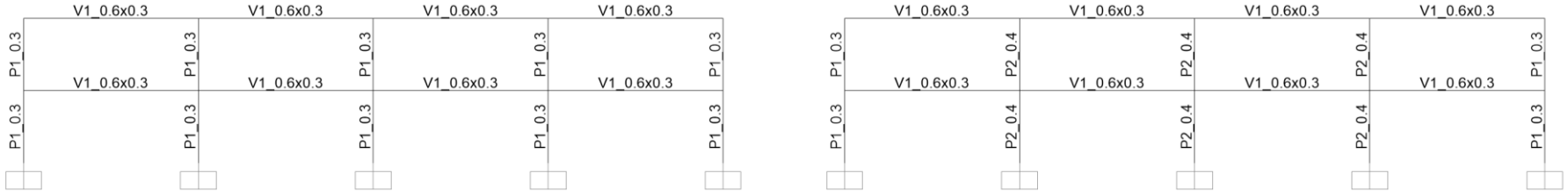

Figure A.8 – Model M_A.II_R for y=0m and y =21m (left) and for y=7m, x=14m (right)

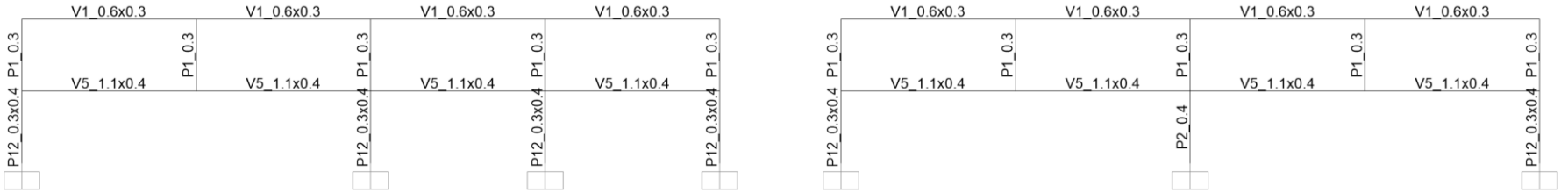

Figure A.9 – Model M_A.II_X-b1 (left) and Model M_A.II_X-bd1 (right) for y=0m

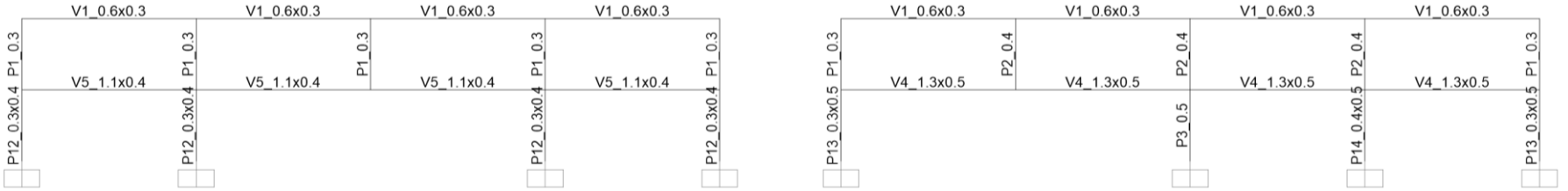

Figure A.10 – Model M_A.II_X-c1 for y=0m (left) and Model M_A.II_X-b2 for y=7m (right)

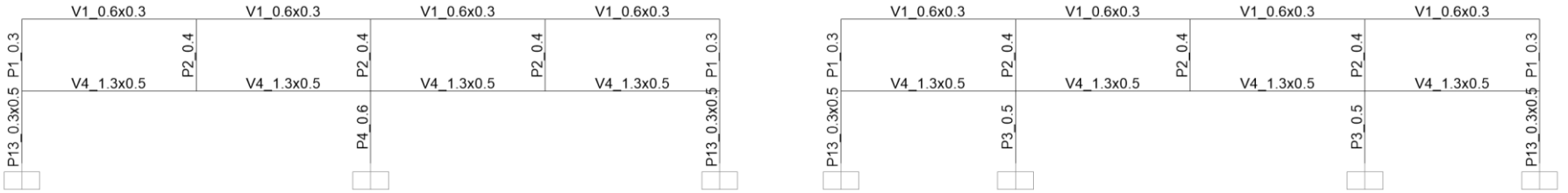

Figure A.11 – Model M_A.II_X-bd2 (left) and Model M_A.II_X-c2 (right) for y=7m

Figure A.12 – Model M_A.II_R for x=0m and x =28m (left) and for x=7m, x=14m and x=21m (right)

Figure A.13 – Model M_A.II_Y-a2 for x=0m (left), M_A.II_Y-b2 for x=7m and M_A.II_Y-c2 for x=14m (right)

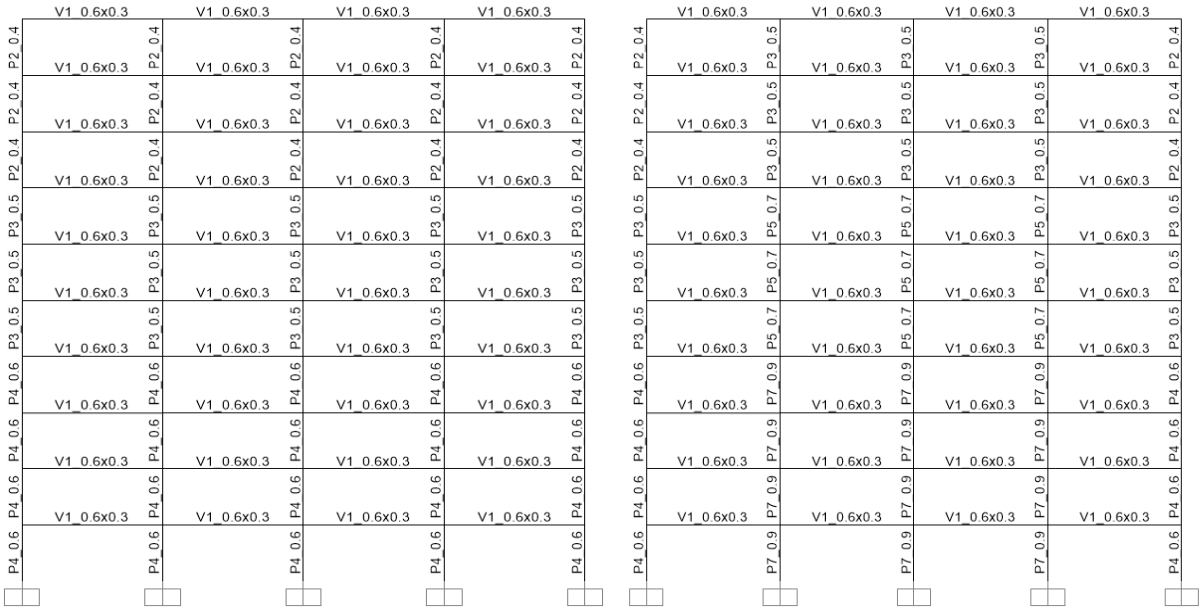

Figure A.14 – Model M_A.III_R for y=0m and y =21m (left) and for y=7m, x=14m (right)

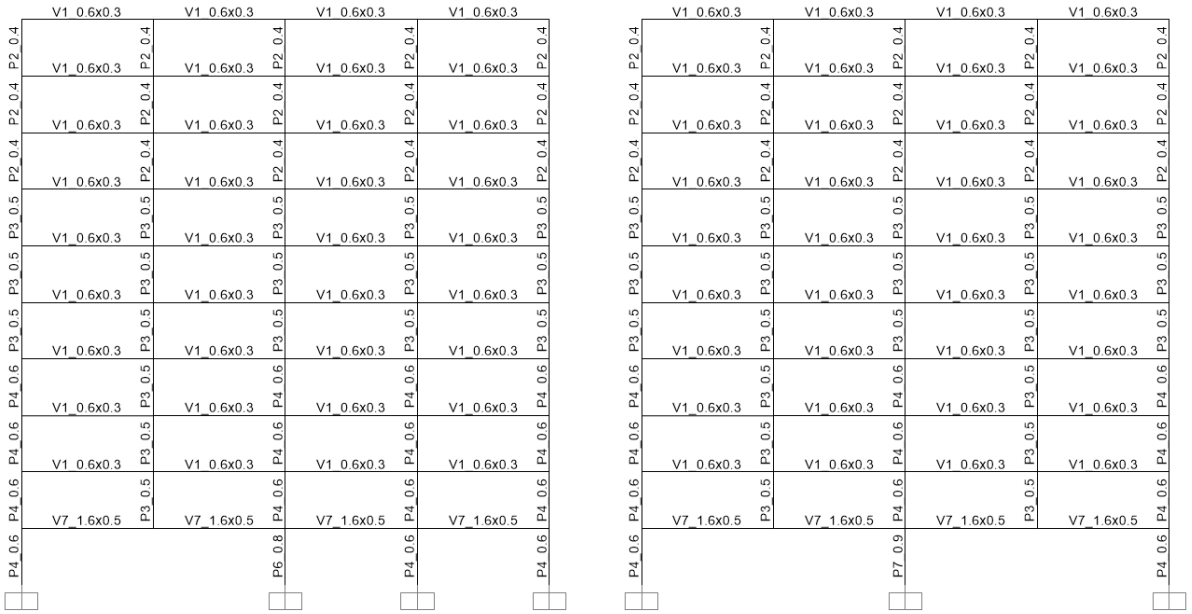

Figure A.15 – Model M_A.III_X-b1 (left) and Model M_A.III_X-bd1 (right) for y=0m

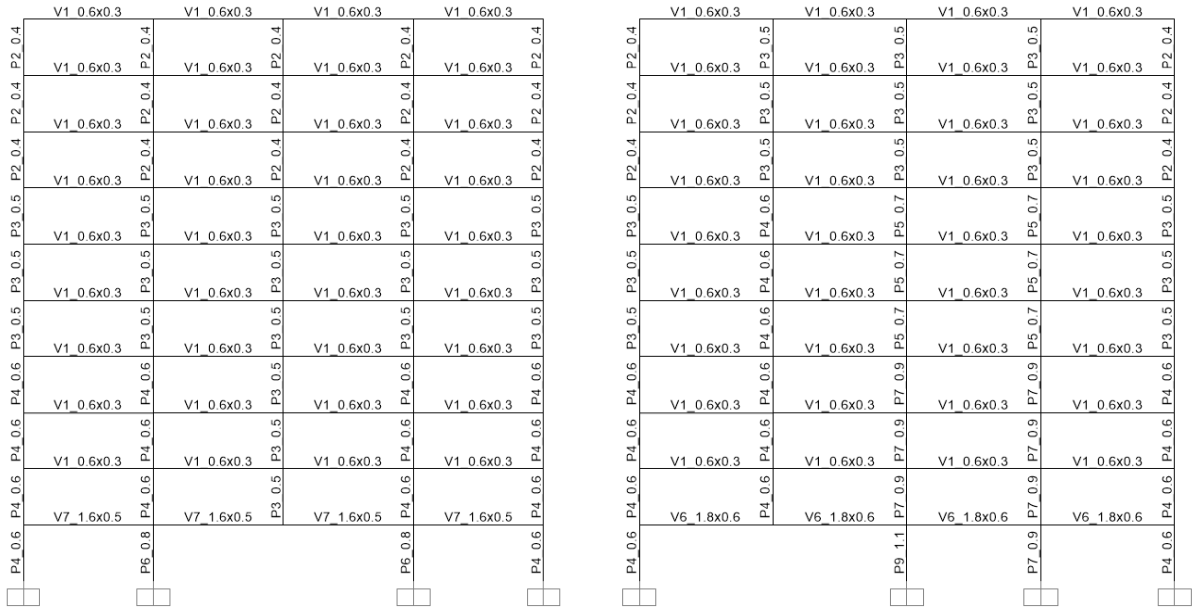

Figure A.16 – Model M_A.III_X-c1 for y=0m (left) and Model M_A.III_X-b2 for y=7m (right)

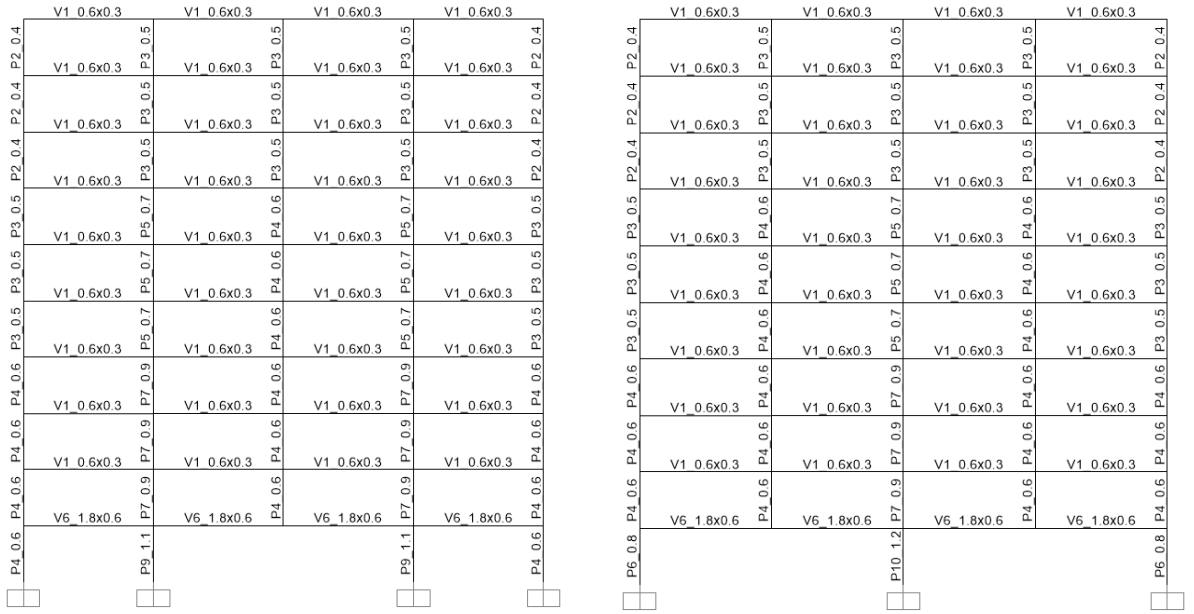

Figure A.17 – Model M_A.III_X-bd2 (left) and Model M_A.III_X-c2 (right) for y=7m

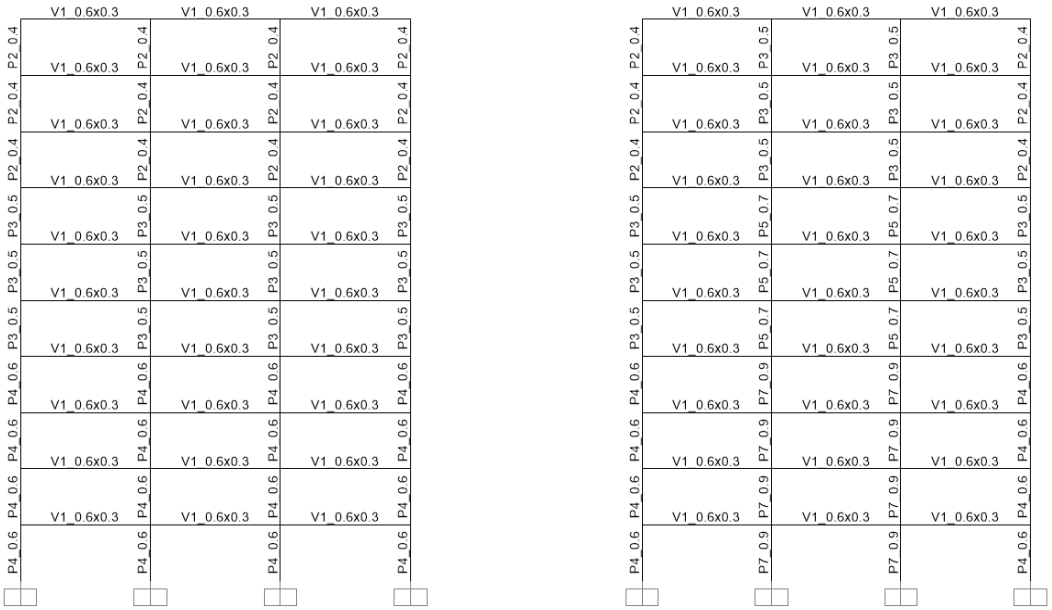

Figure A.18 – Model M_A.III_R for x=0m and x =28m (left) and for x=7m, x=14m and x=21m (right)

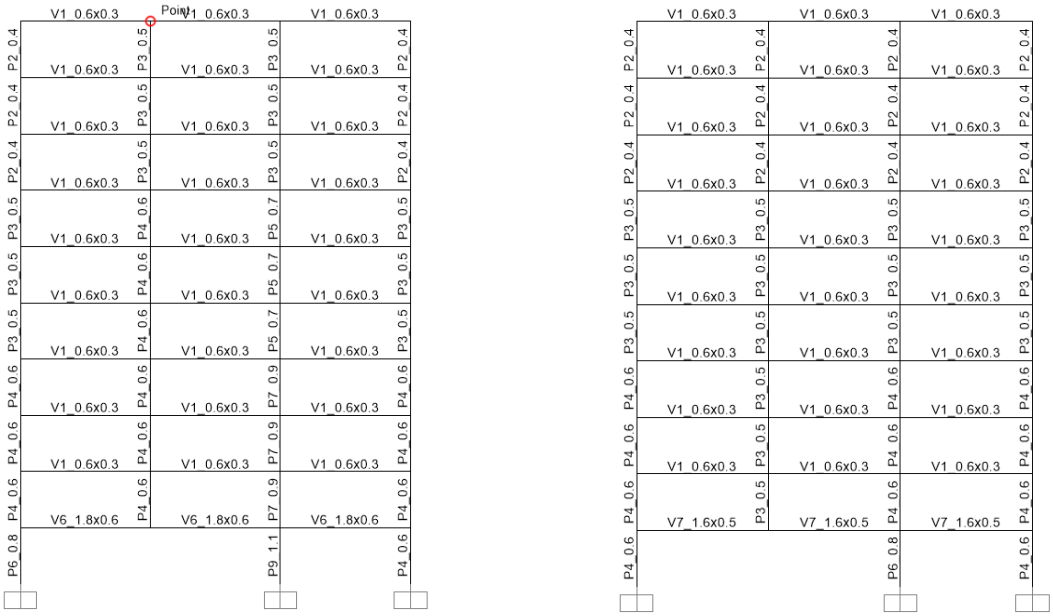

Figure A.19 – Model M_A.III_Y-a2 for x=0m (left), M_A.III_Y-b2 for x=7m and M_A.III_Y-c2 for x=14m (right)

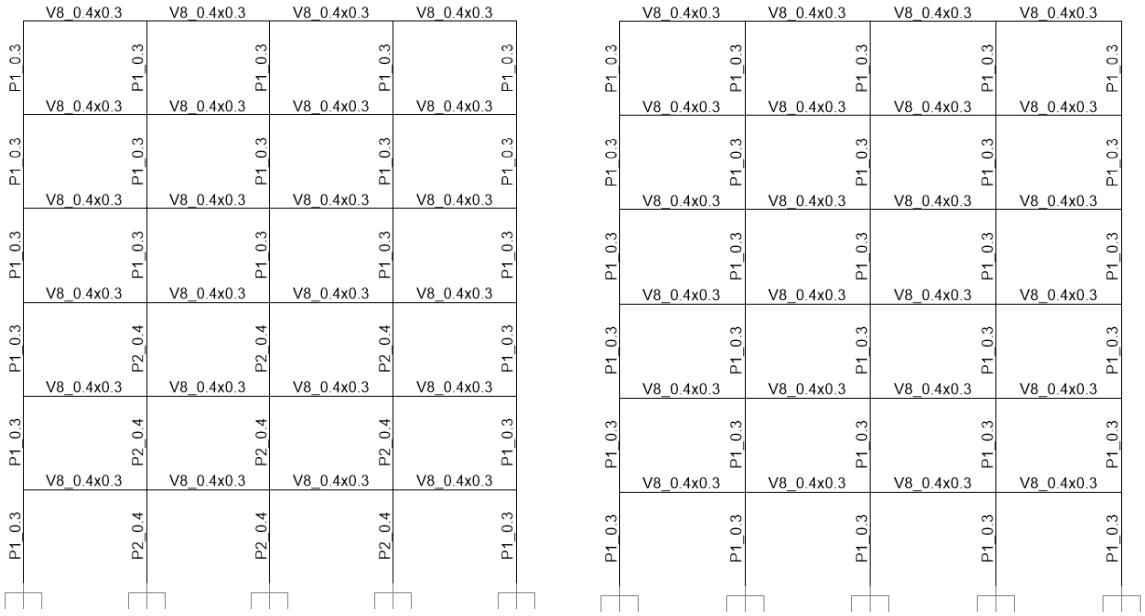

Figure A.20 – Model M_C.I_R for y=0m and y =21m (left) and for y=7m, x=14m (right)

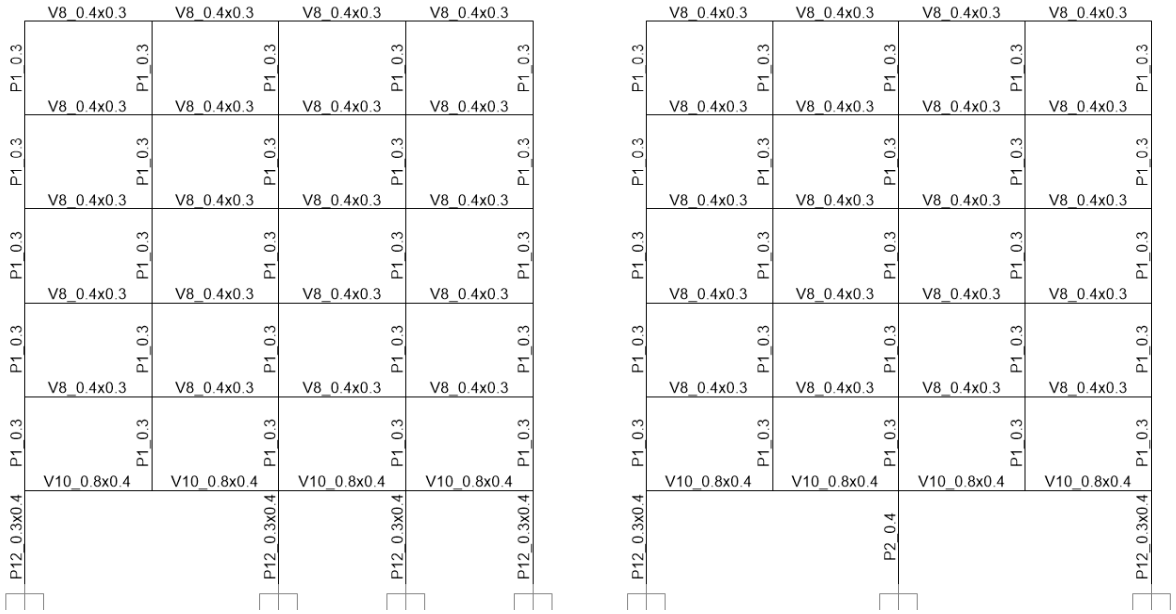

Figure A.21 – Model M_C.I_X-b1 (left) and Model M_C.I_X-bd1 (right) for y=0m

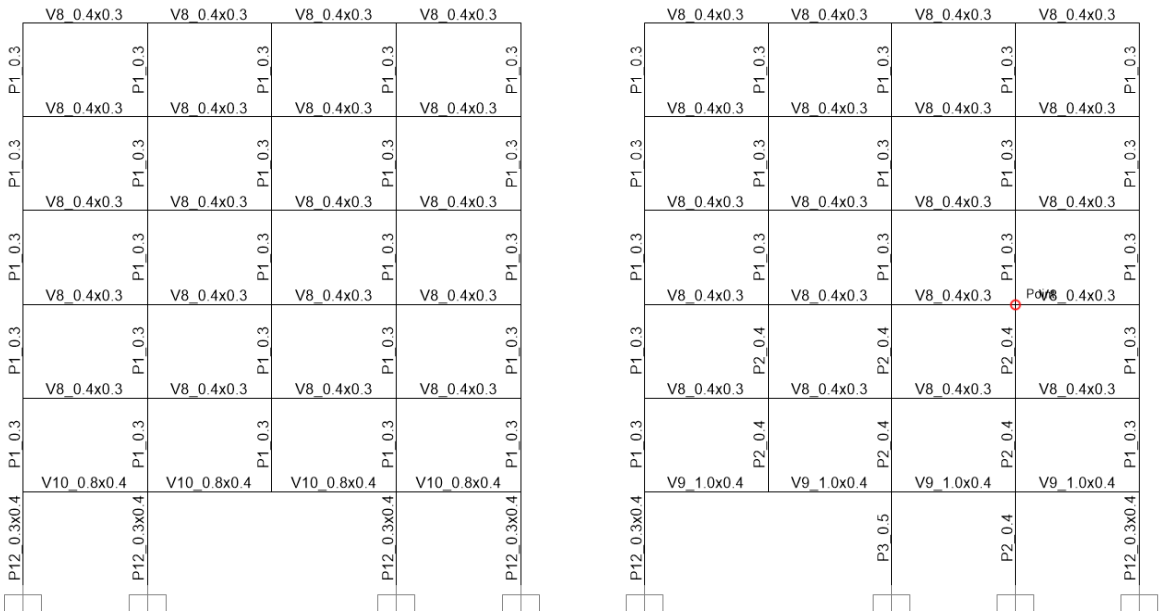

Figure A.22 – Model M_C.I_X-c1 for y=0m (left) and Model M_C.I_X-b2 for y=7m (right)

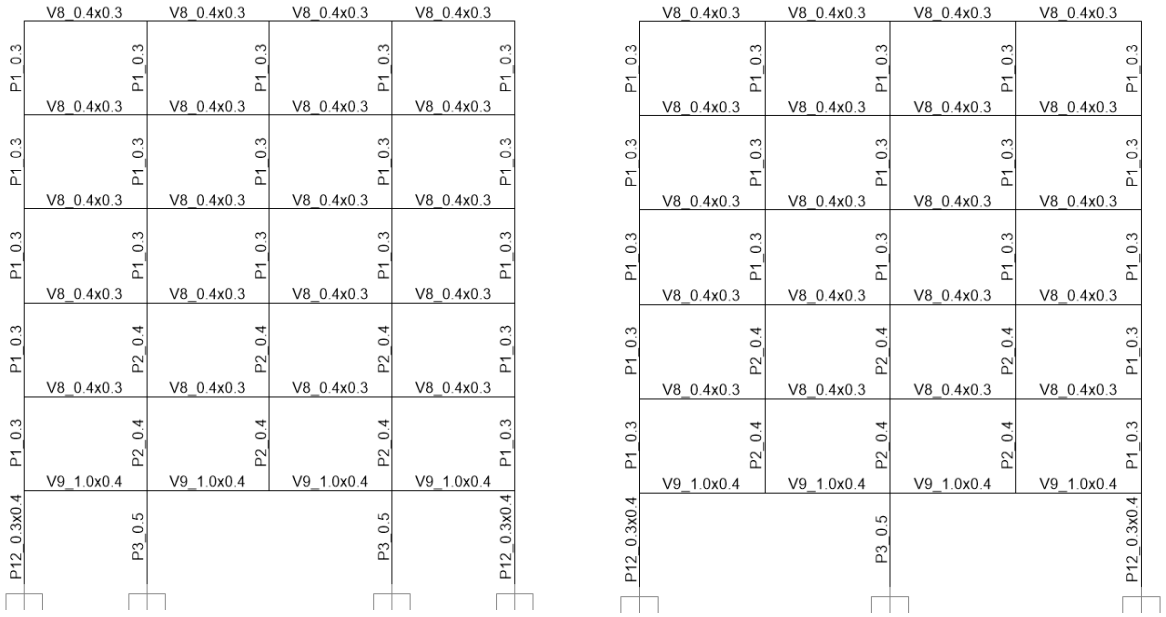

Figure A.23 – Model M_C.I_X-bd2 (left) and Model M_C.I_X-c2 (right) for y=7m

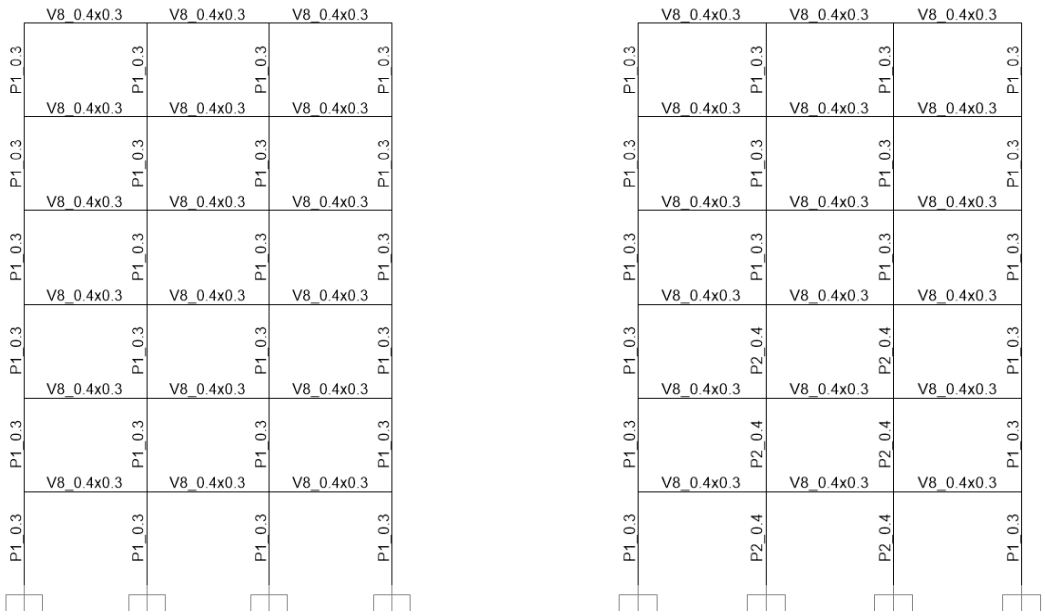

Figure A.24 – Model M_C.I_R for x=0m and x =28m (left) and for x=7m, x=14m and x=21m (right)

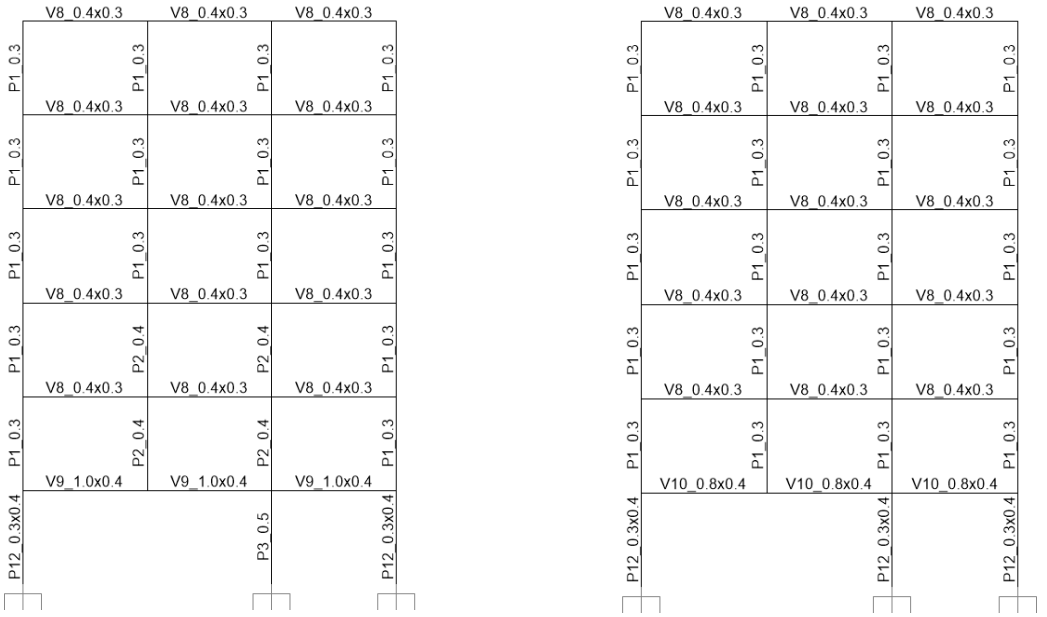

Figure A.25 – Model M_C.I_Y-a2 for x=0m (left), M_C.I_Y-b2 for x=7m and M_C.I_Y-c2 for x=14m (right)

The assignments for the models of the case **M_B.I** were not represented here given that they are equal to the ones for case **M_A.I**, being the only difference, which remains unchanged for all models, the presence of the shear in the positions defined in Figure 3.2 instead of columns **A1**, **A4**, **E1** and **E4**.

Annex B

Bending Moments Diagrams for the Initial Analysis

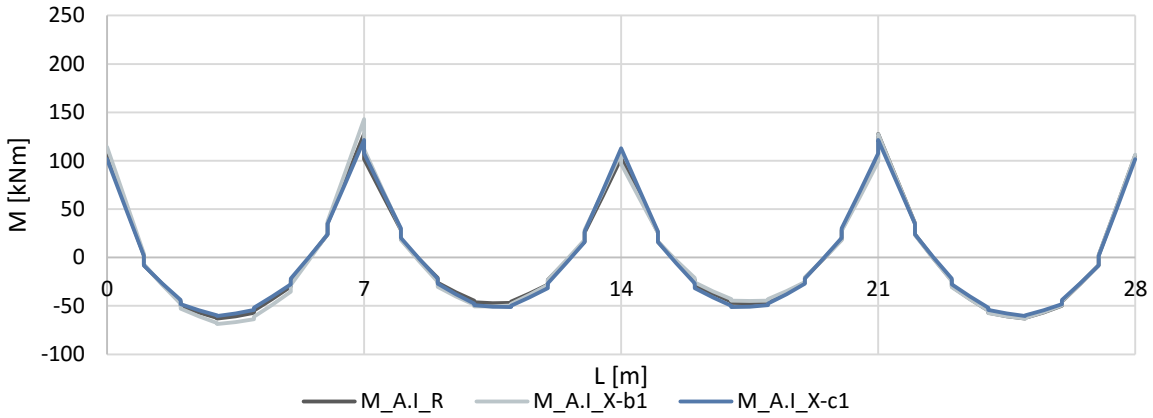

Figure B.1 – Bending moments for the Quasi-Permanent Load Combination on beam X2

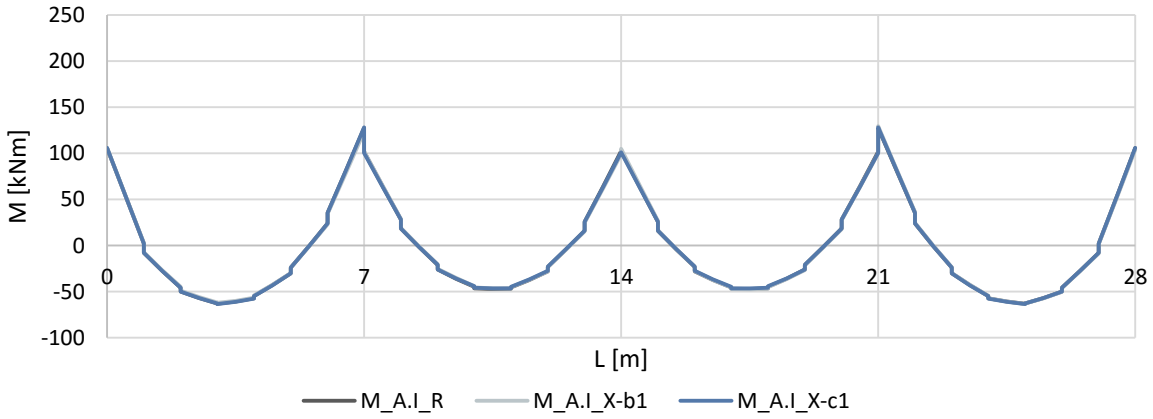

Figure B.2 – Bending moments for the Quasi-Permanent Load Combination on beam X3

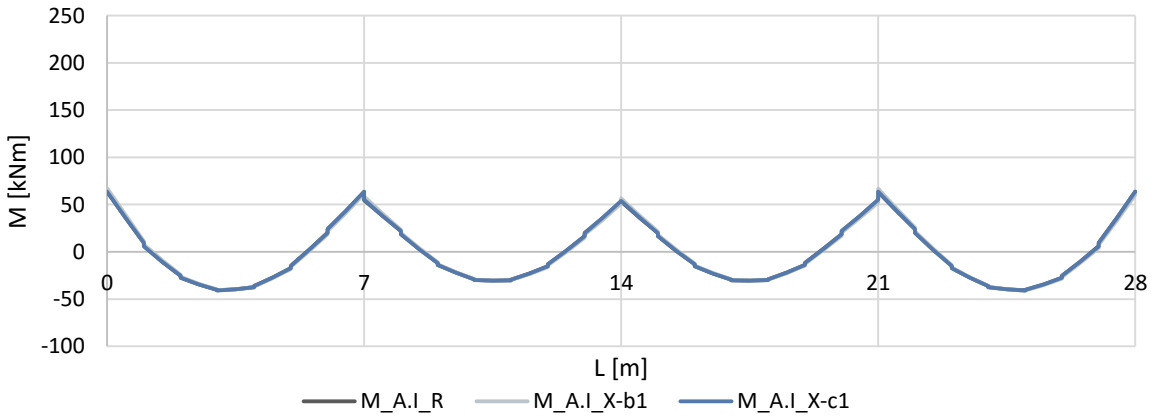

Figure B.3 – Bending moments for the Quasi-Permanent Load Combination on beam X4

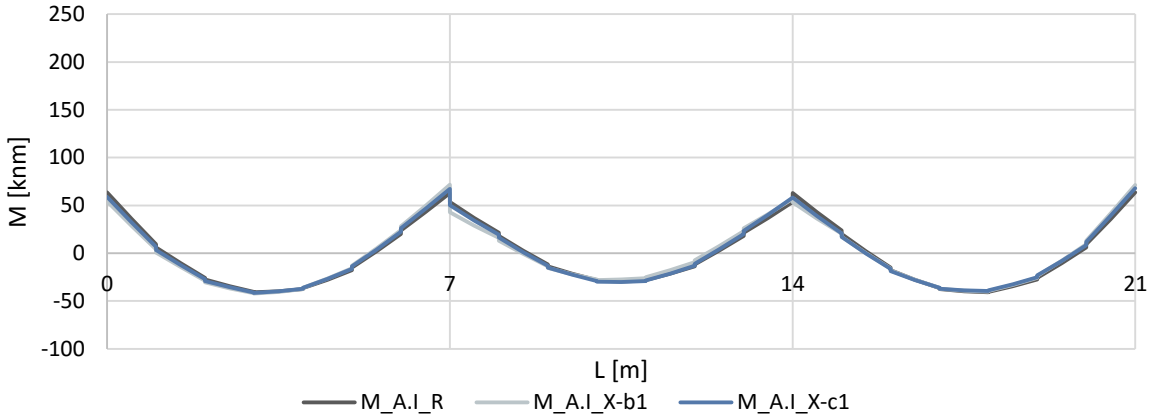

Figure B.4 – Bending moments for the Quasi-Permanent Load Combination on beam YA

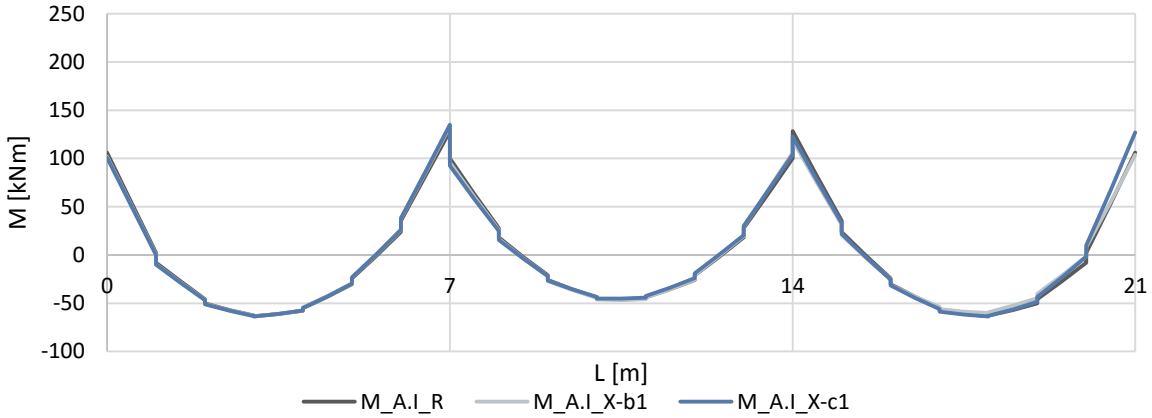

Figure B.5 – Bending moments for the Quasi-Permanent Load Combination on beam YD

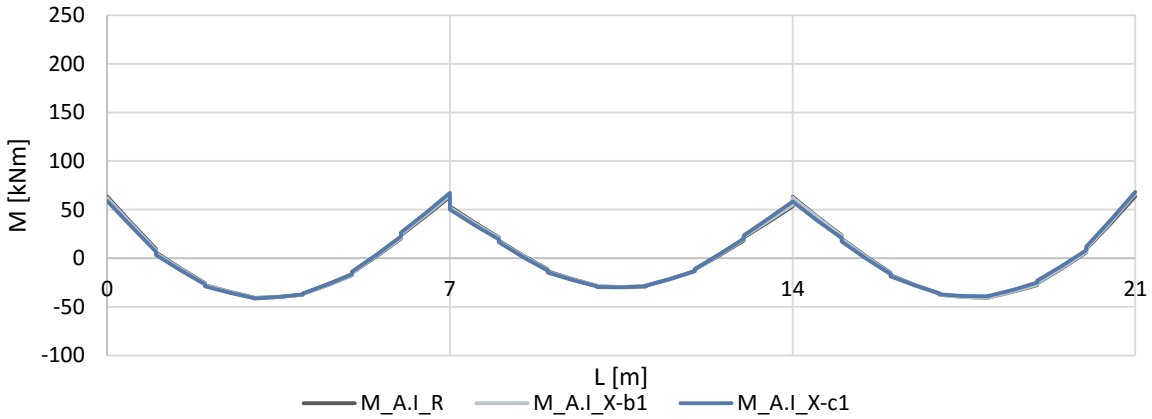

Figure B.6 – Bending moments for the Quasi-Permanent Load Combination on beam YE

Annex C

Displacements on the Models of the Parametric Study

Table C.1 – Horizontal displacements [m] for case M_A.I

Case	R	X-b1	X-c1	X-bd1	X-b2	X-c2	X-bd2	Y-a2	Y-b2	Y-c2
1st Floor	0.015	0.016	0.016	0.016	0.013	0.012	0.013	0.015	0.014	0.014
2nd Floor	0.038	0.041	0.041	0.040	0.035	0.034	0.035	0.038	0.037	0.037
3rd Floor	0.060	0.065	0.064	0.064	0.058	0.057	0.059	0.060	0.060	0.059
4th Floor	0.088	0.094	0.094	0.093	0.087	0.087	0.088	0.088	0.087	0.086
5th Floor	0.108	0.116	0.116	0.115	0.109	0.108	0.109	0.108	0.107	0.106
6th Floor	0.119	0.128	0.128	0.127	0.121	0.120	0.121	0.119	0.118	0.117

Table C.2 – Horizontal displacements [m] for case M_A.II

Case	R	X-b1	X-c1	X-bd1	X-b2	X-c2	X-bd2	Y-a2	Y-b2	Y-c2
1st Floor	0.038	0.040	0.039	0.040	0.039	0.037	0.037	0.035	0.032	0.031
2nd Floor	0.066	0.069	0.069	0.069	0.069	0.068	0.067	0.063	0.061	0.059

Table C.3 – Horizontal displacements [m] for case M_A.III

Case	R	X-b1	X-c1	X-bd1	X-b2	X-c2	X-bd2	Y-a2	Y-b2	Y-c2
1st Floor	0.000	0.000	0.000	0.000	0.000	0.000	0.000	0.000	0.000	0.000
2nd Floor	0.011	0.012	0.012	0.012	0.009	0.009	0.009	0.011	0.011	0.011
3rd Floor	0.032	0.034	0.034	0.034	0.028	0.028	0.028	0.032	0.032	0.031
4th Floor	0.055	0.057	0.058	0.058	0.051	0.051	0.051	0.055	0.055	0.054
5th Floor	0.077	0.081	0.082	0.081	0.074	0.074	0.074	0.077	0.077	0.076
6th Floor	0.100	0.105	0.106	0.106	0.099	0.099	0.099	0.100	0.101	0.099
7th Floor	0.121	0.126	0.128	0.128	0.121	0.120	0.121	0.120	0.121	0.119
8th Floor	0.138	0.145	0.147	0.146	0.140	0.139	0.139	0.138	0.139	0.137
9th Floor	0.159	0.167	0.169	0.168	0.162	0.161	0.162	0.158	0.160	0.157
10th Floor	0.174	0.183	0.185	0.185	0.178	0.178	0.178	0.174	0.175	0.173

Table C.4 – Horizontal displacements [m] for case M_B.I

Case	R	X-b1	X-c1	X-bd1	X-b2	X-c2	X-bd2	Y-a2	Y-b2	Y-c2
1st Floor	0.000	0.000	0.000	0.000	0.000	0.000	0.000	0.000	0.000	0.000
2nd Floor	0.004	0.004	0.004	0.004	0.004	0.004	0.004	0.004	0.004	0.004
3rd Floor	0.012	0.011	0.011	0.011	0.011	0.011	0.011	0.011	0.012	0.012
4th Floor	0.022	0.021	0.021	0.021	0.021	0.021	0.021	0.021	0.022	0.022
5th Floor	0.033	0.033	0.033	0.033	0.033	0.033	0.033	0.033	0.033	0.033
6th Floor	0.045	0.044	0.044	0.044	0.044	0.044	0.044	0.045	0.045	0.045

Table C.5 – Horizontal displacements [m] for case M_C.I

Case	R	X-b1	X-c1	X-bd1	X-b2	X-c2	X-bd2	Y-a2	Y-b2	Y-c2
1st Floor	0.000	0.000	0.000	0.000	0.000	0.000	0.000	0.000	0.000	0.000
2nd Floor	0.004	0.004	0.004	0.004	0.004	0.004	0.004	0.004	0.004	0.004
3rd Floor	0.012	0.011	0.011	0.011	0.011	0.011	0.011	0.011	0.012	0.012
4th Floor	0.022	0.021	0.021	0.021	0.021	0.021	0.021	0.021	0.022	0.022
5th Floor	0.033	0.033	0.033	0.033	0.033	0.033	0.033	0.033	0.033	0.033
6th Floor	0.045	0.044	0.044	0.044	0.044	0.044	0.044	0.045	0.045	0.045

Annex D

Considered Artificial Accelerograms

The artificial accelerograms considered for the non-linear analysis are presented in Figure D.1 to Figure D.6.

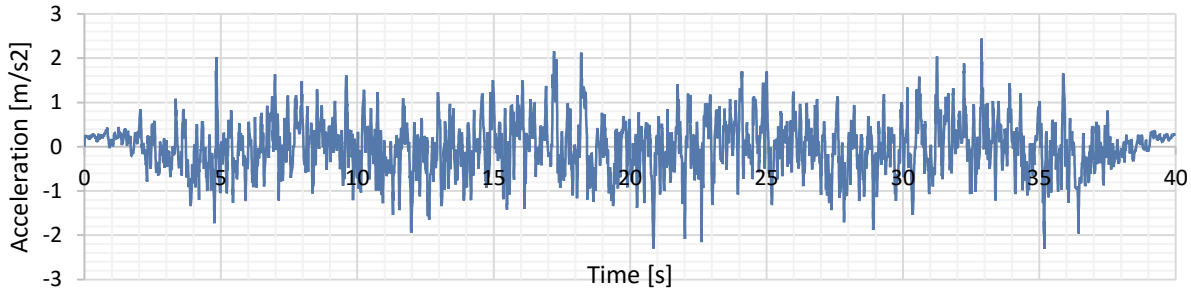

Figure D.1 – Horizontal Time-History record H1

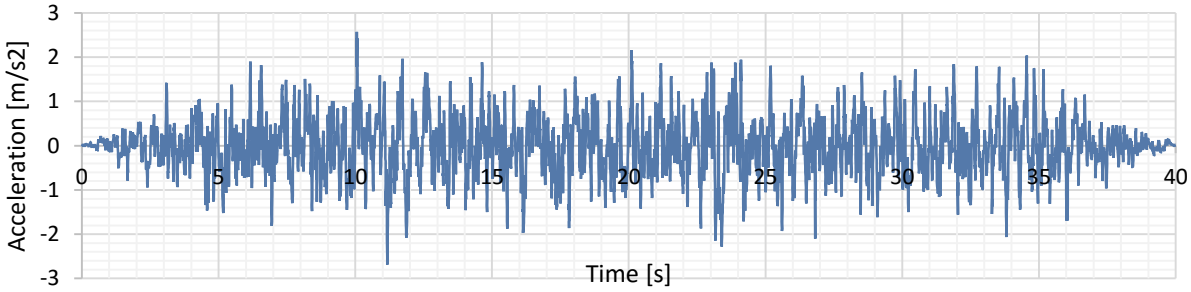

Figure D.2 – Horizontal Time-History record H2

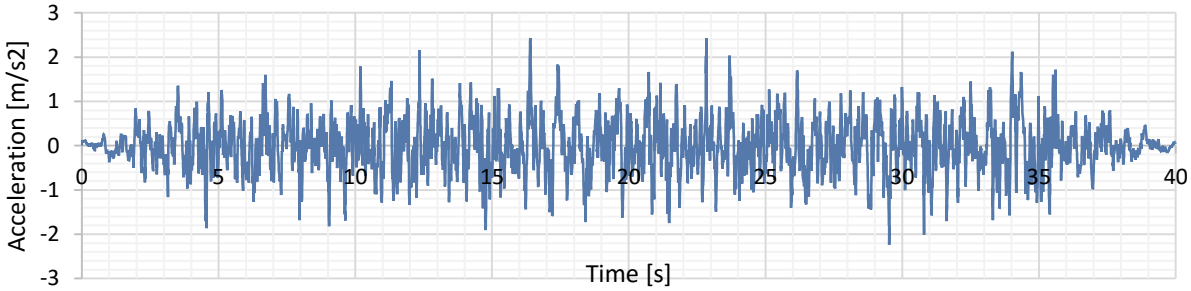

Figure D.3 – Horizontal Time-History record H3

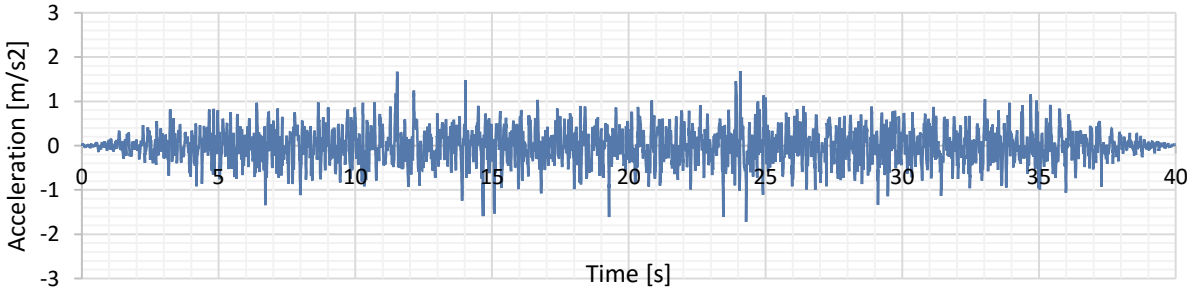

Figure D.4 – Vertical Time-History record V1

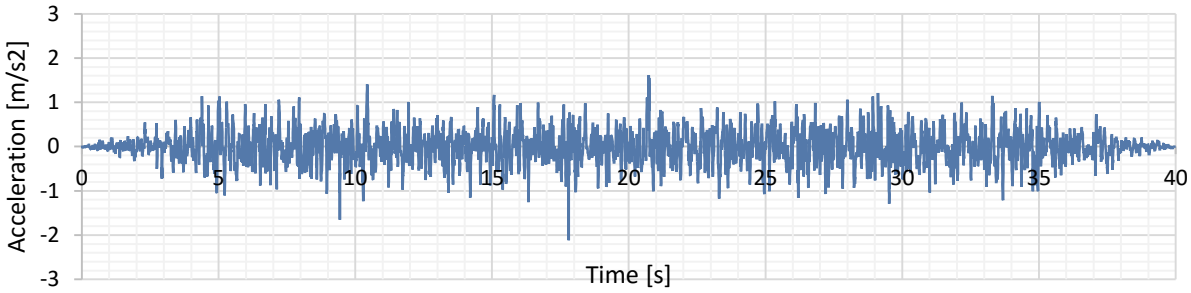

Figure D.5 – Vertical Time-History record V2

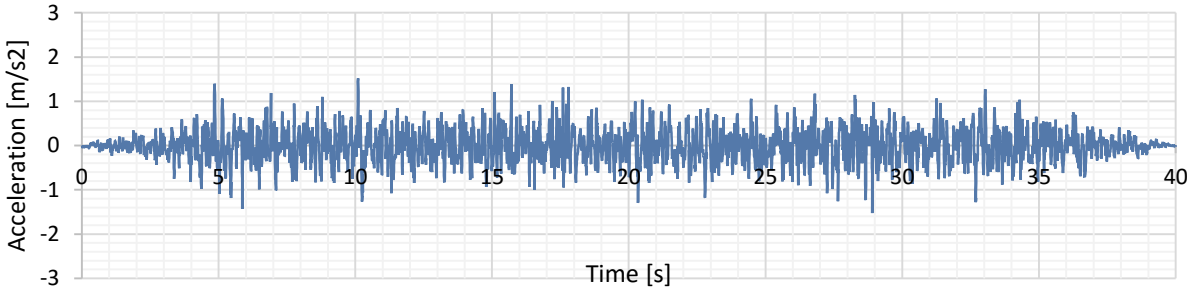

Figure D.6 – Vertical Time-History record V3

Annex E

Chord Rotation of the Elements of the Non-Linear Models

Table E.1 – Chord Rotation [mrad] on the beams oriented in the x direction

	Alignment 1		Alignment 2		Alignment 3		Alignment 4		Irregular / Regular			
	Irregular	Regular	Irregular	Regular	Irregular	Regular	Irregular	Regular	Alignment 1	Alignment 2	Alignment 3	Alignment 4
A_{right}	3.59	5.00	4.84	5.33	5.14	5.37	4.95	4.98	0.72	0.91	0.96	0.99
B_{left}	1.80	1.29	3.06	3.46	3.20	3.42	1.29	1.31	1.39	0.89	0.94	0.99
B_{right}	2.07	1.28	3.00	3.40	3.20	3.40	1.28	1.30	1.62	0.88	0.94	0.99
C_{left}	1.75	1.38	2.91	3.33	3.14	3.34	1.37	1.37	1.27	0.88	0.94	1.00
C_{right}	1.31	1.38	2.89	3.31	3.12	3.32	1.36	1.37	0.95	0.87	0.94	0.99
D_{left}	1.16	1.28	3.01	3.46	3.14	3.36	1.28	1.41	0.91	0.87	0.93	0.91
D_{right}	1.08	1.26	3.10	3.55	3.18	3.43	1.26	1.39	0.86	0.87	0.93	0.90
E_{left}	3.81	4.82	4.69	5.15	4.93	5.22	4.79	4.84	0.79	0.91	0.95	0.99
F_{right}	1.08	6.83	6.39	7.16	6.95	7.18	6.99	6.83	0.16	0.89	0.97	1.02
G_{left}	1.19	4.06	5.82	6.27	6.13	6.30	4.11	4.08	0.29	0.93	0.97	1.01
G_{right}	0.77	4.07	5.85	6.28	6.15	6.31	4.13	4.10	0.19	0.93	0.97	1.01
H_{left}	0.54	4.16	5.56	6.11	5.99	6.15	4.22	4.17	0.13	0.91	0.97	1.01
H_{right}	0.72	4.16	5.54	6.10	5.98	6.14	4.21	4.17	0.17	0.91	0.97	1.01
I_{left}	0.32	4.02	5.79	6.33	6.18	6.36	4.11	4.04	0.08	0.91	0.97	1.02
I_{right}	0.24	3.99	5.78	6.32	6.18	6.36	4.08	4.01	0.06	0.91	0.97	1.02
J_{left}	0.64	6.43	6.15	6.77	6.65	6.77	6.77	6.50	0.10	0.91	0.98	1.04

Table E.2 – Chord Rotation [mrad] on the columns oriented in the x direction

	Alignment 1		Alignment 2		Alignment 3		Alignment 4		Irregular / Regular			
	Irregular	Regular	Irregular	Regular	Irregular	Regular	Irregular	Regular	Alignment 1	Alignment 2	Alignment 3	Alignment 4
A_{down}	4.05	4.32	5.11	5.80	5.38	5.76	4.35	4.34	0.94	0.88	0.93	1.00
B_{down}	4.97	6.23	3.73	4.26	3.90	4.17	6.14	6.12	0.80	0.88	0.93	1.00
C_{down}	4.83	5.88	3.47	3.91	3.76	3.99	5.81	5.84	0.82	0.89	0.94	0.99
D_{down}	5.05	6.13	3.77	4.11	3.74	4.00	6.04	6.06	0.82	0.92	0.93	1.00
E_{down}	4.16	4.60	5.25	6.02	5.64	6.02	4.51	4.52	0.91	0.87	0.94	1.00
F_{up}	6.00	1.52	2.15	2.09	2.02	2.08	1.54	1.65	3.95	1.03	0.97	0.94
G_{up}	6.48	3.56	1.47	1.68	1.49	1.67	3.39	3.41	1.82	0.88	0.89	0.99
H_{up}	5.99	3.17	1.36	1.59	1.39	1.61	3.08	3.16	1.89	0.86	0.86	0.97
I_{up}	5.96	3.41	1.53	1.75	1.53	1.76	3.31	3.42	1.75	0.87	0.87	0.97
J_{up}	6.26	1.52	1.89	2.00	1.86	1.97	1.38	1.53	4.11	0.95	0.94	0.90
F_{down}	9.29	4.64	6.19	5.54	6.28	5.63	5.47	4.82	2.00	1.12	1.12	1.14
G_{down}	-	6.12	4.35	3.88	4.28	3.90	6.70	6.21	-	1.12	1.10	1.08
H_{down}	9.99	6.14	4.75	4.21	4.58	4.21	6.72	6.26	1.63	1.13	1.09	1.07
I_{down}	9.72	6.51	4.71	4.29	4.60	4.28	6.97	6.52	1.49	1.10	1.07	1.07
J_{down}	9.19	5.53	6.88	6.42	6.75	6.43	5.97	5.54	1.66	1.07	1.05	1.08
K_{up}	10.69	9.85	9.97	10.13	10.44	10.20	10.56	9.99	1.09	0.98	1.02	1.06
L_{up}	-	10.12	10.03	10.04	10.29	10.08	10.73	10.24	-	1.00	1.02	1.05
M_{up}	10.06	10.25	10.23	10.22	10.46	10.27	10.86	10.37	0.98	1.00	1.02	1.05
N_{up}	9.89	10.37	10.39	10.53	10.67	10.56	10.96	10.48	0.95	0.99	1.01	1.05
O_{up}	9.73	10.85	10.89	11.15	11.27	11.18	11.35	10.87	0.90	0.98	1.01	1.04

Table E.3 – Chord Rotation [mrad] on the beams oriented in the y direction

	Alignment A		Alignment B		Alignment C		Alignment D		Alignment E		Irregular / Regular				
	Irr.	Reg.	Irr.	Reg.	Irr.	Reg.	Irr.	Reg.	Irr.	Reg.	Align. A	Align. B	Align. C	Align. D	Align. E
I_{right}	4.81	4.78	5.16	5.27	5.17	5.19	5.17	5.27	4.62	4.73	1.01	0.98	1.00	0.98	0.98
II_{left}	1.27	1.26	3.07	3.32	3.20	3.37	3.20	3.32	1.27	1.27	1.01	0.92	0.95	0.97	1.00
II_{right}	1.27	1.26	3.30	3.29	3.19	3.32	3.11	3.28	1.27	1.26	1.01	1.00	0.96	0.95	1.00
III_{left}	1.40	1.41	3.24	3.34	3.28	3.43	3.22	3.34	1.40	1.42	0.99	0.97	0.96	0.96	0.99
III_{right}	1.39	1.40	3.26	3.40	3.32	3.48	3.29	3.39	1.42	1.41	0.99	0.96	0.95	0.97	1.01
IV_{left}	4.61	4.58	5.06	5.09	4.95	5.01	5.00	5.11	4.62	4.60	1.01	0.99	0.99	0.98	1.01
V_{right}	6.64	6.37	5.35	6.82	7.03	6.93	6.80	6.83	6.18	6.40	1.04	0.78	1.01	0.99	0.97
VI_{left}	4.21	4.02	6.08	6.05	6.04	6.02	5.91	6.05	3.89	4.00	1.05	1.01	1.00	0.98	0.97
VI_{right}	4.23	4.04	6.44	6.06	6.04	6.03	5.91	6.07	3.91	4.02	1.05	1.06	1.00	0.97	0.97
VII_{left}	4.10	4.00	6.24	6.13	6.06	6.06	6.02	6.13	3.86	3.97	1.02	1.02	1.00	0.98	0.97
VII_{right}	4.06	3.97	6.23	6.11	6.05	6.04	6.02	6.11	3.87	3.96	1.02	1.02	1.00	0.99	0.98
$VIII_{left}$	6.60	6.27	6.88	6.60	6.60	6.51	6.51	6.59	6.04	6.23	1.05	1.04	1.01	0.99	0.97

Table E.4 – Chord Rotation [mrad] on the columns oriented in the y direction

	Alignment A		Alignment B		Alignment C		Alignment D		Alignment E		Irregular / Regular				
	Irr.	Reg.	Irr.	Reg.	Irr.	Reg.	Irr.	Reg.	Irr.	Reg.	Align. A	Align. B	Align. C	Align. D	Align. E
I_{down}	4.36	4.40	5.26	5.67	5.50	5.63	5.61	5.66	4.49	4.48	0.99	0.93	0.98	0.99	1.00
II_{down}	5.79	5.89	3.70	3.89	3.72	3.78	3.83	3.92	5.61	5.84	0.98	0.95	0.98	0.98	0.96
III_{down}	5.75	5.74	3.75	3.82	3.83	3.90	3.73	3.80	5.75	5.70	1.00	0.98	0.98	0.98	1.01
IV_{down}	4.29	4.45	5.69	5.88	5.73	5.93	5.73	5.89	4.32	4.37	0.96	0.97	0.97	0.97	0.99
V_{up}	2.24	1.59	3.71	2.12	2.65	2.09	2.60	2.09	2.35	1.64	1.41	1.75	1.26	1.25	1.43
VI_{up}	3.15	3.27	1.43	1.54	1.45	1.47	1.56	1.54	3.17	3.29	0.96	0.93	0.98	1.02	0.96
VII_{up}	3.09	3.13	1.46	1.54	1.58	1.61	1.54	1.55	3.32	3.17	0.99	0.94	0.98	1.00	1.05
$VIII_{up}$	1.80	1.57	2.20	2.10	2.17	2.12	2.19	2.13	1.74	1.59	1.15	1.05	1.02	1.03	1.09
V_{down}	5.78	4.24	-	5.01	5.86	4.80	5.90	5.03	5.42	4.38	1.36	-	1.22	1.17	1.24
VI_{down}	6.46	5.27	3.78	3.30	3.76	3.33	3.48	3.33	5.22	5.35	1.23	1.15	1.13	1.04	0.98
VII_{down}	6.75	5.46	4.08	3.40	3.97	3.51	3.60	3.40	5.34	5.54	1.24	1.20	1.13	1.06	0.96
$VIII_{down}$	5.81	4.49	6.02	5.23	5.90	5.34	5.41	5.22	4.30	4.43	1.29	1.15	1.11	1.04	0.97
IX_{up}	10.23	9.26	-	9.49	9.62	9.32	9.62	9.52	9.32	9.36	1.11	-	1.03	1.01	1.00
X_{up}	10.59	9.24	10.03	9.21	9.71	9.28	9.23	9.23	8.91	9.30	1.15	1.09	1.05	1.00	0.96
XI_{up}	10.76	9.40	10.25	9.46	9.94	9.52	9.49	9.47	9.07	9.46	1.15	1.08	1.05	1.00	0.96
XII_{up}	11.03	9.54	10.62	9.78	10.45	9.90	9.93	9.79	9.24	9.60	1.16	1.09	1.06	1.02	0.96